Technische Universität München

Lehrstuhl für Anorganische Chemie

Multiphase Epoxidation Catalysis of Olefins with Metal-Organic Frameworks and Ionic Liquids

Marlene Kaposi

Vollständiger Abdruck der von der Fakultät für Chemie der Technischen Universität München zur Erlangung des akademischen Grades eines

Doktors der Naturwissenschaften (Dr. rer. nat.)

genehmigten Dissertation.

Vorsitzende(r):	Univ.-Prof. Dr. F. E. Kühn
Prüfer der Dissertation:	1. Univ.-Prof. Dr. Dr. h.c. mult. W. A. Herrmann
	2. Prof. Dr. Dr. h.c. J. Mink, Universität Budapest/Ungarn

Die Dissertation wurde am 25.06.2015 bei der Technischen Universität München eingereicht und durch die Fakultät für Chemie am 23.07.2015 angenommen.

Für Tobias
und meine Eltern,
Susanne und Harald

I do not know what I may appear to the world,
but to myself I seem to have been only like a boy playing on the seashore,
and diverting myself in now and then finding a smoother pebble or a prettier shell
than ordinary, whilst the great ocean of truth lay all undiscovered before me.
- Sir Isaac Newton

Die vorliegende Arbeit wurde zwischen Juli 2012 und Juli 2015 am Lehrstuhl für Anorganische Chemie I der Technischen Universität München angefertigt.

Besonders danken möchte ich meinem Doktorvater

Herrn Professor Dr. Dr. h.c. mult. Wolfgang A. Herrmann

für die Aufnahme in seinen Arbeitskreis, das uneingeschränkte Vertrauen, das er mir und meiner Arbeit entgegenbrachte, die exzellenten Bedingungen und hervorragende Infrastruktur am Lehrstuhl sowie den finanziellen Rückhalt während der Durchführung meiner Arbeit.

Weiterhin gilt mein besonderer Dank

Herrn Professor Dr. Fritz E. Kühn

für die schnelle und unkomplizierte Aufnahme in den Arbeitskreis, die wertvollen wissenschaftlichen Gespräche und die große Unterstützung in allen Belangen meiner Promotion.

Acknowledgments

The support of a lot of people made this work possible. Therefore my special thanks go to:

Dr. Mirza Cokoja for his kind supervision, his advice, proof reading of all my works, and for always supporting me,

Dr. Alexander Pöthig for his words of encouragement, our nice conversations, and for teaching me single crystal X-ray diffractometry,

Dr. Markus Drees for enjoyable conversations during coffee breaks and for helping with all issues regarding the Graduate School,

Dr. Gabriele Raudaschl-Sieber for the measurement of the solid state ^{13}C-MAS-NMR spectra,

Patricia Wand, **Daniel Weiß**, **Markus Anneser**, **Anja Lindhorst** and **Simone Hauser**, I always enjoyed our lunch and coffee breaks and our talks, professionally and personally,

Michael Wilhelm, **Michael Anthofer**, and **Robert Reich**, who have become great friends, it was a pleasure to work with you on the imidazolium catalysts,

all my other colleagues – my time at TUM has been wonderful, thanks for all the help, advice, good food, fruitler, jokes, and laughter,

Christine Hutterer for her great Master's Thesis and her friendship,

my internship students who assisted me in the lab,

Jürgen Kudermann for his uncomplicated nature and always trying to find a solution to characterization problems, and **Ulrike Ammari**, **Petra Ankenbauer**, and **Bircan Dilki** for the characterizatation of countless compounds,

all secretaries, **Irmgard Grötsch**, **Roswitha Kaufmann**, **Renate Schuhbauer-Gerl**, and **Ulla Hifinger**, for helping with official business.

Last but not least I want to thank my family – especially my parents, who have always supported me, and my husband, Tobias, for sharing all the good and bad experiences. His encouragement and love have enlightened all successes and helped me through all though times.

Abstract

The goal of this thesis was the study of the catalytic epoxidation of olefins in multiphasic systems and the recyclability of the investigated catalysts.

In the first part of this work, a solid/liquid biphasic system was investigated. A series of different amino-functionalized metal-organic frameworks (MOFs) of the UiO-type and IRMOF-3 were prepared and post-synthetically modified with a molecular molybdenum catalyst. Variable pore sizes were achieved through the use of different linkers and by preparing mixed MOFs containing only a fraction of functionalized linkers. The materials were characterized and tested in epoxidation catalysis of *cis*-cyclooctene using *tert*-butylhydroperoxide as oxidant. Four UiO-type MOFs were found to be stable during modification and epoxidation catalysis. Mo@UiO-67 mixed, being the framework with the largest pore size, can be reused several times without significant loss in activity. Furthermore, this catalyst can be applied in oxidation catalysis of the more demanding substrates 1-octene and styrene.

In the second part, differently substituted imidazolium perrhenates or nitrates were prepared and applied for biphasic liquid/liquid epoxidation catalysis of *cis*-cyclooctene. With this system hydrogen peroxide could be used as oxidant leading to water as the only by-product. Introduction of alkyl chains in different positions of the imidazolium moiety can significantly influence the ion pairing and solubility of the compounds, thus affecting catalytic performance. On the basis of the perrhenate ILs the effects of the substitution patterns on the catalytic activity were investigated. Methylation of the C2 position decreased cation–anion interactions, leading to the highest activities observed. Octyl and dodecyl chains in one of the N-positions enabled the imidazolium perrhenate to act as a better phase transfer catalyst and therefore further increased activity. Additionally, recycling experiments were performed to examine stability and reusability of the catalysts. Using nitrate ILs similar substitution patterns of the imidazolium ring were investigated in *cis*-cyclooctene epoxidation. It was found that nitrate is able to activate hydrogen peroxide. However, dramatically lower activities were observed, most probably due to the higher solubility of the compounds in aqueous phase thereby reducing the phase transfer capabilities.

Kurzfassung

Das Ziel dieser Arbeit ist die Untersuchung der katalytischen Epoxidation von Olefinen in Mehrphasensystemen und der Wiederverwendbarkeit der angewandten Katalysatoren.

Im ersten Teil wurde eine Serie amino-funktionalisierter metallorganischer Netzwerke (MOFs), basierend auf dem UiO- oder dem IRMOF-Typ, hergestellt und postsynthetisch mit einem molekularen Molybdänkomplex modifiziert. Durch die Verwendung verschiedener Linker und die Synthese von gemischten MOFs, die nur einen kleinen Anteil funktionalisierter Linker enthalten, konnten verschiedene Porengrößen eingestellt werden. Die MOF-Materialien wurden charakterisiert und in der Epoxidationskatalyse von *cis*-Cycloocten mit *tert*-Butylhydroperoxid als Oxidans getestet. Vier der UiO-Netzwerke blieben während der Modifikation und unter den katalytischen Bedingungen stabil. Der MOF mit den größten Poren, Mo@UiO-67 mixed, konnte ohne Aktivitätsverlust mehrfach wiederverwendet und auch in der Oxidation von 1-Octen und Styrol erfolgreich angewandt werden.

Im zweiten Teil der Arbeit wurden unterschiedlich substituierte ionische Flüssigkeiten (ILs), aufgebaut aus Imidazoliumkationen und Perrhenat oder Nitrat als Anionen, synthetisiert und in der Flüssig-Flüssig-Mehrphasenkatalyse zur Epoxidation von *cis*-Cycloocten eingesetzt. Diese Systeme sind in der Lage, Wasserstoffperoxid zu aktivieren, weshalb als einziges Nebenprodukt Wasser entsteht. Substituierung verschiedener Positionen am Imidazolium Ring ändert die Stärke der Ionenpaarung und die Löslichkeit, wodurch die katalytische Aktivität der ILs erheblich beeinflusst wird. Diese Effekte wurden mit Hilfe der Imidazoliumperrhenate untersucht. Methylierung der C2 Position bewirkt verringerte Wechselwirkungen zwischen den Ionen, was zu den aktivsten Katalysatoren führt. Werden Octyl- oder Dodecylgruppen an einem der Stickstoffatome eingeführt, sind die ILs in der Lage als Phasentransferkatalysatoren zu wirken, wodurch die Aktivität weiter gesteigert wird. Die Stabilität der Verbindungen konnte durch mehrfaches Wiederverwenden derselben Verbindung gezeigt werden. Auch Nitrat ist in der Lage Wasserstoffperoxid zu aktivieren, was mit ILs mit ähnlichen Substitutionsmustern gezeigt wurde. Die Aktivität der Verbindungen wird allerdings dramatisch verringert, was wahrscheinlich an der erhöhten Löslichkeit der Nitrate in der wässrigen Phase liegt.

Abbreviations

acac	acetylacetonato
AER	anion exchange resin
BET	Brunauer-Emmett-Teller
DCM	dichloromethane
DFT	density functional theory
DMF	*N*,*N*-dimethylformamide
DMSO	dimethyl sulfoxide
EBHP	ethylbenzene hydroperoxide
EO	ethylene oxide
HPPO	hydrogen peroxide propylene oxide
IL	ionic liquid
IR	infrared
IRMOF	isoreticular metal-organic framework
MAS	magic angle spinning
MOF	metal-organic framework
MTO	methyltrioxorhenium
NMR	nuclear magnetic resonance
ORTEP	Oak Ridge thermal ellipsoid plot
PO	propylene oxide
PXRD	powder X-ray diffraction
RTIL	room temperature ionic liquid
SBU	secondary building unit
SC-XRD	single crystal X-ray diffraction
SI	salicylimide
SILP	supported ionic liquid phases
SIP	supramolecular ion pairs
TBHP	*tert*-butyl hydroperoxide
THF	tetrahydrofuran
TOF	turn over frequency
UHP	urea hydroperoxide
UiO	Universitetet i Oslo
XPS	X-ray photoelectron spectroscopy

Contents

Introduction 1

1 Industrial Epoxidation of Olefins 3

1.1 Chlorohydrin process . . . 3
1.2 Hydroperoxide Processes . . . 4
1.3 Hydrogen-Peroxide-Propylene-Oxide (HPPO) process . . . 5
1.4 Ethylene Oxide . . . 6

2 Homogeneous Epoxidation Catalysis 6

3 Immobilization of Molecular Molybdenum Epoxidation Catalysts 10

3.1 Metal-organic Frameworks as Supports for Epoxidation Catalysts . 11

4 Ionic Liquids in Epoxidation Catalysis 14

Objective 21

5 Metal-organic Frameworks 23

6 Ionic Liquids 24

Results and Discussion 25

7 Immobilization of a Molecular Epoxidation Catalyst on UiO-type MOFs 27

7.1 Synthesis . . . 27
    7.1.1 Linker Preparation . . . 27
    7.1.2 Catalyst Preparation . . . 29
7.2 Characterization . . . 33
    7.2.1 Powder X-ray Diffraction . . . 33
    7.2.2 Solid-State ^{13}C-MAS-NMR . . . 35

7.2.3 Specific Surface Area Determination from N_2 Adsorption Measurements 36
7.2.4 X-ray Photoelectron Spectroscopy 37
7.2.5 Single Crystal X-ray Diffraction (SC-XRD) 37
7.2.6 Elemental Analysis 40
7.3 Catalytic Epoxidation of Olefins and Recycling 41

8 Epoxidation of Olefins using Perrhenate Containing Ionic Liquids 46
8.1 Synthesis 46
8.1.1 Preparation of Imidazolium Halides 46
8.1.2 Preparation of Imidazolium Perrhenates 47
8.2 Characterization 48
8.2.1 NMR Spectroscopy 49
8.2.2 IR Spectroscopy 51
8.3 Catalytic Epoxidation of Olefins 51
8.4 Recycling of the Catalyst 56

9 Imidazolium Nitrate based Ionic Liquids 57
9.1 Synthesis 57
9.2 Characterization 58
9.2.1 NMR Spectroscopy 58
9.2.2 Single Crystal X-ray Diffraction and Hirshfeld Surface Analysis 58
9.2.3 Solubility tests 62
9.3 Catalytic Epoxidation of Olefins 63
9.3.1 Influence of Stirring 63
9.3.2 Catalyst Comparison 63

Conclusions and Outlook 67

10 Metal-organic Frameworks 69

11 Imidazolium Based Ionic Liquids 70
11.1 Imidazolium Perrhenates 70
11.2 Imidazolium Nitrates 71

Experimental Part 73

12 General Remarks 75

13 Analytical Methods 75

14 Metal-organic Frameworks 79
14.1 Linker Preparation 79
14.2 Catalyst Preparation 83
14.3 Catalytic Epoxidation Experiments 88

15 Imidazolium Bromides 89
15.1 Synthesis 89

16 Imidazolium Perrhenates 90
16.1 Synthesis 90
16.2 Analysis 90
16.3 Catalysis 96

17 Imidazolium Nitrates 97
17.1 Synthesis 97
17.2 Analysis 97

References 105

List of Publications and Curriculum Vitae 117

18 Journal or Book Chapter Contributions 119

19 Talks and Poster Presentations 120

Introduction

R
R'
catalyst
R'
R

1 Industrial Epoxidation of Olefins

The epoxidation of olefins is of high interest in industry and academia.[1,2] Epoxides are being used as monomers for various polymers, such as polyglycol, polyamides and polyurethanes. They are also important intermediates in the production of fine chemicals like pharmaceuticals, food additives or flavor and fragrance compounds.[3]

Propylene oxide (PO) and ethylene oxide (EO) are the most important epoxides in industry. PO is the second most important propylene derivative after polypropylene.[1] In 2013, 8.06 tons of PO were produced and the market is expected to grow by 3.5-4 % annually.[4] While it is possible to directly oxidize EO with molecular oxygen over a Ag/Al_2O_3 catalyst,[5] economical oxidation routes for PO require chemical mediators.

1.1 Chlorohydrin process

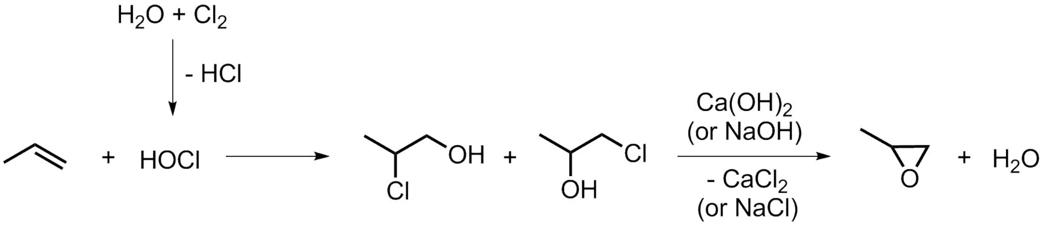

Scheme 1.1: PO synthesis via the chlorohydrin route.

The chlorohydrin process for PO and EO synthesis was first described by Wurtz in 1859.[6] The course of the reaction for propylene is shown in Scheme 1.1. First, the alkene reacts with hypochlorous acid, which is formed in situ from water and chlorine, to give chlorohydrin. Subsequently, dehydrochlorination occurs with calcium or sodium hydroxide, and the epoxide forms.[7] The main drawback of this process is the large amount of waste products. Per ton of propylene oxide produced, 40t of waste water and 2t of chloride salts accrue. Additional by-products are 1,2-dichloropropane and smaller amounts of dichloropropanols. Recently, no plants using this process have been built, due to the high waste production. Because of high investment costs, however, older plants are still operational and are kept up-to-date, often integrated with Cl_2 production.[1]

1.2 Hydroperoxide Processes

In hydroperoxide processes alkanes are oxidized to their respective hydroperoxides, which can react with propylene to form PO and alcohol.

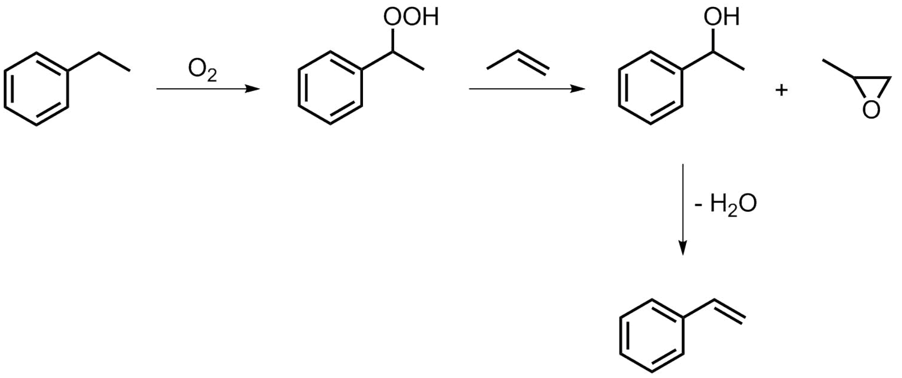

Scheme 1.2: Halcon/ARCO process for PO synthesis (analogous route for isobutane).

Halcon and ARCO developed a process using ethylbenzene hydroperoxide (EBHP)[8–10] or *tert*-butyl hydroperoxide (TBHP)[11,12] as oxidants. The epoxidation step is catalyzed by either homogeneous molybdenum, tungsten or vanadium catalysts or a heterogeneous titanium-based catalyst. Furthermore, α-methylbenzyl alcohol or *tert*-butyl alcohol are formed as co-products (2.5 t and 2.1 t per ton PO respectively[1]). Scheme 1.2 shows the reaction pathway for the epoxidation of propylene using EBHP. α-Methylbenzyl alcohol can be dehydrated to styrene and *tert*-butyl alcohol to isobutene or converted to methyl-*tert*-butyl ether with methanol. The Halcon/ARCO process produces far less waste than the chlorohydrin process, but the market value of the produced PO is dependent on the market of the co-products.

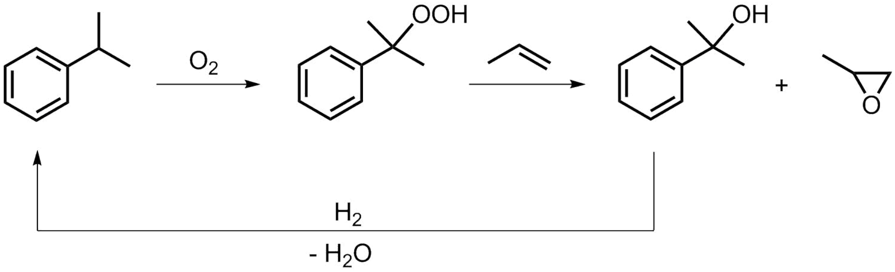

Scheme 1.3: Sumitomo process for propylene epoxidation.

Sumitomo Chemical developed an alternative hydroperoxide process using cumene (Scheme 1.3). Cumyl hydroperoxide is more selectively produced and more stable than ethylbenzene hydroperoxide. Cumyl alcohol is formed as co-product in the epoxidation step. The alcohol is dehydrated to α-methylstyrene which is then hydrogenated back to cumene to be reused in the process. These steps can be combined into a single hydrogenolysis step and are catalyzed by a copper-chromium oxide catalyst.[2]

1.3 Hydrogen-Peroxide-Propylene-Oxide (HPPO) process

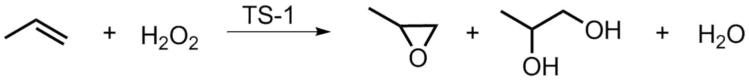

Scheme 1.4: HPPO process.

Enichem, Dow and BASF developed a process using aqueous H_2O_2 as oxidant for PO synthesis.[13–16] H_2O_2 is produced on-site in an integrated facility to avoid expensive transportation with water being the only by-product. In the presence of water, however, PO can easily undergo ring opening to form 1,2-propanediol. For the epoxidation process a heterogeneous titania-doped zeolite, TS-1, is used as catalyst, which is easily recycled but needs to be regenerated prior to reuse. Although this leads to additional expenses, the HPPO process is now state of the art for propylene epoxidation.

1.4 Ethylene Oxide

Ethylene oxide was, together with PO, first prepared in 1859 by Wurtz using the chlorohydrin process.[6] In 1931 the direct oxidation of ethylene with a Ag@Al_2O_3 catalyst was achieved.[17] Since the 1940s all newly built plants have been based on that principle.[2] However, the conditions for direct oxidation are very harsh and the gaseous phase, containing ethylene oxide and oxygen, is highly explosive and therefore poses a significant security risk. Furthermore, large amounts of CO_2 are formed as a by-product during the process through combustion of ethylene.

2 Homogeneous Epoxidation Catalysis

At present, industry favors heterogeneous catalysts since their recycling is much easier to accomplish compared to homogeneous compounds. However, for selective and asymmetric synthesis it is necessary to use homogeneous catalysts.[18]

A plethora of very active homogeneous epoxidation catalysts based on transition metals like molybdenum, titanium, vanadium, manganese, rhenium, and, more recently, iron have been reported.[18–20] Most of the catalytic reactions, however, are only done with simple olefins and recycling is often not reported.

Figure 2.1 shows four of the most active homogeneous epoxidation catalysts known so far.[19] In order to easily compare catalysts the turn over frequency (TOF) is used. It is determined by the amount of substrate (in mol) converted by the applied amount of catalyst (in mol) per unit time (usually given in hours). For the catalytic epoxidation of *cis*-cyclooctene with a catalyst loading of 0.05 mol% TOFs as high as 25000 h^{-1} per Mo for $[Mo_2(O\mathit{t}Bu)_6]$ (**1**)[21] and 44000 h^{-1} for the ansa-complex $[Mo(\eta5\text{-}C_5H_4(CH(CH_2)_3)\text{-}\eta1\text{-}CH)(CO)_3]$ (**2**)[22] could be reached. TOFs of around 40000 h^{-1} are observed with Methyltrioxorhenium (MTO, **3**) even at catalyst loadings of only 0.01 mol%.[23] The highest reported TOF of around 53000 h^{-1}

for a Mo compound is achieved with $[CpMo(CO)_2(ImPyMes)(NCCH_3)]BF_4$ (**4**) with catalyst loadings of 0.01 mol%.[24]

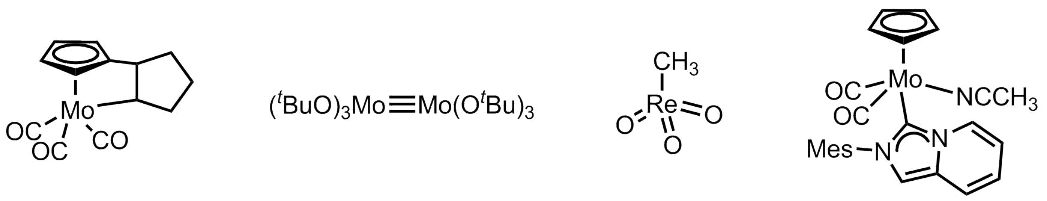

1 **2** **3** **4**

Figure 2.1: Four very active homogeneous epoxidation catalysts.[19,24]

Cis-cyclooctene is the benchmark substrate in academia, since it is easy to epoxidize and generates a relatively stable epoxide, which is not prone to ring opening. To evaluate a catalytic system better, however, a broader range of substrates should be tested. The most commonly used model substrates are 1-octene (for an aliphatic terminal olefin) and styrene (for an aromatic olefin). In both cases MTO (**3**) shows the best performance.[23,25] While the molybdenum based catalysts are working with TBHP as oxidant, MTO is able to activate H_2O_2 for epoxidation. Methyltrioxorhenium was first described in 1979[26] and the synthesis has been improved twice by Herrmann et al.[27,28] Apart from epoxidation catalysis it has been applied successfully in olefin metathesis[29], dehydration of alcohols[30], aldehyde olefination[31,32], deoxydehydration of diols[33–35], and C-O cleavage in lignin model compounds.[36] The proposed mechanism for olefin epoxidation is shown in Scheme 2.1.

In the first step, MTO reacts with one equivalent H_2O_2 to form the monoperoxo complex. This species can either react directly with the olefin or first form the bisperoxo complex, which then activates the alkene. Since both the mono- and bisperoxo species can react with the olefin a concerted mechanism is proposed.[37]

Three reports are dealing with potential industrial application of MTO in propylene epoxidation. The first report was published in 1991 by Herrmann et al.[38] The catalytic reaction shows only moderate conversions and a selectivity of 50 % towards the epoxide and formation of propylene glycol. The latter suggests ring opening of propylene oxide to the diol due to the catalyst's Lewis acidity and the

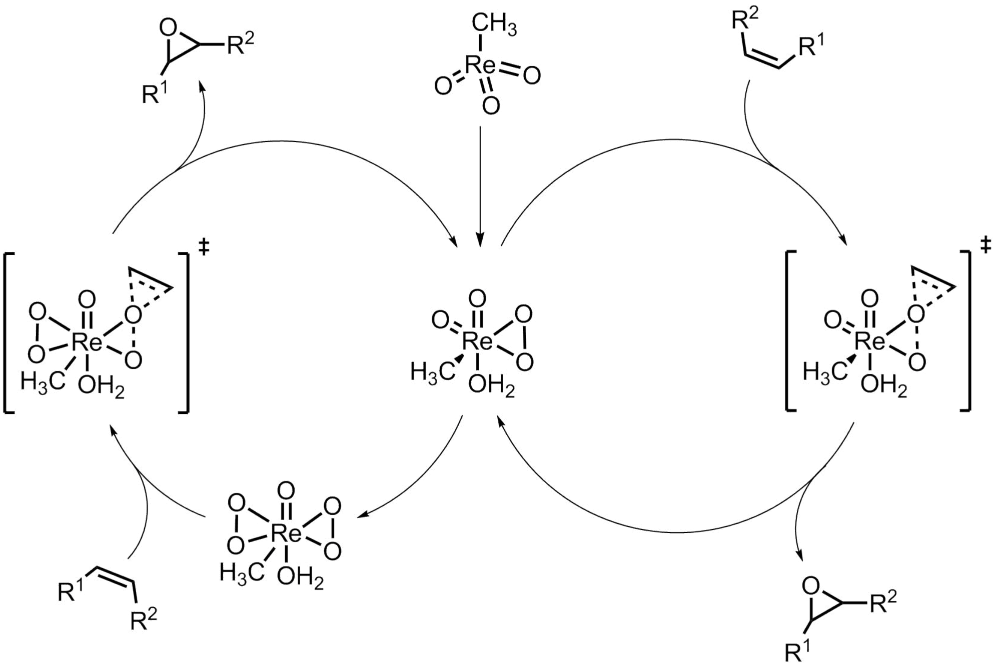

Scheme 2.1: Mechanism of olefin epoxidation catalyzed by MTO using aqueous H_2O_2.

presence of water.[38] Subramaniam and coworkers reported a biphasic system (gas/liquid) using a solution of MTO and aqueous H_2O_2 in methanol.[39] To stabilize the catalyst, pyridine-N-oxide was used and the authors claim PO yields of 98 % at near-ambient temperatures. However, in order to enhance the solubility of propylene in the liquid phase, a high N_2 pressure (20 bar) is necessary.[39] In 2014 Cokoja, Fehrmann, Kühn, and coworkers described the efficient epoxidation of propylene using a MTO/H_2O_2 system in acetonitrile.[40] Under mild conditions (40 ℃, 3 bar propylene) and using pyridine functionalized imidazolium salts as additives high conversions (up to 96 %) and selectivities could be achieved. However, recycling of the presented system was not possible. The authors attribute this to slow degradation of the active species during catalysis.[40]

In contrast to MTO's great catalytic performance there are still major drawbacks for its use in epoxidation catalysis. Both asymmetric epoxidation with MTO and immobilization of the catalyst could not be achieved so far. Furthermore, rhenium is a very expensive metal and catalyst recycling has proven to be difficult.

Molybdenum complexes are more promising in regards to asymmetric epoxidation and immobilization, since they can easily be modified. However, the use of H_2O_2 as oxidant is not possible, because of decomposition of both H_2O_2 and the catalyst. Therefore, hydroperoxides (mostly TBHP) are used with molybdenum compounds. In the 1970s two mechanistic pathways were proposed. Both involve a Mo-peroxo compound, but Mimoun et al.[41] suggested that the olefin attacks at the metal center, whereas it is proposed to attack directly at the peroxo-oxygen in the mechanism by Sharpless et al. (Scheme 2.2).[42] 20 years later, Thiel et al. proposed a Sharpless-like mechanism specifically for epoxidation with *tert*-butyl hydroperoxide as oxidant, where the olefin attacks at the coordinated *tert*-butyl peroxo ligand.[43–45] DFT calculations showed that in all proposed pathways the energies of all transition states were in a reasonable range, so that neither one could be excluded or preferred uniquely.[46–48]

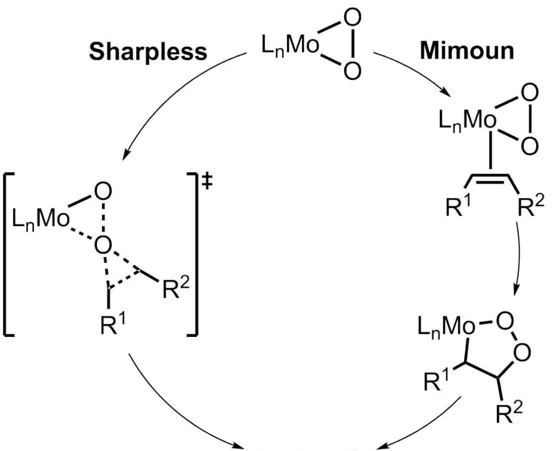

Scheme 2.2: Proposed epoxidation mechanisms of olefin with molybdenum compounds.

3 Immobilization of Molecular Molybdenum Epoxidation Catalysts

Myriads of molecular catalysts for epoxidation reactions are known (see chapter 2), but they have been neglected in industry so far. This can be attributed to the fact that homogeneous catalysts cannot be easily recycled and additionally are usually very expensive. Nevertheless, molybdenum complexes have been used in the industrial Halcon/ARCO and Sumitomo processes.[3] Industry would benefit greatly from the ability to replace a homogeneous catalyst with a heterogeneous one, while working at the same or at least comparable conditions.[49]

Over the last 15 years molecular molybdenum based epoxidation catalysts have been immobilized on various supports to facilitate recycling. The most common supports are mesoporous silicas, e.g. MCM-41[50–55] and SBA-15[56–58], and polymers. Polymer supported epoxidation catalysts have been known since the late 70's.[59,60] Molybdenum complexes have been immobilized on ion exchange resins,[59–61] poly(ethylene oxide),[62] poly(vinylpyridine),[63,64] imidazolium containing polymers[65], and various other materials.[66,67] Even nanoparticles[68] and carbon nanotubes[69] have been used as supports. However, immobilization is often associated with lower activity compared to the homogeneous analogues or leaching of the catalyst into the reaction mixture due to instability of the compounds. The loss in activity can be explained through diminished access of the substrates to the metal centers and limitations due to diffusion.[70] Therefore, highly tunable porous coordination polymers, more specifically metal-organic frameworks (MOFs), seem to be interesting supports for molecular catalysts. Details are covered in the following chapter.

3.1 Metal-organic Frameworks as Supports for Epoxidation Catalysts

The first report of a material, which today would be included in the family of "coordination polymers" or "metal-organic frameworks", was published by Kinoshita et al. in 1959.[71] Other reports of coordination polymers followed in the early 1960's[72–74] and the topic has even been reviewed in 1964.[75] However, those materials did not receive too much attention until the late 1990's, when the subject was rediscovered. Pioneering work was done by Robson et al., demonstrating that the formation of porous frameworks was easily achievable.[76,77] Especially the synthesis of the MOF-5 material by Yaghi and coworkers raised the research interest in this field.[78]

Nowadays, metal-organic frameworks (MOFs) can be defined as crystalline, highly porous frameworks composed of metal ions or clusters, also known as secondary building units (SBUs), and multidentate organic molecules, called linkers.[79] Thereby, the metal-linker coordinative bonds are stronger than H-bonds and other weak interactions, such as π-π stacking.[80] Due to these strong metal-ligand bonds it is possible to completely remove solvent molecules from the pores without structural collapse of the frameworks.[81] Their hybrid design allows an easy variation of pore size and form, and introduction of functional groups by choosing different building units (linkers and SBUs).[82] Because of their very high pore volumes and their variability the field of applications ranges from gas storage and separation trough petrochemistry, drug delivery and sensoring to catalysis.[82–84]

Synthesis of MOFs is usually carried out in liquid phase, generally by mixing a solution of a metal precursor with a solution of the organic linker molecule. The crystalline network is formed by self-assembly either at room temperature or at solvothermal conditions ($>$100 ℃).[79] To ensure the formation of stable, porous and crystalline frameworks rigid molecules are usually preferred over flexible ones.[85–87] Typical examples of organic linker molecules are shown in Figure 3.1.[79,82]

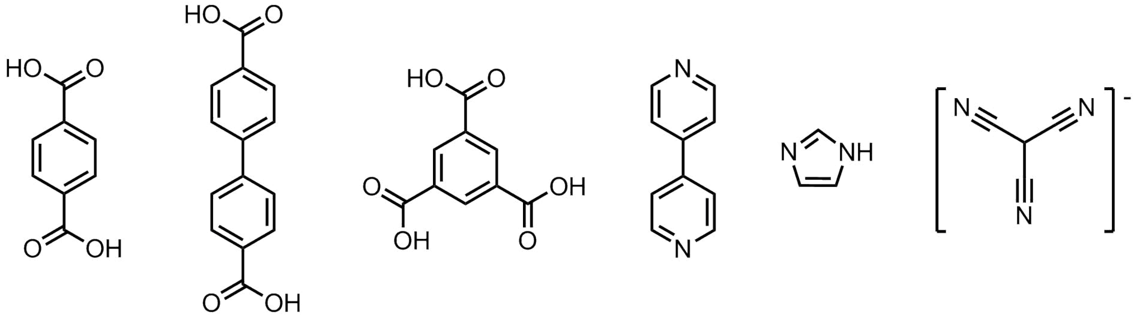

Figure 3.1: Examples of linker molecules used in metal-organic frameworks.[79,82]

There are various ways to apply MOFs in catalysis.[79] On the one hand, the frameworks can be used as catalysts by themselves. Such materials can either be synthesized by using organometallic linker molecules, such as the paddle-wheel MOF reported by Cho et al.,[88] or by introducing unsaturated metal sites at the inorganic SBUs. The latter is achieved when labile ligand molecules are added during synthesis, which can be removed through heating (activation step) prior to catalysis. On the other hand, complexes known to be catalytically active can be trapped inside the pores (so-called “ship in a bottle”)[89] or covalently immobilized through post-synthetic modification steps. This modification is a very versatile approach and has already been used for epoxidation catalysts. For example, post-synthetic modification was used by Farha et al. to exchange metals of the organometallic linker of a paddle-wheel MOF.[90] More importantly, post-synthetic modification of the organic linker molecules can facilitate covalent immobilization of complexes. Rosseinsky and coworkers reported a method where the amino-functionalized IRMOF-3 was treated with salicylaldehyde to form an imide. In a second step, $V(O)(acac)_2{\cdot}H_2O$ was immobilized on the MOF via a simple ligand exchange reaction.[83] A similar method has been used to immobilize manganese(II) acetylacetonate on IRMOF-3 in a one-pot reaction.[91] Furthermore, using post-synthetic modifications allows for the introduction of synergetic effects. This can be achieved when a MOF with already active metal sites is additionally modified to carry a different metal immobilized as a complex.[92]

To the best of our knowledge there are three reports dealing with immobilization of molybdenum(VI) species on MOFs. However, either the conversions reported are significantly lower compared to the homogeneous analogoues,[93] or the materials decompose slowly under oxidative reaction conditions.[94] For the third report a comparison is difficult, since the authors did not report a catalyst loading.[95]

The application of MOFs in catalysis is limited, mostly due to the low stability of the compounds towards temperature, moisture and various chemical compounds. Therefore, a few criteria concerning the framework have to be considered for it to be suitable for epoxidation catalysis. First of all, the material must be stable in the presence of air, water, and oxidants. Furthermore, the immobilized catalyst in a post-synthetically modified MOF must be strongly bound to the framework. Lastly, the pore size of the network must be chosen large enough to enable diffusion of both substrate and product.

The most promising MOFs to meet the aforementioned points are the Zr-based frameworks UiO-66 and -67 (UiO = Universitetet i Oslo) first reported by Lillerud et al.[96,97] Their stability can be attributed to the bond strength of a Zr-O bond and thus high stability of the inorganic building unit and high bonding strength between SBU and organic linker.[84] The structures of the inorganic metal cluster and UiO-67 are shown in Figure 3.2 (a and b, respectively). The secondary building unit is a $Zr_6O_4(OH)_4$ unit, which was first described by Schubert et al. in 2006.[98] The triangular faces of the octahedron are alternately capped by μ_3-OH and μ_3-O groups (Figure 3.2a). Dicarboxylic acids like terephthalic acid (for UiO-66) or 4,4'-biphenyldicarboxylic acid (for UiO-67) were used as organic linkers[84] connecting each Zr-cluster to twelve further $Zr_6O_4(OH)_4$ units. Therefore, UiO-type MOFs can be described as expanded cubic closed-packed structures (Figure 3.2b).[99] By using a carboxylate linker, which contains amino groups, post-synthetic modification can be applied for catalyst immobilization. Van Bokhoven et al. modified UiO-66-NH_2 using vapor diffusion to introduce a salicylidene moiety.[100]

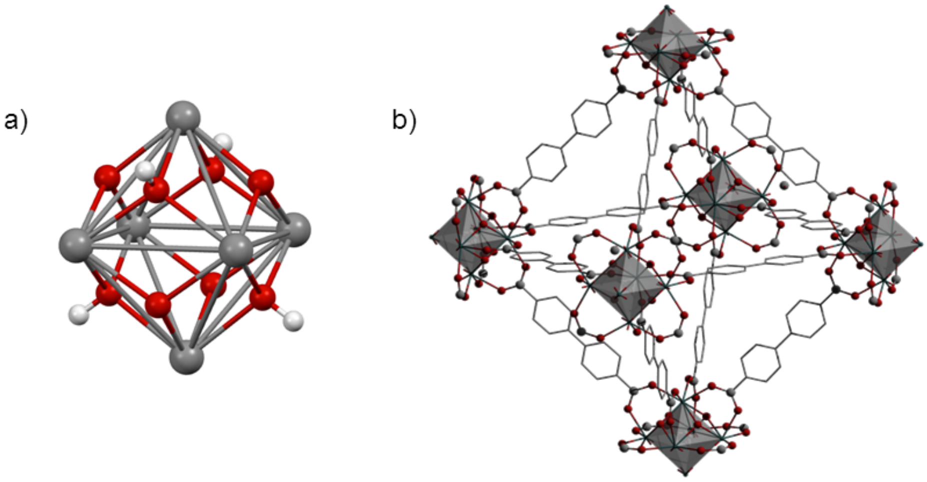

Figure 3.2: a) $Zr_6O_4(OH)_4$ cluster; b) UiO-67 with 4,4'-biphenyldicarboxylate linker (hydrogen atoms in b) are omitted for clarity).

As already described for V(V)[83], Au(III)[101], Ni(II)[102] and Ir(I)[103] this moiety can be used for immobilization of complexes. However, the incorporation of Mo(VI) into an amino-containing MOF has not been reported yet.

4 Ionic Liquids in Epoxidation Catalysis

Multiphase liquid/liquid systems offer another approach for straightforward catalyst recycling. At the same time the process should be environmentally benign. Therefore, the use of conventional organic solvents with high vapor pressures should be avoided. Ionic liquids seem to be the optimal alternative.

The first ionic liquid (IL) was synthesized in 1914,[104] but scientific interest in these compounds only rose in the last two decades of the 20th century with the pioneering work of Wilkes and coworkers.[105,106] ILs are commonly defined as liquids, which are entirely composed of ions with a melting point around or below 100 °C. A smaller subgroup are the room-temperature ionic liquids (RTILs) with melting points below 25 °C.[107]

In recent years ILs have been promoted as "green" solvents to an increasing degree, the reason behind this being their unique physical and chemical properties such as low volatility, low flash-point, and good thermal stability. They are also claimed to be relatively nontoxic.[107] Although the last point may not always be correct,[108,109] the other properties mentioned together with high polarity and therefore low miscibility with non-polar, organic solvents render ILs interesting alternatives to conventional solvents.[110] The characteristics of ionic liquids can additionally be tuned by choosing the right composition of anion and cation.[110] Properties like viscosity, conductivity, solvation, thermal and (electro)chemical stability can be adjusted to the application of the IL.[108] Typical ions used in ionic liquids are shown in Figure 4.1. Due to the multitude of available anions and cations, limitless combinations for ionic liquids are possible.

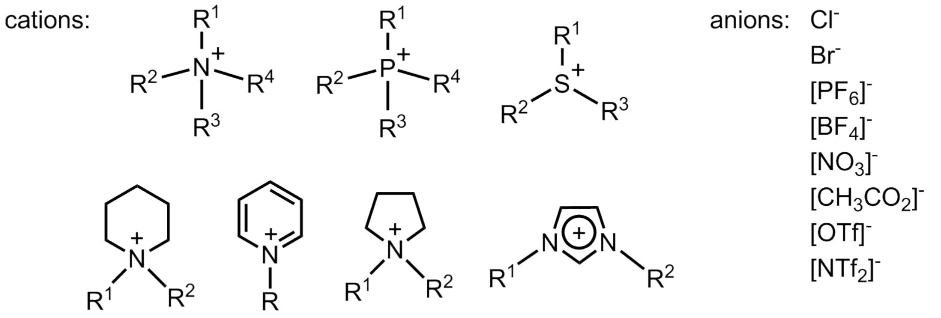

Figure 4.1: Examples of typical anions and cations used in ionic liquids.[111]

In the late 1980's first reports of the application of ILs as reaction media in organic synthesis were published.[112,113] Their use as solvents in homogeneous transition metal catalysis was first reported in 1990 by Chauvin et al.[114] Since then, interest in ILs and SILPs (Supported Ionic Liquid Phases)[115,116] as solvents for liquid/liquid extractions, synthesis and catalysis[117] has grown, as has been shown in works from Rogers,[118,119] Seddon,[120–122] Welton,[123–125] Wasserscheid,[126] Dupont[127] and others.[128–130] It has been shown that in addition to being interesting solvents for catalysis ILs can also be applied as catalysts, co-catalysts and ligands.[123]

Some ILs are already applied in industrial processes,[111] the most prominent example being the BASIL process of BASF.[131] In this alkoxyphenylphosphine synthesis 1-methylimidazole is applied to scavenge the formed hydrochloric acid (see Scheme 4.1). Methylimidazolium chloride and thereby a biphasic system is formed. After the completion of the reaction the product can be obtained by simple phase separation. The IL can be regenerated by deprotonation with sodium hydroxide.[132]

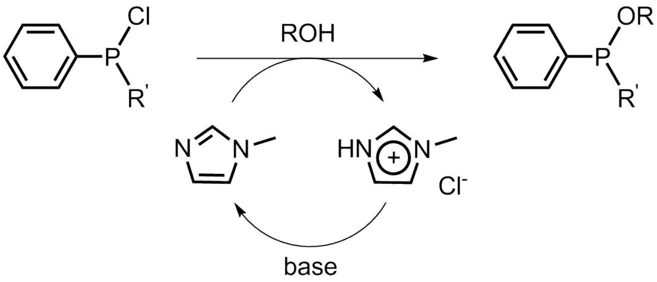

Scheme 4.1: Schematic representation of the BASIL process.[111]

The stability of ionic liquids in oxidative conditions allows their use in epoxidation catalysis. Song and Roh published the first report of an IL being used as solvent for a manganese(III) (salen) complex for asymmetric epoxidation in 2000.[133] Shortly thereafter more reports followed, including the application of various molybdenum complexes[134] and MTO[135] in ionic liquids. Initially, ILs were used to replace volatile solvents and to facilitate product separation and recycling. The latter could be achieved in only a few cases, but in addition an increase in catalytic activity of several systems could be observed.[136] For example, the molybdenum ansa-complex **2** mentioned in chapter 2 only reaches its full potential in ionic liquids.[22]

Surprisingly, even catalytically inactive inorganic compounds, such as perrhenates, have been found to activate oxidants for olefin epoxidation when applied as anions of ionic liquids. Zhang, Rösch, Kühn and coworkers[137] showed the efficient stoichiometric epoxidation of *cis*-cyclooctene to the corresponding cyclooctene oxide in excellent yields using aqueous H_2O_2 as oxidant (Scheme 4.2).

Different perrhenate containing imidazolium based ILs were applied in an equimolar mixture with *cis*-cyclooctene and 2.5 equivalents of oxidant. Compared to MTO substantially higher reaction temperatures (70 °C) and reaction times (4h) were necessary. However, the reported ILs could be recycled for at least eight

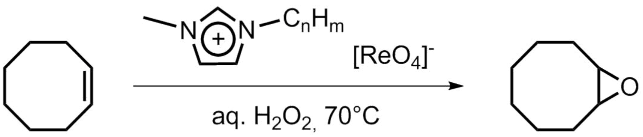

Scheme 4.2: Epoxidation of *cis*-cyclooctene with perrhenate containing ILs (n = 4, 8, 12; m = 2n+1).

runs without any loss in activity. The epoxide was extracted with *n*-hexane and the IL was dried in high vacuo at 50 ℃ for 4h to remove remaining *n*-hexane, water, and hydrogen peroxide.

Urea hydrogen peroxide (UHP) and TBHP were also tested as oxidants, but a considerable decrease in catalytic activity was observed.

To exclude the activation of H_2O_2 via the ILs' cation $[BF_4]$-salts were applied in the epoxidation reaction. *Cis*-cyclooctene yield dropped to 13 % as opposed to 100 % with $[ReO_4]^-$ containing ILs, showing the necessity of the perrhenate anion. The small but prevailing activity of the $[BF_4]$-ILs might be attributed to the ability of ILs to form H-bonds with H_2O_2 thus resulting in slight activation of the oxidant. Such strong interactions of ILs have previously been described for water by Welton et al.[138] In the presence of strong H-bond acceptors, such as perrhenate, it is proposed that such interactions between the cation and H_2O_2 are inhibited. An outer-sphere mechanism for the activation with perrhenate is therefore suggested. This differs from the usually proposed (hydro)peroxo metal complexes as active species.[139]

Scheme 4.3 shows the most feasible mechanism according to DFT calculations by Kühn et al.[137] The assumptions were proven spectroscopically by NMR, IR and Raman measurements. In the first step, H_2O_2 is activated through addition to the perrhenate anion, forming an outer-sphere complex. From this pre-coordinated H_2O_2 molecule one oxygen atom can be transferred to an olefin. Thereby, the desired epoxide is formed and water is produced as the only side product. After extraction of the product and drying of the ionic liquid the next reaction cycle can be started again.

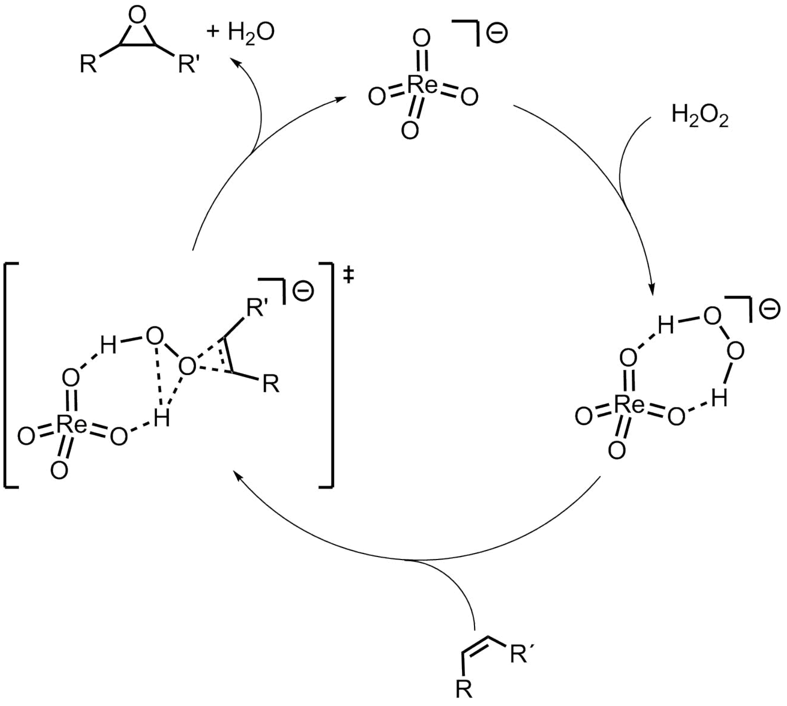

Scheme 4.3: Proposed mechanism for the epoxidation of olefins with $[ReO_4]^-$ containing ILs and H_2O_2 as oxidant.

Since the mechanism suggests that perrhenate is not consumed during the reaction, it should be possible to apply only catalytic amounts of it. Furthermore, it has been shown that the nature of the cation influences the activity of perrhenate. In the aforementioned work NH_4ReO_4 and $KReO_4$ were also tested for their catalytic activity in ILs. Considerably lower yields were achieved than with the imidazolium perrhenates. This effect was ascribed to the hydrophobic environment created by the imidazolium ion, rendering a protic solvent shell unnecessary. Very recently, Cokoja, Kühn, Love, and co-workers reported the catalytic epoxidation of olefins with perrhenate containing organic-phase supramolecular ion pairs (SIPs).[140] Amido-ammonium and -pyridinium receptors were investigated regarding their ability to transfer $[ReO_4]^-$ into a hydrophobic environment. It was shown, that perrhenate SIPs are indeed able to catalytically activate hydrogen peroxide and therefore enable epoxidation reactions.

Nevertheless, a few possibilities to optimize the reaction need to be addressed. Investigation of imidazolium perrhenates as catalysts instead of stoichiometric reaction partners for epoxidation reactions can be beneficial, because of their straightforward synthesis compared to the reported, sophisticated SIPs. Furthermore, the low Coulomb interactions between cation and anion in the IL facilitate the formation of H-bonds of H_2O_2 with $[ReO_4]^-$. Therefore, tailoring of the imidazolium counter ion should be considered (Figure 4.2).

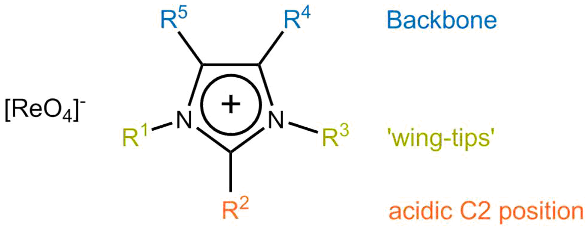

Figure 4.2: Possible optimization sites of the imidazolium moiety for functionalization and tailoring for certain applications.

On the one hand, replacement of the acidic proton in C2-position with alkyl groups decreases the anion-cation interactions, which should facilitate the formation of the outer-sphere complex. On the other hand, variation of the alkyl chains in the wingtip positions allows for adjustment in solubility and solvation properties. Furthermore, using imidazolium based ILs, where perrhenate is substituted by a metal-free alternative seems possible, since rhenium is not directly involved in the proposed mechanism.

Objective

Heterogeneous catalyst systems are preferred by industry due to their easy recycling. However, often homogeneous catalysts provide higher activities and selectivities. Therefore, two systems are investigated as suitable solutions.

5 Metal-organic Frameworks

The first part of this work deals with the heterogenization of molecular catalysts on metal-organic frameworks (MOFs). This approach offers the possibility to combine the properties of homogeneous catalysts with the easy recyclability of heterogeneous ones. MOFs are chosen as supports, since they offer both easy variation of pore size and a defined chemical microenvironment in the cages. Different UiO-type frameworks with varying contents of amino groups are synthesized and modified for the immobilization of a molecular molybdenum catalyst. The materials are fully characterized and applied for the epoxidation of olefins with special regard to material recycling and stability. Diffusion limitations arise from framework materials, showing that the investigation of the influence of pore sizes on catalytic activity is important. IRMOF-3 is synthesized and modified in a similar fashion for stability comparisons.

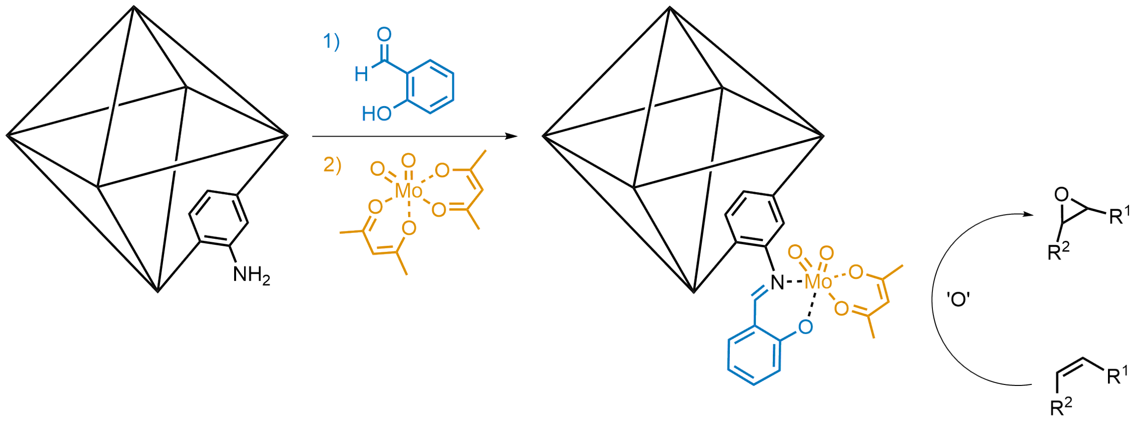

Scheme 5.1: Schematic representation of MOF modification and application in epoxidation catalysis.

6 Ionic Liquids

In the second part of this thesis ionic liquids are investigated as catalysts in biphasic epoxidation catalysis. Multiphase liquid/liquid systems provide easy recyclability similar to solid/liquid systems, but with lower diffusion limitations. Various imidazolium perrhenate and nitrate ILs are synthesized, characterized and applied in the catalytic epoxidation of *cis*-cyclooctene as model substrate. To understand the catalytic activity of these compounds, the influence of different substitution patterns (Figure 6.1, R1, R2 and R3) are investigated. Furthermore, stability and recycling possibilities for imidazolium perrhenates are studied.

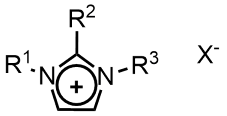

$X^- = [ReO_4]^-, [NO_3]^-$
R^1 = Me, ^{n}Oc
R^2 = H, Me, ^{n}Bu
R^3 = Me, ^{n}Bu, ^{n}Oc, ^{n}Hex, Bn^F

Figure 6.1: General formula of the imidazolium salts examined (Me = methyl, ^{n}Bu = *n*-butyl, ^{n}Oc = *n*-octyl, ^{n}Do = *n*-dodecyl, ^{n}Hex = *n*-hexadecyl, Bn^F = 2',3',4',5',6'-pentafluorobenzyl).

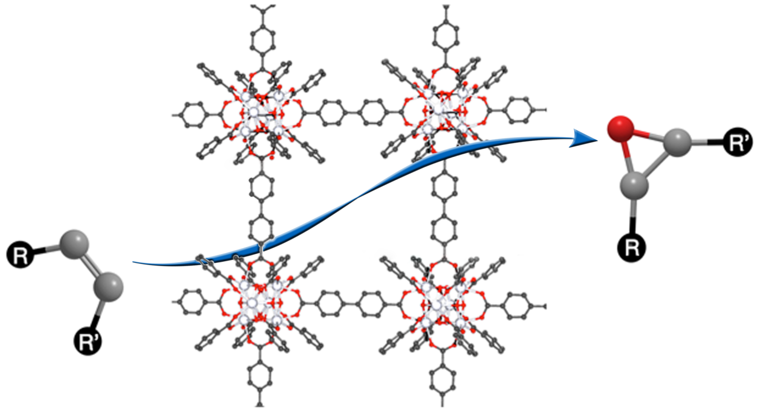

Results and Discussion

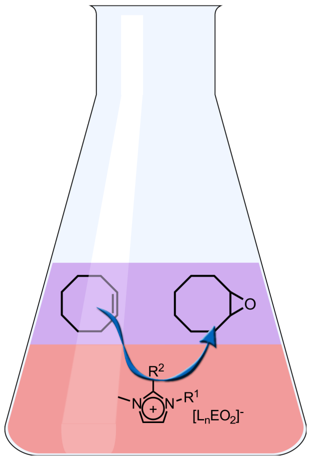
O
R^2
N
+
N
-R^1
[L$_n$EO$_2$]$^-$

7 Immobilization of a Molecular Epoxidation Catalyst on UiO-type MOFs

7.1 Synthesis

The syntheses of the precursors of UiO-67[141,142] and -68[99] containing amino groups have been reported in literature and were, for the most part, performed accordingly. Preparation procedures of the frameworks were also reported before.[96] However, slight adjustments to both literature procedures were made to obtain the materials in sufficient yields and high crystallinity.

7.1.1 Linker Preparation

The synthesis of 2-aminobiphenyl-4,4'-dicarboxylic acid was described by Telfer and co-workers in 2010.[142] Starting from dimethyl biphenyl-4,4'-dicarboxylate a three-step synthesis route was used as shown in Scheme 7.1.

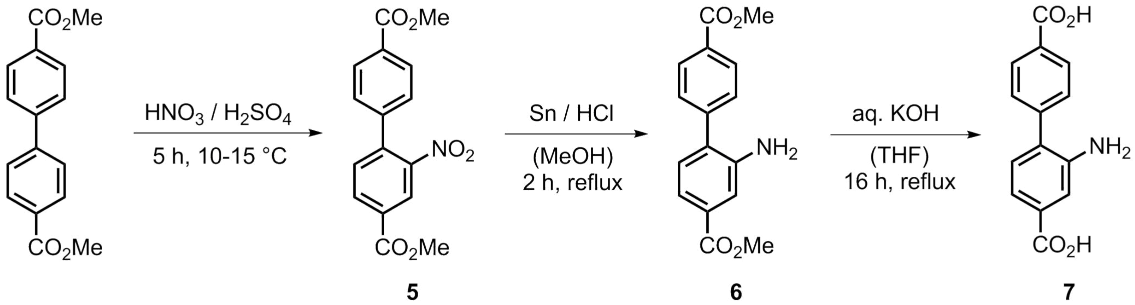

Scheme 7.1: Synthesis steps for the preparation of 2-aminobiphenyl-4,4'-dicarboxylic acid.

First, dimethyl biphenyl-4,4'-dicarboxylate was converted to dimethyl-2-nitrobiphenyl-4,4'-dicarboxylate (**5**) using nitrosulfuric acid. This step is slightly altered from the procedure described in literature by Olkhovik et al.[141] To optimize purity and yield of the reaction the reaction time had to be prolonged to 5 h. Additionally, the resulting product was recrystallized in a mixture of isopropanol and acetone. In the second step the nitro moiety of **5** was reduced with tin and hydrochloric acid to an amino group. The crude product was purified by flash chromatography, since the reported recrystallization[142] did not yield the pure dimethyl-2-aminobiphenyl-4,4'-dicarboxylate (**6**). To obtain 2-aminobiphenyl-4,4'-dicarboxylic acid (**7**) necessary for MOF formation deprotection was achieved by reacting **6** with aqueous potassium hydroxide in tetrahydrofuran (THF).[142]

The organic linker molecule for UiO-68 with amino-functionalization, 2'-amino-1,1':4',1"-terphenyl-4,4"-dicarboxylic acid (**9**), was previously reported by Behrens and co-workers.[99] Two equiv. of 4-(methoxycarbonyl)phenylboronic acid are cross-coupled with 2,5-dibromoaniline (Scheme 7.2) and subsequently deprotected. The previously reported yields are given as 91 % of dimethyl 2'-amino-1,1':4',1"-terphenyl-4,4"-dicarboxylate (**8**), but the product contained trace amounts of an unidentified by-product. The reaction was therefore optimized by prolonging the reaction time to 24 h, since after the reported time of 17 h the starting material could still be found in ^{1}H NMR spectra. Furthermore, the purification via column chromatography was improved by using a different solvent ratio (CH_2Cl_2:Et_2O = 25:1 instead of 50:1). With these changes yields of 70% were obtained with no by-products whatsoever. The deprotection was carried out as described above for **7** using ethanol instead of THF, since higher yields (98 %) could be obtained by changing the solvent.

1,1':4',1"-terphenyl-4,4"-dicarboxylate (**10**) was synthesized in a similar fashion using 1,4-dibromobenzene as starting material. Longer reaction times of four days were necessary to complete the reaction and the solvent system for the column chromatography had to be changed to ethylacetate/hexane (2:1). For the Suzuki cross-coupling a yield of 72 % was reached, but the deprotection step only resulted in 42 % of 1,1':4',1"-terphenyl-4,4"-dicarboxylic acid (**11**).

All prepared linker molecules were characterized by ^{1}H- and ^{13}C-NMR measurements. The results matched the ones described in literature (for details see experimental part).

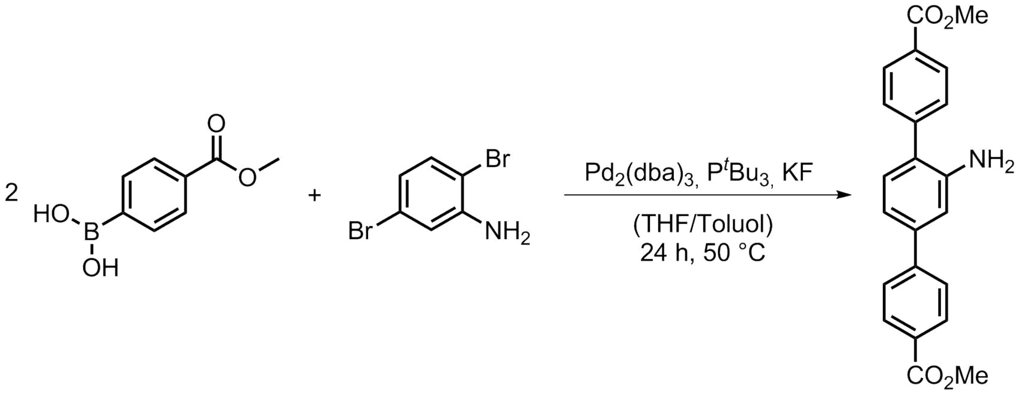

8

Scheme 7.2: Synthesis of 2’-amino-1,1’:4’,1”-terphenyl-4,4”-dicarboxylic acid via Suzuki cross-coupling reaction.

7.1.2 Catalyst Preparation

A set of four UiO-type materials was synthesized, including the fully amino-functionalized UiOs, as well as mixed UiOs (see below for details). The synthetic method applied in this work is based on the preparation described by Lillerud et al. in 2010.[96] However, four equivalents of water had to be added to the reaction mixture to obtain a crystalline powder. Without addition of water the frameworks did not form or the reaction gave only amorphous materials. This effect has previously been described by Behrens et al.[99] The fully functionalized materials UiO-66-NH_2 and UiO-67-NH_2 were synthesized using zirconium(IV) chloride and the amino-containing linker molecules, 2-aminoterephthalic acid and 2-aminobiphenyl-4,4’-dicarboxylic acid, respectively. The starting materials were dissolved in N,N-dimethylformamide (DMF), heated to 80 ℃ for 12 h and then kept at 100 ℃ for an additional 24 h. (Scheme 7.3 for UiO-66-NH_2)

To obtain mixed frameworks, UiO-66 mixed and UiO-67 mixed, only 1/6 of the amino-linkers were used and combined with unfunctionalized analogues, terephthalic acid and 4,4’-dicarboxylic acid. Cohen and co-workers found this simple method to yield truly mixed materials over a conglomerate of two different MOFs.[143] The use of linkers with different lengths and decrease of functionalization gives access to materials with varying pore sizes, schematically depicted in Figure 7.1.

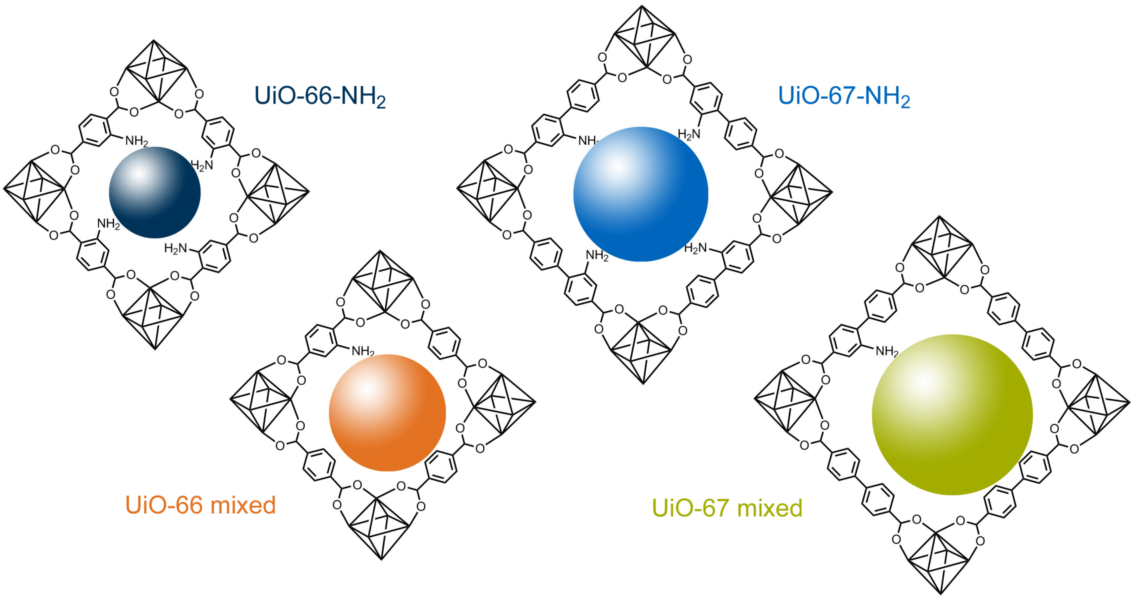

Figure 7.1: Schematic representation of accessible pore diameters in UiO-type MOFs.

Synthesis of UiO-68 mixed proved more difficult compared to the other UiO-type MOFs. The route described above only yielded amorphous materials, wherefore a modulated synthesis with benzoic acid[99] (30 equiv.) had to be applied. This method was also used for single crystal preparation of UiO-67-NH_2. 30 equiv. of benzoic acid were added to the standard reaction mixture for the MOF described above. The solution was then heated stepwise to 120 °C over the course of four days and left at that temperature for another 12 days.

In addition to the UiO-type MOFs, IRMOF-3 was synthesized as described by Cohen et al.[144] using $Zn(NO_3)_2 \cdot 4H_2O$ and 2-aminoterephthalic acid as starting materials.

The amino groups in all the dried MOF materials mentioned above were post-synthetically modified with salicylaldehyde to a salicylidene (SI) substituent as shown in Scheme 7.4. A vapor diffusion reaction was applied, previously reported by van Bokhoven et al.[100]

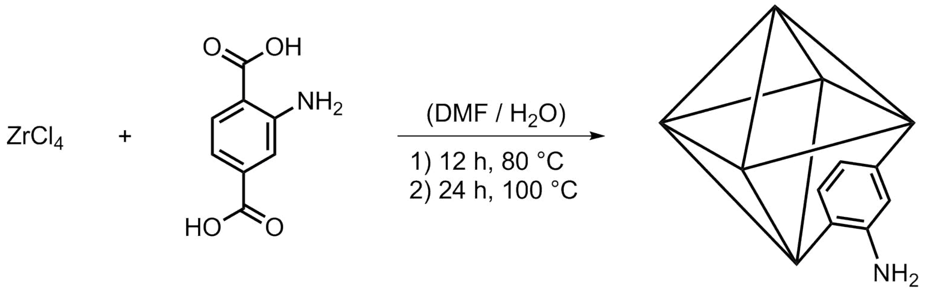

Scheme 7.3: Schematic representation of UiO-type MOF synthesis shown for UiO-66-NH_2.

The materials were placed on a filter paper, which was then transferred into a Schlenk tube containing salicylaldehyde (3 equiv.). The Schlenk tube, cooled with an ice bath to prevent evaporation of salicylaldehyde, was subsequently evacuated. After the pressure had stabilized the Schlenk tube was sealed and heated to 100 °C for 16 h. Afterwards the solids were transferred to a clean Schlenk tube and washed several times before drying. For the purification of UiO-type MOFs dry ethanol was used instead of the reported toluene in order to accelerate the drying process. Henceforth, the resulting materials are denoted as UiO-SI and IRMOF-3-SI.

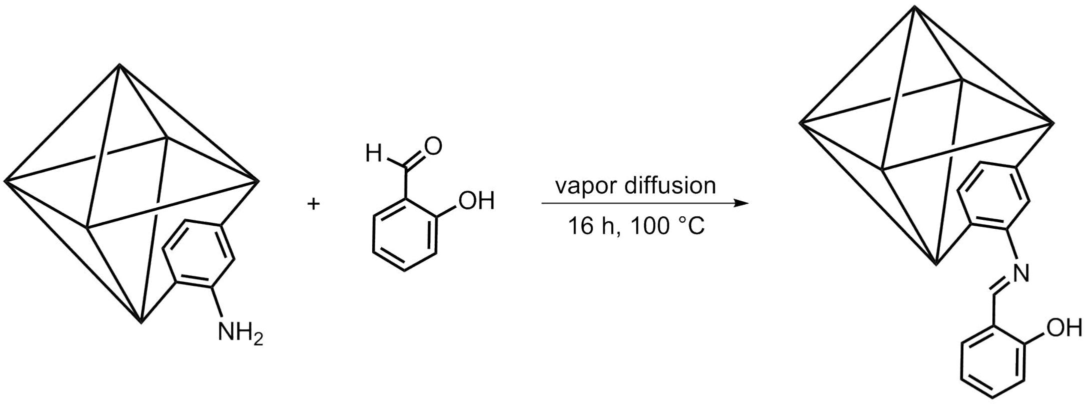

Scheme 7.4: Post-synthetic modification of UiO-type MOFs with salicylaldehyde.

In a second modification step bis(acetylacetonato)dioxomolybdenum(VI) was immobilized by a ligand exchange reaction (Scheme 7.5). The MOF-SI materials were placed in a Schlenk tube, which was subsequently flushed with argon. A solution of [$MoO_2(acac)_2$] in dry dichloromethane (DCM) was added and the mixture was kept at room temperature under exclusion of light for seven days. After the supernatant solution had been removed the remaining solid was washed with dry DCM until the solvent remained colorless. This was then dried under vacuum, yielding the Mo@MOF materials.

For UiO-67-SI mixed the optimal reaction time was investigated by determination of the molybdenum content in the material after 2 to 7 days. It was found that after 4 days the reaction was complete. However, this reaction time can only be applied to UiO-67-SI mixed, since the pore sizes of the materials and thereby the diffusion times of the reactants vary.

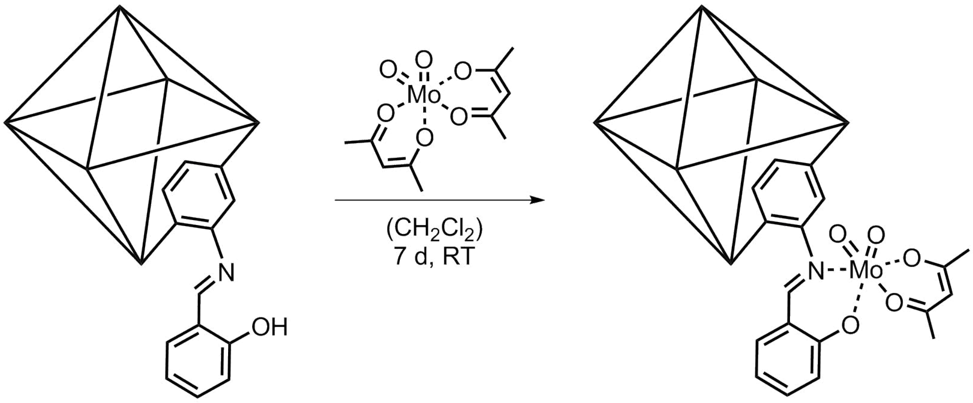

Scheme 7.5: Modification of UiO-SI MOFs with $MoO_2(acac)_2$.

Synthesis of the Schiff base ligand **13** for the preparation of the homogeneous complex [MoO_2(acac)(PhN=C-PhO)] (**14**) was reported by Bhaw-Luximon, Mapolie, and coworkers.[145] It was achieved by simple Schiff base condensation of salicylaldehyde with aniline at room temperature (Scheme 7.6).

Complex **14** was then prepared by Simone Hauser[146] similarly to the procedure reported for other *cis*-dioxidomolybdenum(VI) complexes with ligands derived from (+)-α-pinene.[147] A solution of molybdenum precursor [$MoO_2(acac)_2$] and an equimolar amount of ligand **13** was stirred at room temperature overnight (Scheme 7.7). Since the reaction gave a mixture of the desired compound **14**, the disubstituted complex [$MoO_2(PhN{=}C\text{-}PhO)_2$], and unreacted [$MoO_2(acac)_2$]

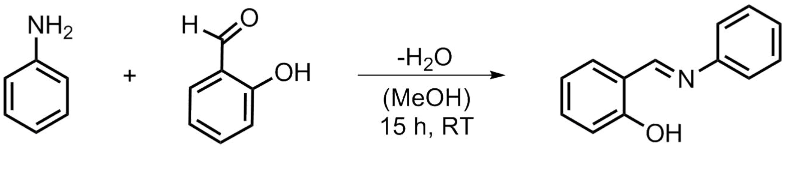

13

Scheme 7.6: Preparation of the Schiff base ligand PhN=C-PhO (**13**).

a solution in diethylether was left overnight to give single crystals of **14** in small amounts. These crystals were identified by ^1H and ^{13}C NMR spectroscopy and X-ray diffraction crystallography and then applied in catalysis.

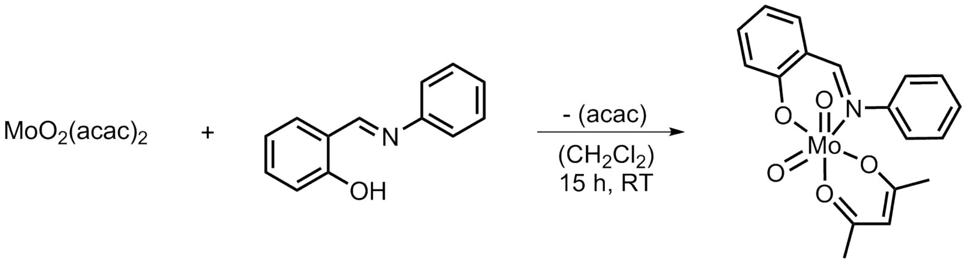

Scheme 7.7: Synthesis of $[MoO_2(acac)(PhN{=}C{-}PhO)]$ (**14**).

7.2 Characterization

7.2.1 Powder X-ray Diffraction

All synthesized MOFs were characterized by powder X-ray diffraction (PXRD) measurements to confirm formation of the correct framework as well as crystallinity of the materials.

The resulting diffractograms for the UiO-66 and -67 MOFs are shown in Figure 7.2. The patterns are similar to previous reports, showing that the UiO-type structure is formed.[96,99] Figure 7.2 shows patterns of the unfunctionalized UiO materials (a), after functionalization with salicylaldehyde (b) and $[MoO_2(acac)_2]$ (c). The fourth pattern displayed was recorded after catalysis, suggesting that the framework is still intact and stable towards oxidative conditions (see chapter 7.3).

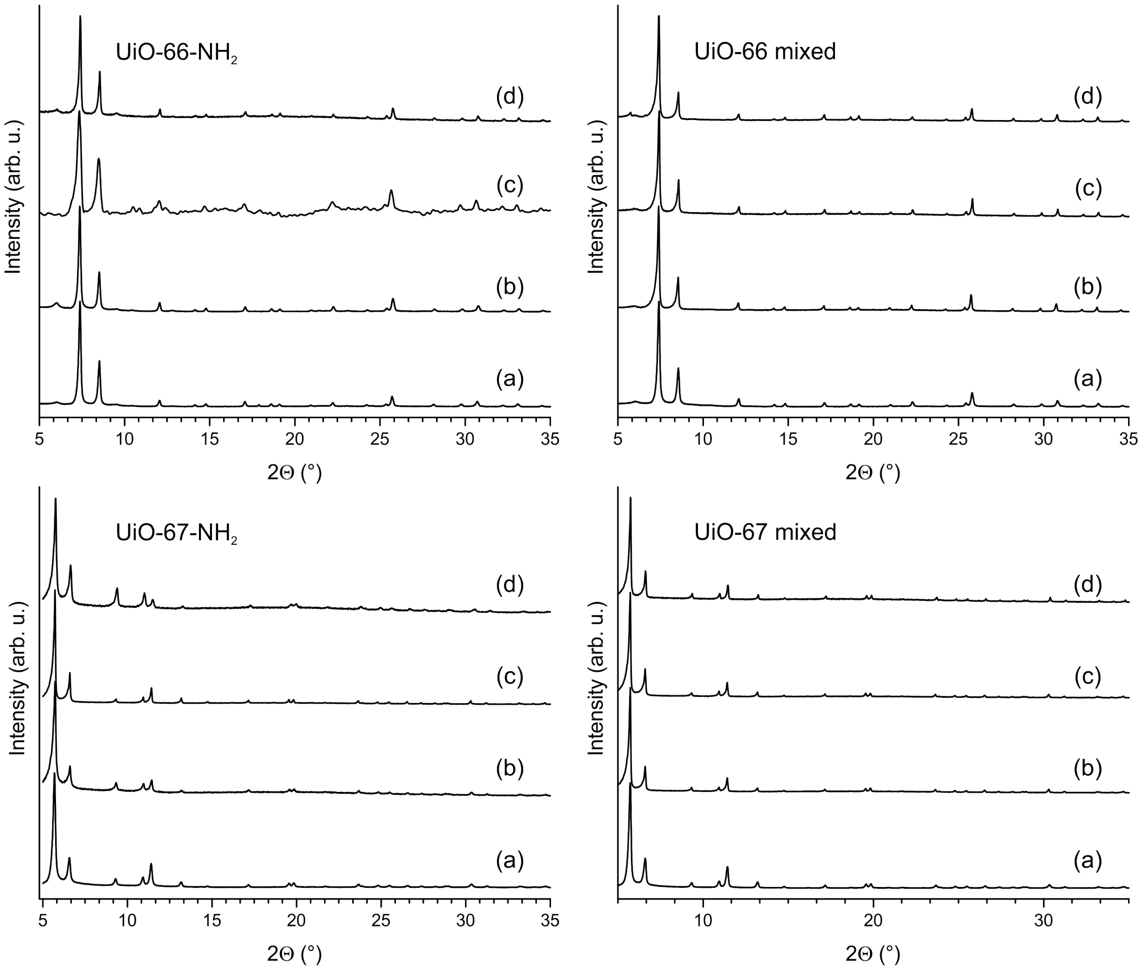

Figure 7.2: PXRD patterns of (a) UiO, (b) UiO-SI, (c) Mo@UiO and (d) Mo@UiO after catalysis.

For UiO-68 mixed the patterns of the unfunctionalized MOF were comparable to the literature, but the framework decomposed during modification showing only amorphous material for Mo@UiO-68 mixed (Figure 7.3).

Figure 7.4 shows that the IRMOF-3 framework was also formed and that the first modification step had had no influence on the crystallinity of the MOF. However, the framework exhibited a decrease in crystallinity after immobilization, which becomes apparent as a significant rise in PXRD background (see Fig. 7.4c). The diffractogram after catalysis in turn shows complete decomposition of the material under oxidative conditions.

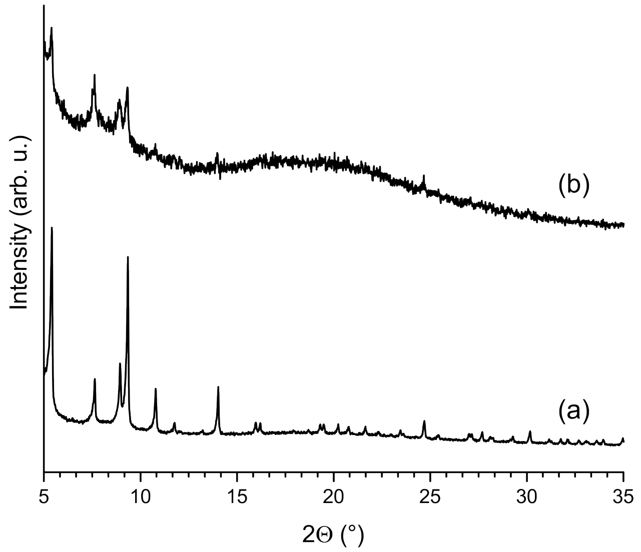

Figure 7.3: PXRD patterns of (a) UiO-68 and (b) Mo@UiO-68.

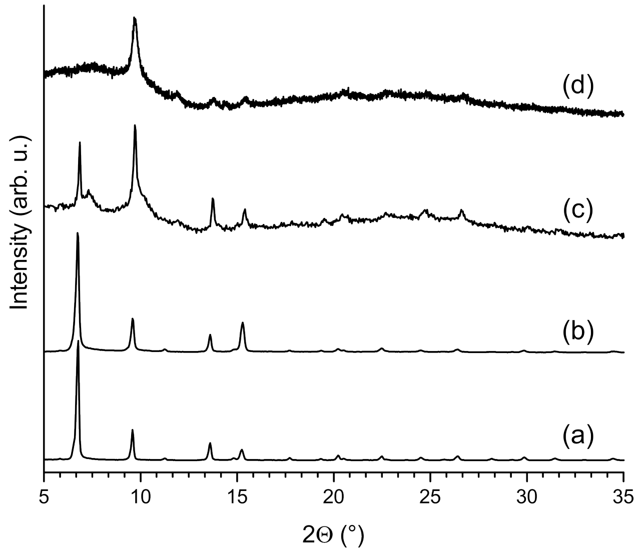

Figure 7.4: PXRD patterns of (a) IRMOF-3, (b) IRMOF-3-SI, (c) Mo@IRMOF-3 and (d) Mo@IRMOF-3 after catalysis.

7.2.2 Solid-State ^{13}C-MAS-NMR

Solid-state ^{13}C-MAS-NMR spectra of the pure UiO and Mo@UiO materials were recorded. The obtained spectra of the UiO-67 mixed series are shown exemplarily in Figure 7.5. The spectral data for the other MOF materials is summarized in the experimental part. The peaks of the amino functionalized linker have very low intensities and are therefore overlapped by the intense signals of the unfunctionalized linker. For the same reason the only signal visible appertaining to the immobilized molybdenum complex stems from the two methyl groups of the acetylacetonate ligand.

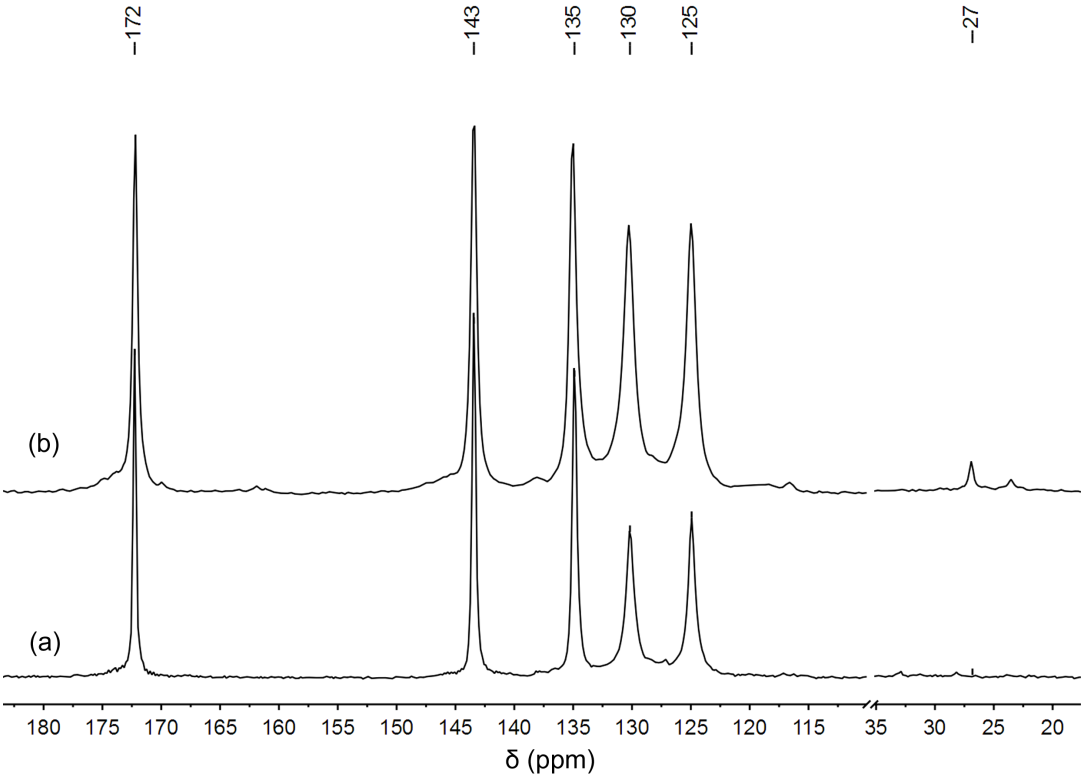

Figure 7.5: ^{13}C-MAS-NMR spectra of (a) UiO-67 mixed and (b) Mo@UiO-67 mixed.

7.2.3 Specific Surface Area Determination from N_2 Adsorption Measurements

For the fully functionalized UiO-67-NH_2 specific surface areas of 1800 m^2g^{-1} have been reported.[148] To compare the mixed counterpart, specific surface areas of UiO-67 mixed and Mo@UiO-67 mixed were determined by the Brunauer, Emmett and Teller (BET) method of adsorption of nitrogen gas. The adsorption isotherms used for surface area calculations are shown in Figure 7.6. A surface area of 2200 m^2g^{-1} was found for the unfunctionalized UiO-67 mixed, clearly showing the effect of reduced amino-group content in the framework on pore sizes. In Mo@UiO-67 mixed the surface area of 2000 m^2g^{-1} is still higher than in UiO-

67-NH_2. This result suggests that the pores of the MOF are not obstructed by immobilization of the complex.

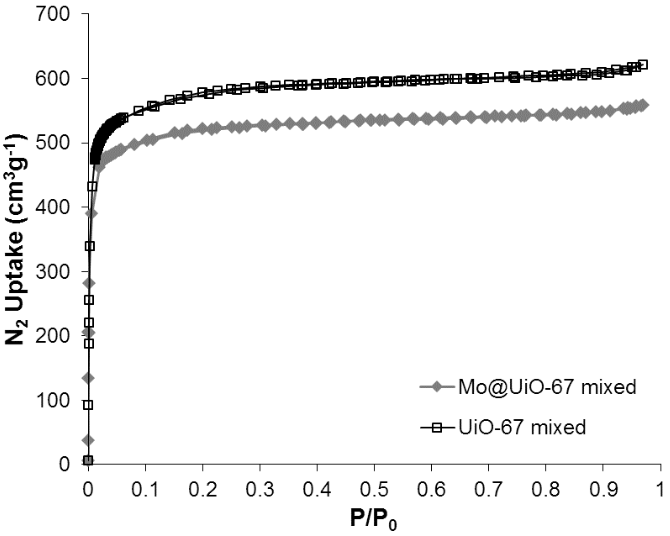

Figure 7.6: N_2 adsorption isotherms of UiO-67 mixed and Mo@UiO-67 mixed.

7.2.4 X-ray Photoelectron Spectroscopy

The oxidation state of the immobilized molybdenum species can be determined by X-ray photoelectron spectroscopy (XPS). In Figure 7.7 the area of the resulting XPS spectrum pertaining to the molybdenum 3d region is shown. Two peaks are clearly visible, one at 232.8 eV and one at 236.0 eV, the peak splitting arising from spin-orbit interactions. The value of the binding energy splitting (3.2 eV) and the relative peak intensities (59:41) match the data for molybdenum(VI) described in literature.[93] Thus, the catalyst's oxidation state is not influenced by immobilization to the framework.

7.2.5 Single Crystal X-ray Diffraction (SC-XRD)

The single crystal structure of UiO-67-NH_2 (Figure 7.8) was determined by SC-XRD of a crystal obtained by the modulated synthesis described above. UiO-67-NH_2 crystallizes in the $Fm\bar{3}m$ space group and shows the same expanded cubic closed packed topology as described for the unfunctionalized analogue.[84]

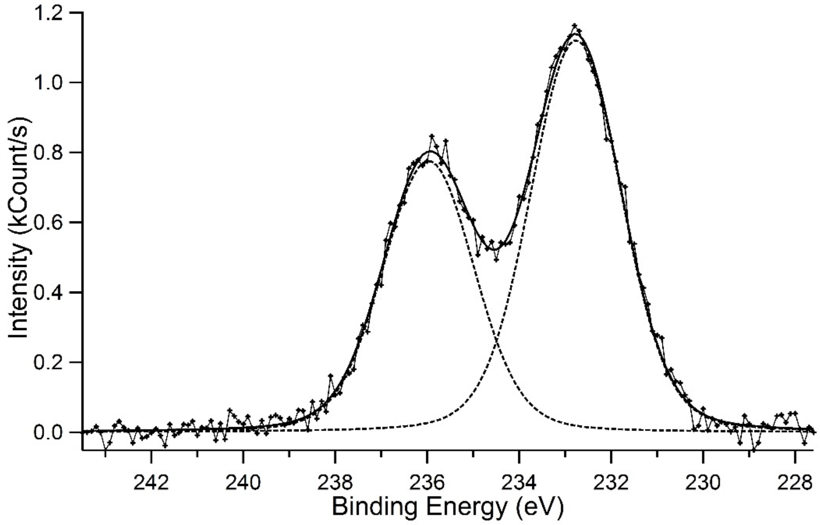

Figure 7.7: Mo 3d XPS line with binding energies of 232.8 and 236.0 eV for the Mo 3d5/2 and 3d3/2 levels, respectively.

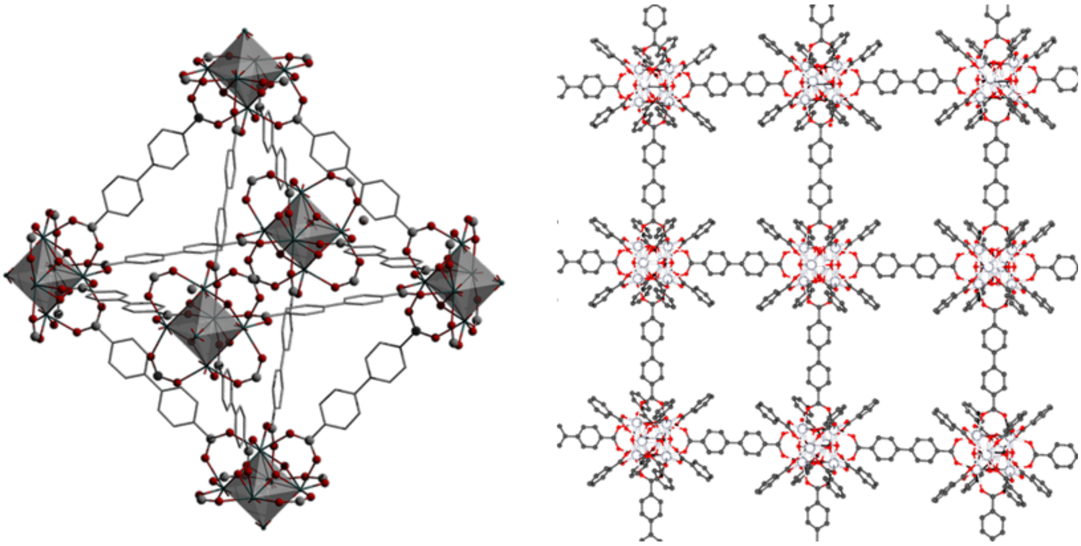

Figure 7.8: X-ray single crystal structure of UiO-67-NH_2 (Amino groups and hydrogen atoms are omitted for clarity).

Even though the measurements were performed at -123 °C the benzene rings are distorted, thus showing large displacement parameters perpendicular to their ring plane (Figure 7.9). Since the amino groups have a statistical probability of being bound at four different positions (two on each benzene ring), the distortion of the rings enables eight possible positions. The remaining single crystals were

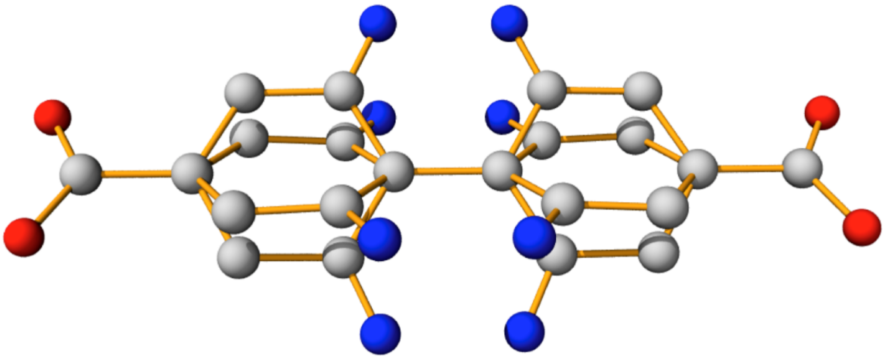

Figure 7.9: Disorder of aromatic rings in UiO-67-NH_2 (H atoms omitted for clarity).

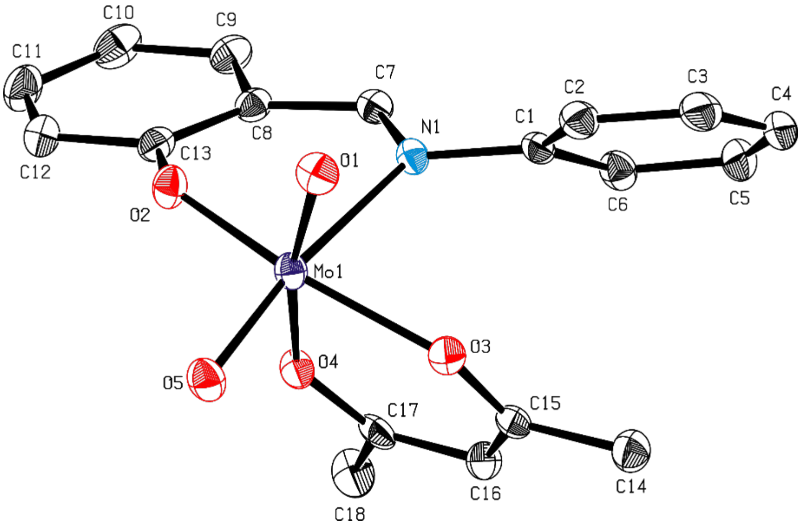

Figure 7.10: ORTEP style drawing of [MoO_2(acac)(PhN=C-PhO)] (**14**) in the solid state. Thermal ellipsoids are drawn at the 50 % probability level. Selected bond lengths (Å) and bond angles (°): Mo1–O1 1.703(1), Mo1–O2 1.920(1), Mo1–O3 2.016(1), Mo1–O4 2.181(1), Mo1–O5 1.712(1), Mo1–N1 2.358(1); O1–Mo1–O2 100.03(6), O1–Mo1–O3 93.53(5), O1–Mo1–O5 104.34(6), O2–Mo1–O4 81.02(5), O2–Mo1–O5 99.71(6), O3–Mo1–O4 80.72(5), O3–Mo1–O5 95.51(5), O1–Mo1–N1 89.37(6), O2–Mo1–N1 80.94(5), O3–Mo1–N1 79.94(5).

subjected to the post synthetic method with salicylaldehyde as used for the UiO powders. A color change was observed, indicating the formation of the imine moiety. However, the XRD measurements did not differ from the unmodified crystals. The residual electron densities in the pores could not be reasonably assigned to the salicylidene groups of the linker or to guest molecules due to the aforementioned distortion and statistical distribution of binding sites.

To confirm the structure of the homogeneous molybdenum compound prepared for comparisons of catalytic activity, single crystals obtained during the synthesis procedure were measured. Figure 7.10 shows that the Schiff base complex was formed, wherein the molybdenum atom is coordinated in an octahedral shape by two terminal oxo-oxygen atoms in a *cis*-arrangement, one imino nitrogen and three oxygen atoms from the ligand molecules (two from the acetylacetonato, one from the Schiff base ligand). Observed values of the Mo=O distances (1.703 and 1.712 Å) and the O=Mo=O angle (104.3°) are in the usual range for *cis*-MoO_2-complexes.

7.2.6 Elemental Analysis

The molybdenum content of all Mo@MOF materials used for catalysis was determined by elemental analysis. C, H and N elemental analyses were different for every batch of MOF as different amounts of solvent remained in the pores. The molybdenum values for the MOF series used for the recycling experiments are listed in Table 7.1, since it is of great importance to know the exact amount of catalyst in the system.

Table 7.1: Molybdenum content found by elemental analysis for all Mo@MOFs.

MOF	**Mo calculated[a] (%)**	**Mo found (%)**
Mo@UiO-66	15.41	8.48
Mo@UiO-66 mixed	4.60	5.69
Mo@UiO-67	13.74	3.23
Mo@UiO-67 mixed	3.78	2.43
Mo@IRMOF-3	3.22	3.02

[a] Mo values calculated for complete modification of all possible sites in the MOFs

7.3 Catalytic Epoxidation of Olefins and Recycling

All synthesized and fully characterized Mo@MOF materials were tested in the catalytic epoxidation of *cis*-cyclooctene with *tert*-butyl hydroperoxide (TBHP, 5.5 M in decane) at 50 ℃ (Scheme 7.8). The reactions were carried out under inert gas conditions without additional solvent (neat). The catalyst with the highest activity towards epoxidation of *cis*-cyclooctene (Mo@UiO-67 mixed) at the above mentioned conditions was used at room temperature and tested with the more sophisticated substrates 1-octene and styrene.

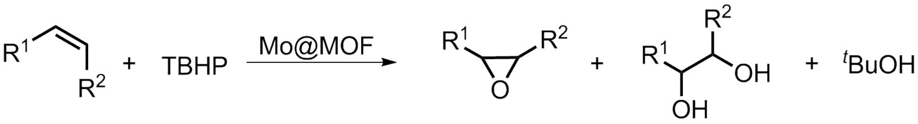

Scheme 7.8: Epoxidation of olefins with Mo@MOF catalysts and TBHP as oxidant.

The results are summarized in Table 7.2. The conversion of *cis*-cyclooctene shows a strong dependence on the pore size of the applied materials (Table 7.2, entries 1-4), whereas the selectivity is very high in all cases. At lower temperatures the conversion drops significantly (Table 7.2, entry 6).

IRMOF-3 was not further investigated after the first catalysis run, as PXRD measurements showed a complete decomposition of the material (Fig. 7.4). Therefore, this framework seems not suitable as support for catalysts in oxidation catalysis.

Kinetic studies were performed using Mo@UiO-67 mixed (1 mol%) at 50 ℃ and the homogeneous analogue [MoO_2(acac)(PhN=C-PhO)] (**14**, 1 mol%) at room temperature as catalysts (Figure 7.11). The turnover frequency (TOF) for the MOF was calculated after 15 minutes and found to be 130 h^{-1}, whereas with **14** after 5 min. TOFs of 870 h^{-1} were reached. The decrease in activity of the immobilized complex can be attributed to the intrinsic diffusion limitations of the MOF framework.

To ensure that the observed catalytic activity is actually due to the immobilized complex, UiO-67-SI mixed was tested in the same reaction. A conversion

Table 7.2: Epoxidation of olefins with different catalysts.

Entry	Catalyst	Substrate	Conv. (%)	Sel.[c] (%)
1	Mo@UiO-66[a]	*cis*-Cyclooctene	63	100
2	Mo@UiO-66 mixed[a]	*cis*-Cyclooctene	94	100
3	Mo@UiO-67[a]	*cis*-Cyclooctene	100	100
4	Mo@UiO-67 mixed[a]	*cis*-Cyclooctene	100	100
5	Mo@IRMOF-3[b]	*cis*-Cyclooctene	66	100
6	Mo@UiO-67 mixed[b]	*cis*-Cyclooctene	66	100
7	Mo@UiO-67 mixed[a]	1-Octene	62	70
8	Mo@UiO-67 mixed[a]	Styrene	38	68

[a] Reaction conditions: 1 mol % catalyst, 150 mol % TBHP, 50 ℃, 4 h,

[b] Reaction conditions: 1 mol % catalyst, 150 mol % TBHP, 25 ℃, 24 h,

[c] Selectivity to epoxide.

of 8 % was reached, which corresponds to the conversion of substrate and oxidant without catalyst, therefore clearly showing the necessity of the molybdenum species.

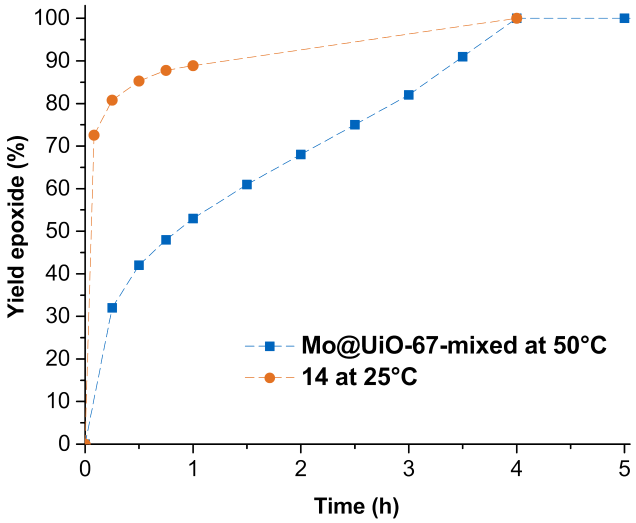

Figure 7.11: Plot of yield versus time in the oxidation of cyclooctene with TBHP and 1 mol % of Mo@UiO-67-mixed at 50 ℃ and [MoO_2(acac)(PhN=C-PhO)] (**14**) at room temperature.

The stability of the complex after immobilization was tested by leaching experiments with Mo@UiO-67. After a conversion of 50 % the catalyst was removed by filtration and the reaction mixture was kept at 50 ℃ for an additional 3 h. An increase in cyclooctene oxide of 12 % was observed (Figure 7.12), which is similar to a conversion of *cis*-cyclooctene without catalyst. These results suggest that no molybdenum species is leaching from the MOF into the reaction mixture.

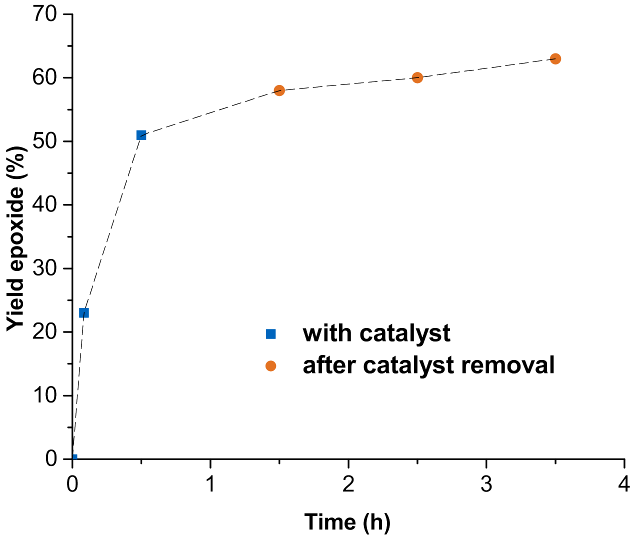

Figure 7.12: Leaching experiment with Mo@UiO-67.

Furthermore, the UiO-type catalysts were investigated for their recycling properties in a series of ten subsequent catalytic runs with *cis*-cyclooctene being the model substrate. After four hours, when one catalytic cycle was completed, the remaining solution was removed, the MOF was washed with dichloromethane (DCM) and dried in vacuum overnight. For the first three runs drying was performed at room temperature. Since a significant decrease in activity of all frameworks but Mo@UiO-67 mixed was observed, the drying temperature was increased to 150 ℃. Figure 7.13 shows the strong dependence of recycling on the pore size of the MOF system used. While the Mo@UiO-66 frameworks show a significant loss in activity even when drying at 150 ℃, the Mo@UiO-67 materials exhibited very high conversions in all ten runs. Mo@UiO-67 benefited from the work up procedure at higher temperatures, whereas Mo@UiO-67 mixed could even be recycled at room temperature. PXRD patterns after all catalytic runs show that all frameworks remain intact (Figure 7.2). The decrease in activity therefore is attributed to blockage of the pores and not to a decomposition of the frameworks. Especially in the UiO-66 systems reactants and products cannot easily be removed, even at elevated temperatures, most probably due to diffusion limitations arising from the small pore size.

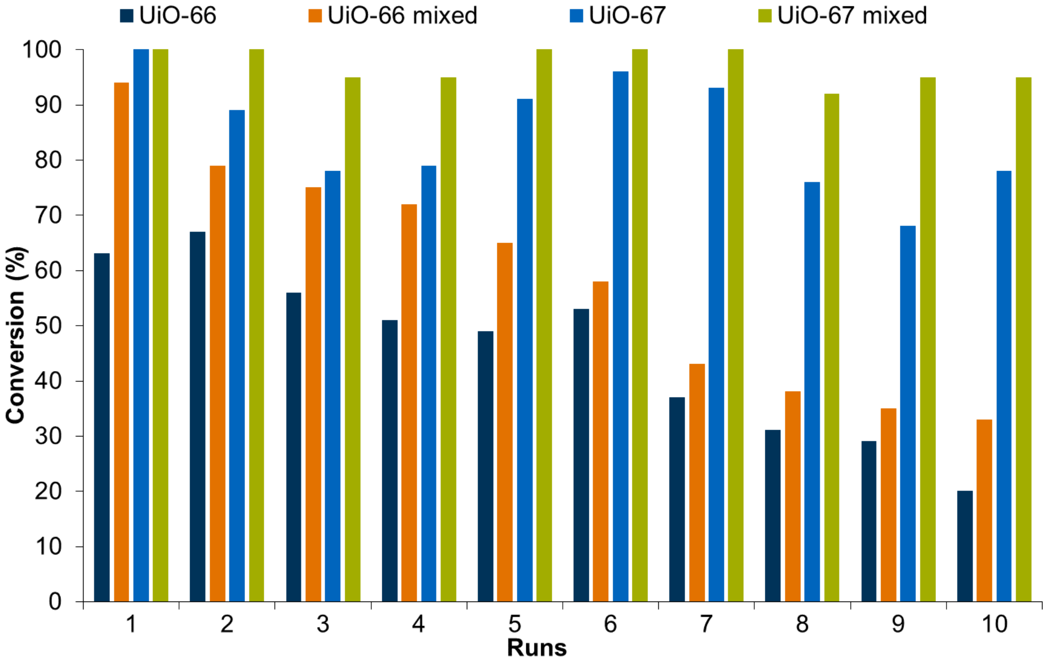

Figure 7.13: Recycling of the different modified MOF catalysts in epoxidation reaction with *cis*-cyclooctene.

While the selectivity for cyclooctene oxide is 100 %, diol formation is observed when more demanding substrates, like 1-octene and styrene, are oxidized (Table 7.2, entries 7 and 8). This is most probably due to the Lewis acidic character of the UiO-type MOFs in combination with OH groups situated on the inorganic building units. Both of these attributes facilitate diol formation from less stable epoxides. It has been reported that the OH groups may be removed by tempering of the MOF.[84] Therefore, UiO-67 mixed was heated to 300 °C for two days prior to modification with salicylaldehyde and [$MoO_2(acac)_2$]. This dehydrated Mo@UiO-67 mixed was applied in catalysis with 1-octene as substrate. The selectivity towards 1,2-epoxyoctane was thus increased to 100 %, but conversion dropped drastically to 13 %. This activity decrease was attributed to the fact that *tert*-

butanol and TBHP can coordinate to the free coordination sites on the zirconium cluster. Thereby, the pore size is lowered substantially, inhibiting further reaction of the substrate with the catalyst. This hypothesis was investigated further by reacting the dehydrated Mo@UiO-67 mixed with *tert*-butanol prior to application in epoxidation. In fact this reaction only yielded minimal amounts of epoxide, which corroborates the theory of coordinated *tert*-butanol limiting substrate and oxidant diffusion and thereby reducing the conversion.

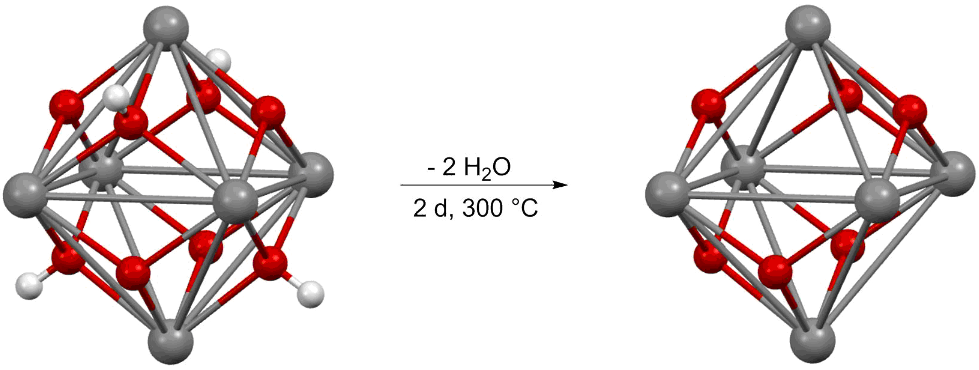

Scheme 7.9: Removal of OH groups on Zr clusters by tempering.

Epoxidation of propylene with Mo@UiO-67 mixed was also attempted. A Fisher-Porter tube was loaded with catalyst and TBHP, sealed, flushed with Argon and then charged with 3 bar of propylene. According to the pressure drop of 0.83 bar over 24 hours a conversion of 27 % could be reached. However, selectivity determinations via NMR were impossible due to formation of side products, since the proton signals could not be distinguished clearly.

8 Epoxidation of Olefins using Perrhenate Containing Ionic Liquids

8.1 Synthesis

8.1.1 Preparation of Imidazolium Halides

Procedures for the synthesis of imidazolium bromides and iodides (see below for details) have previously been reported in various works and were synthesized accordingly.[149–154] Scheme 8.1 shows the general procedure used for the imidazolium bromides with protons or methyl groups in C2-position (**16a**-**18a** and **20a**-**22a**). 1-methyl- or 1,2-dimethylimidazole was dissolved in toluene or tetrahydrofuran (THF) and a slight excess of the respective alkyl bromide was added. After a reaction time of 24 hours the remaining solvents were evaporated. The crude products were washed with diethylether, ethylacetate or hexane. To obtain 1,3-dimethyl- (**15a**) and 1,2,3-trimethylimidazolium iodides (**19a**) a similar reaction was performed with methyl iodide as starting material at room temperature instead of reflux conditions. Purity of the compounds was determined with ^{1}H- and ^{13}C-NMR spectroscopy as well as with elemental analysis.

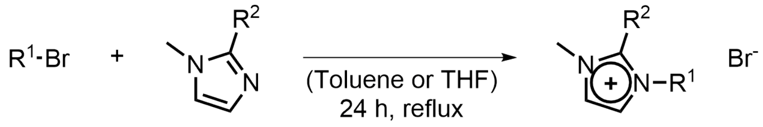

R^1 = Bu; R^2 = H (**16a**), Me (**20a**)
R^1 = Oc; R^2 = H (**17a**), Me (**21a**)
R^1 = Do; R^2 = H (**18a**), Me (**22a**)

Scheme 8.1: General synthesis of imidazolium bromides **16a**-**18a** and **20a**-**22a** (Me = methyl, Bu = *n*-butyl, Oc = *n*-octyl, Do = *n*-dodecyl).

1-Alkyl-2-butyl-3-methylimidazolium iodides (**23a**) as well as bromides (**24a**-**26a**) were prepared according to a synthesis route described by Ennis and Handy

(Scheme 8.2).[155] Previously prepared 1-alkyl-3-methylimidazolium halides were deprotonated using NaH. After four hours a fourfold excess of 1-iodobutane (for **23a**) or 1-bromobutane (for **24a**-**26a**) was added to the mixture. The workup procedure mentioned above was also applied for the obtained butylated imidazolium salts. All obtained products were characterized by means of ^{1}H-, ^{13}C-NMR spectroscopy, and elemental analysis. The previously unknown 2-butyl-1-dodecyl-3-methyl-imidazolium bromide (**26a**) was obtained with a high purity and moderate yield.

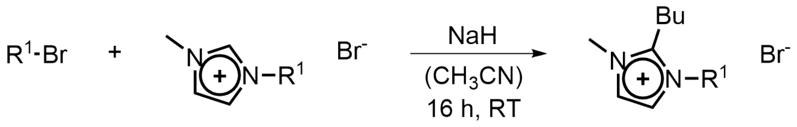

R^1 = Bu (**24a**), Oc (**25a**), Do (**26a**)

Scheme 8.2: General synthesis of 1-alkyl-2-butyl-3-methylimidazolium bromides **24a**-**26a** (Me = methyl, Bu = *n*-butyl, Oc = *n*-octyl, Do = *n*-dodecyl).

8.1.2 Preparation of Imidazolium Perrhenates

A simple route for the preparation of perrhenate containing ionic liquids described by Kühn and co-workers[137] was applied in this work. Bromides and iodides of the previously synthesized imidazolium halides were exchanged by hydroxide on an anion-exchange resin (AER). Subsequently, a slight excess of ammonium perrhenate (1.1 equiv.) was added to the aqueous solution and the mixture was stirred at 70 ℃ for 24 h (Scheme 8.3). The only side products, water and ammonia, can easily be removed in vacuo at elevated temperatures. The obtained oily or solid residues were dissolved in dichloromethane and filtered to remove excess of NH_4ReO_4. All compounds, except for **19b**, were received in high purities and yields (72-95 %). The low yield of 33 % for **19b** can be explained by the low solubility of the compound in dichloromethane. Therefore, large amounts of product were lost in the filtration step, even though the residue in the filter was washed thoroughly.

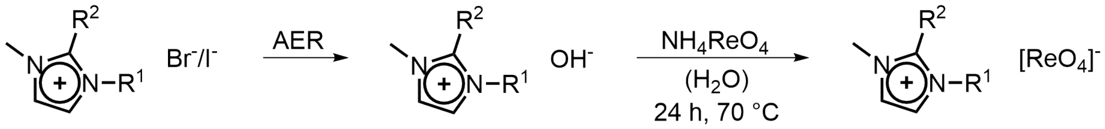
R^2
Br$^-$/I$^-$
AER
OH$^-$
NH$_4$ReO$_4$
(H$_2$O)
24 h, 70 °C
[ReO$_4$]$^-$
N–R^1

Scheme 8.3: Anion exchange procedure for all synthesized imidazolium bromides (AER = anion exchange resin).

A complete list of all synthesized imidazolium cations used in the perrhenate ILs is given in Figure 8.1.

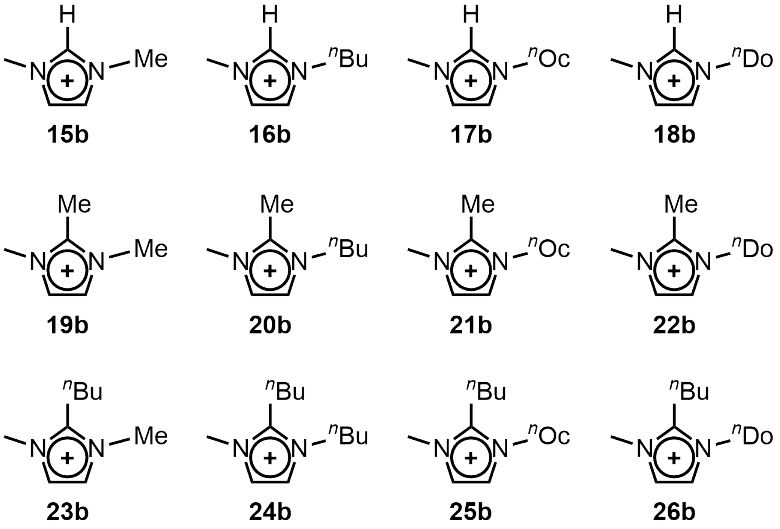
15b
16b
17b
18b
19b
20b
21b
22b
23b
24b
25b
26b
H
Me
^{n}Bu
^{n}Oc
^{n}Do

Figure 8.1: Illustration of imidazolium cations used in this study (Me = methyl, ^{n}Bu = *n*-butyl, ^{n}Oc = *n*-octyl, ^{n}Do = *n*-dodecyl) and numbering for the resulting perrhenates.

8.2 Characterization

All synthesized compounds were characterized by means of ^{1}H-, ^{13}C-NMR, IR spectroscopy, elemental analysis, and melting point determinations to confirm their purity. Results of the spectroscopic methods are discussed exemplarily for 1,2-dimethyl-3-octylimidazolium perrhenate (**17b**) in this chapter, full listings for all compounds can be found in the experimental part.

8.2.1 NMR Spectroscopy

To compare the spectra of a bromide with a perrhenate containing IL **17a** and **17b** were chosen as examples. In the ^{1}H-NMR spectra of the imidazolium salts the most prominent difference is the change in chemical shift of the C2 proton. The signal is shifted upfield from 10.40 ppm in the bromide salt (Figure 8.2) to 8.85 ppm in the case of imidazolium perrhenate (Figure 8.3), due to the change in chemical environment caused by the anion exchange. The perrhenate anion represents a stronger hydrogen bond acceptor compared to halides and withdraws electron density from the C2 proton to a greater degree. Most of the other signals are also shifted upfield, but to a much lower extent and the shift decreases the farther away the groups are from the imidazolium moiety, i.e. there is no difference observable for the CH_3-group of the octyl chain.

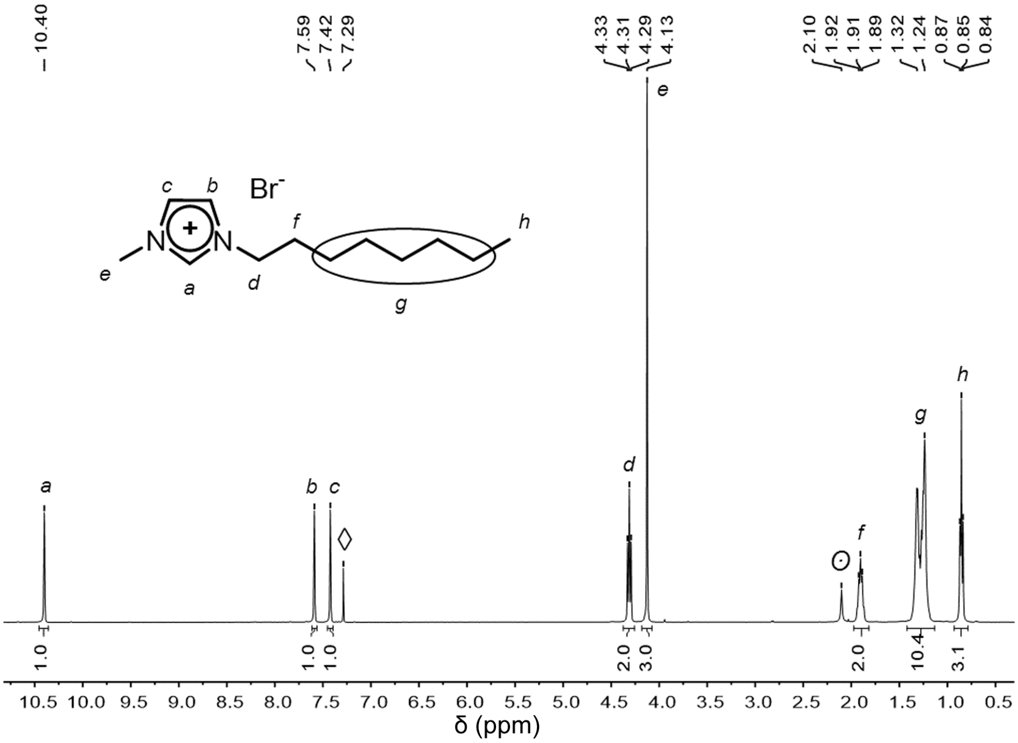

Figure 8.2: ^{1}H-NMR spectrum of **17a** (◇ = $CDCl_3$, ⊙ = H_2O).

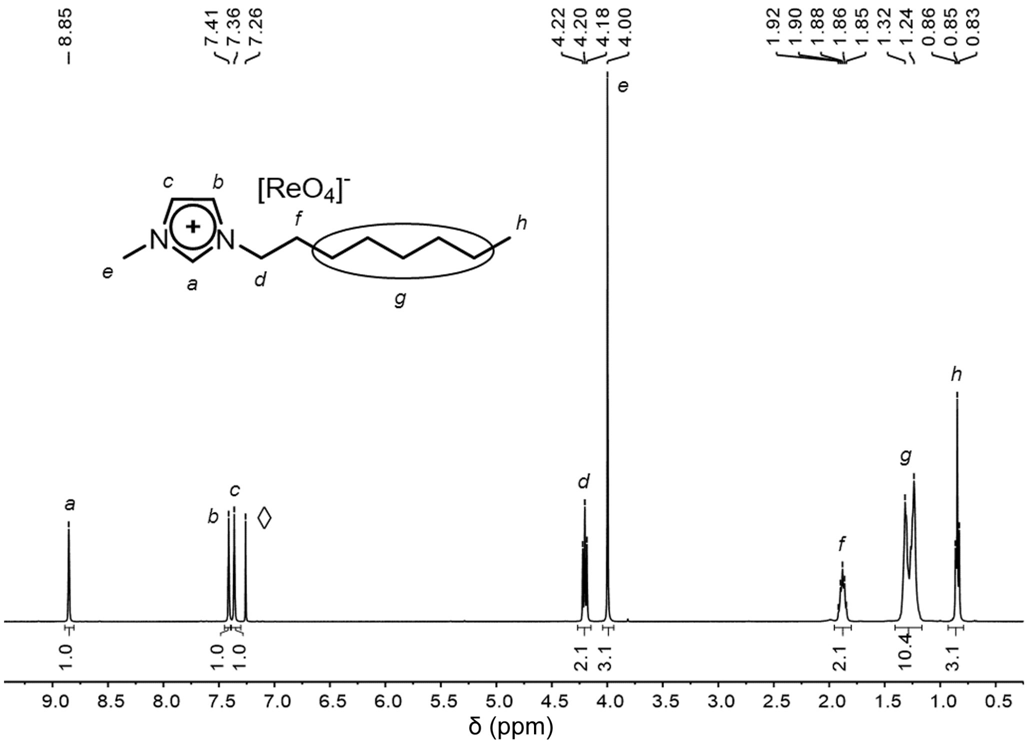

Figure 8.3: ^{1}H-NMR spectrum of **17b** (◊ = $CDCl_3$).

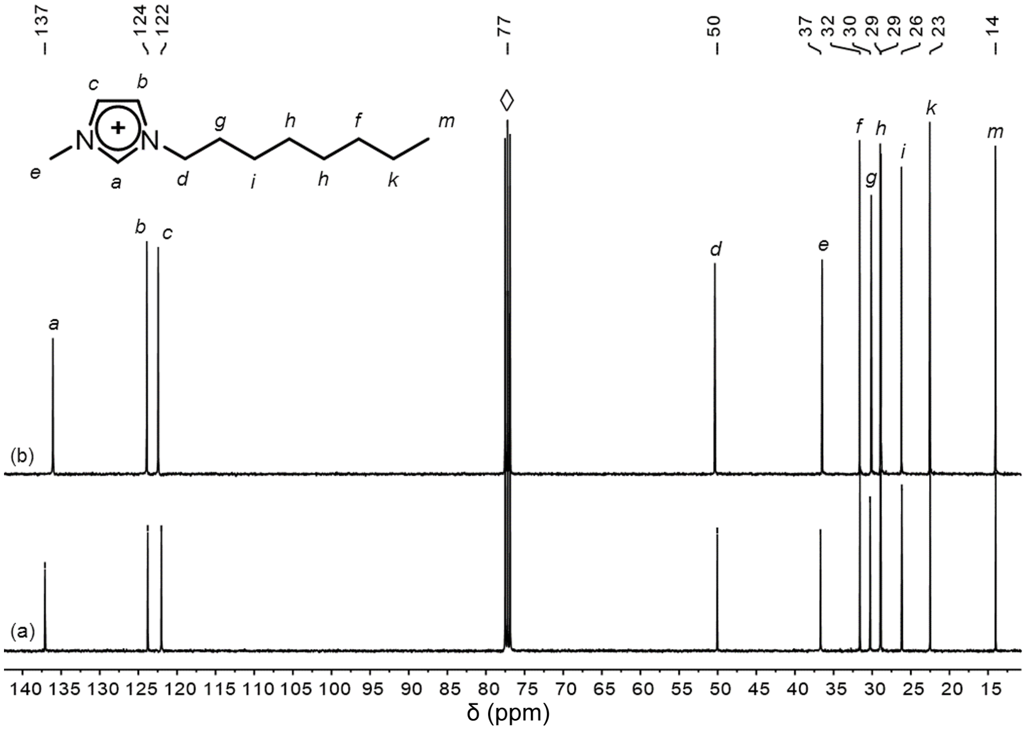

Figure 8.4: ^{13}C-NMR spectra of (a) **17a** and (b) **17b.**

The influence of the anion on the chemical shifts is much weaker in the ^{13}C spectra (Figure 8.4). Only very minor shifts of the imidazolium carbons ($<$1 ppm) can be observed.

8.2.2 IR Spectroscopy

IR spectra confirm the successful anion exchange, as the strong Re=O asymmetric stretching vibration can clearly be seen for all imidazolium perrhenates in the range from 890 to 905 cm^{-1}. Exemplarily, the IR spectrum of **17b** is shown in Figure 8.5 with the mentioned band marked at 895 cm^{-1}.

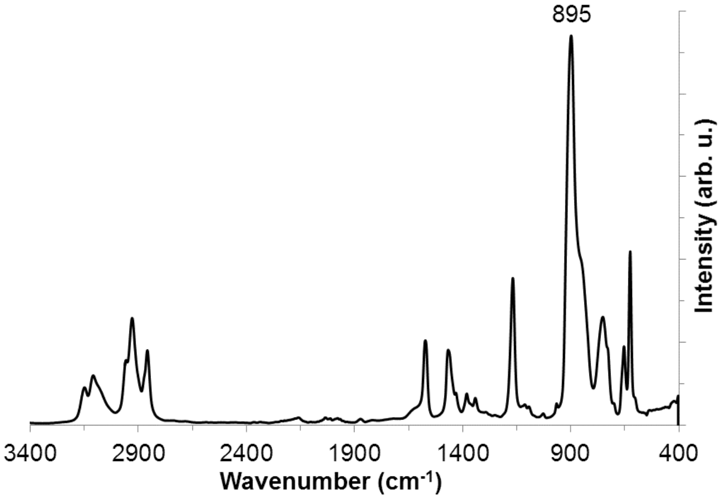

Figure 8.5: IR spectrum of **17b**.

8.3 Catalytic Epoxidation of Olefins

All prepared and fully characterized imidazolium perrhenates were tested in epoxidation catalysis using *cis*-cyclooctene as model substrate (Scheme 8.4). The reactions were carried out at 70 ℃ using aqueous H_2O_2 as oxidant. A catalyst loading of 5 mol% was used and the reaction was carried out without additional solvent (neat), since these conditions achieved the best results in previous studies by Christian Münchmeyer and Robert Reich.[156,157]

The results obtained with samples taken after 4 and 24 h are summarized in Table 8.1. To further investigate the activity of the catalysts depending on

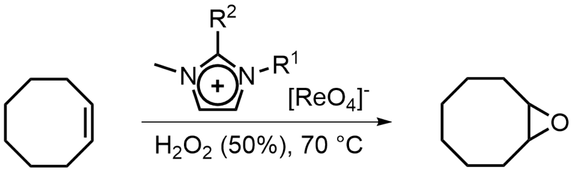

Scheme 8.4: Catalytic epoxidation of *cis*-cyclooctene with perrhenate containing ILs.

Table 8.1: Yield of cyclooctene oxide after 4 and 24h reaction time.

Entry	Catalyst	Yield after 4h (%)	Yield after 24h (%)
1	**15b**	3	22
2	**16b**	7	55
3	**17b**	44	98
4	**18b**	64	96
5	**19b**	4	60
6	**20b**	8	70
7	**21b**	88	100
8	**22b**	85	100
9	**23b**	5	59
10	**24b**	24	100
11	**25b**	21	34
12	**26b**	2	8

[a] Reaction conditions: 0.5 mmol catalyst (5 mol%), 10 mmol (100 mol%) *cis*-cyclooctene, 25 mmol (250 mol%) oxidant, 70 °C.

the substituents the cyclooctene oxide yield over time at the standard conditions mentioned above was analyzed. The resulting plots are shown in Figures 8.6 and 8.7.

Catalysts from imidazolium cations with unsubstituted C2 positions and short N-alkyl chains lead to low conversions even after 24 h (Table 8.1, entries 1 and 2). This may be attributed to the rather strong ion contacts (Imidazolium-H—$OReO_3$). However, substitution of the C2 proton with methyl or *n*-butyl groups to increase

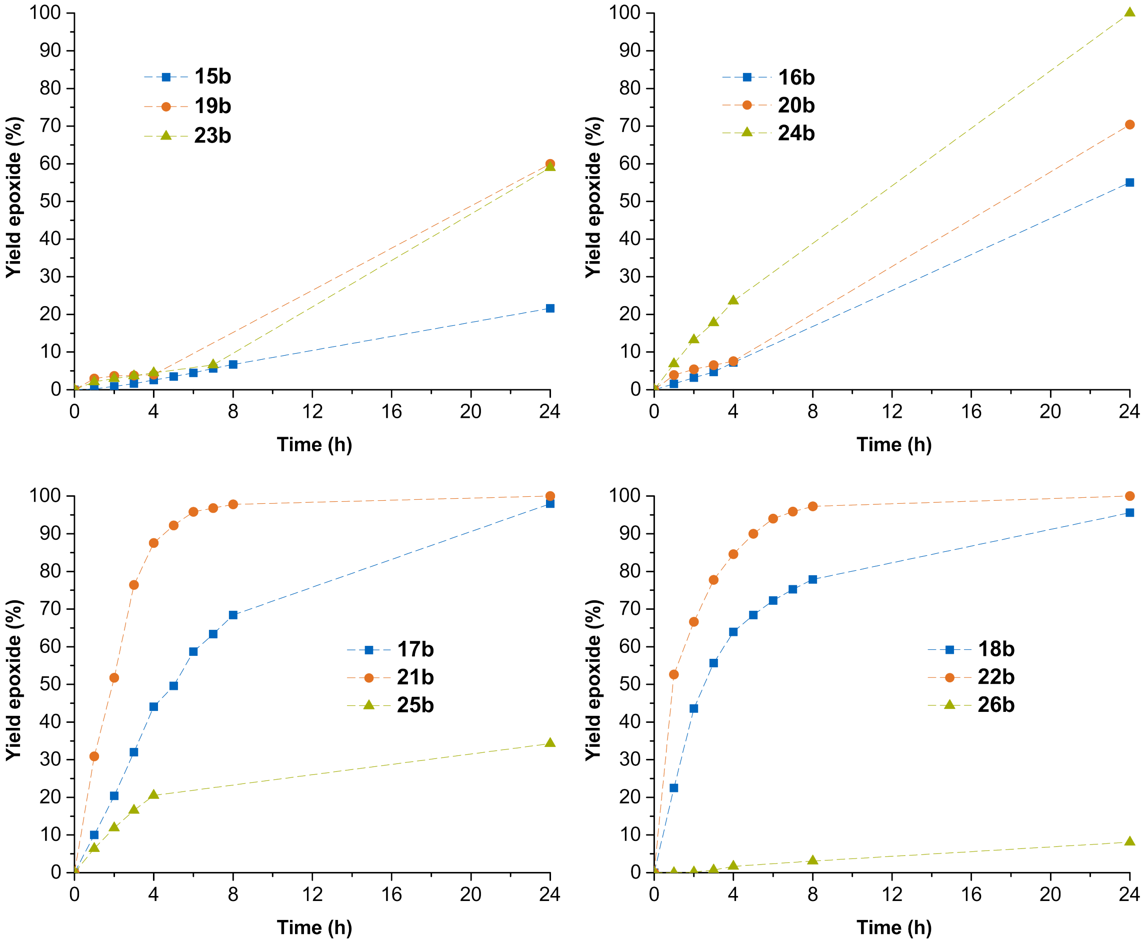

Figure 8.6: Comparison of the kinetic curves of imidazolium perrhenates with varying substituents in C2 position.

the activity is not particularly effective in these cases (Table 8.1, entries 5, 6 and 9 and Figure 8.6). Especially after the first 4 h conversion is virtually the same with substituted and unsubstituted imidazolium cations. This suggests that other factors than ion contact strengths are influencing the activity of the $[ReO_4]^-$ anion. Since *n*-octyl and *n*-dodecyl groups in N-position lead to higher activities (Table 8.1, entries 3 and 4 and Figure 8.7), hydrophobicity of the catalysts seems to be important. This hypotheses are supported by the fact that the catalysts bearing both a methyl group in C2 position as well as longer alkyl chains on the N-wingtip moiety exhibit the highest activities (Table 8.1, entries 8 and 9). The difference between *n*-octyl (**21b**) and *n*-dodecyl (**22b**) substituents, however, is minor, indicating sufficient hydrophobicity of the 1,2-dimethyl-3-octylimidazolium cation.

According to these suppositions introduction of *n*-butyl groups in C2 position should further decrease the ion contacts and increase hydrophobicity and therefore enhance the catalytic performance. On the contrary catalysts **25b** and **26b** (Table 8.1, entries 11 and 12 and Figure 8.6) show a tremendous decrease in activity compared to their methyl substituted analogues.

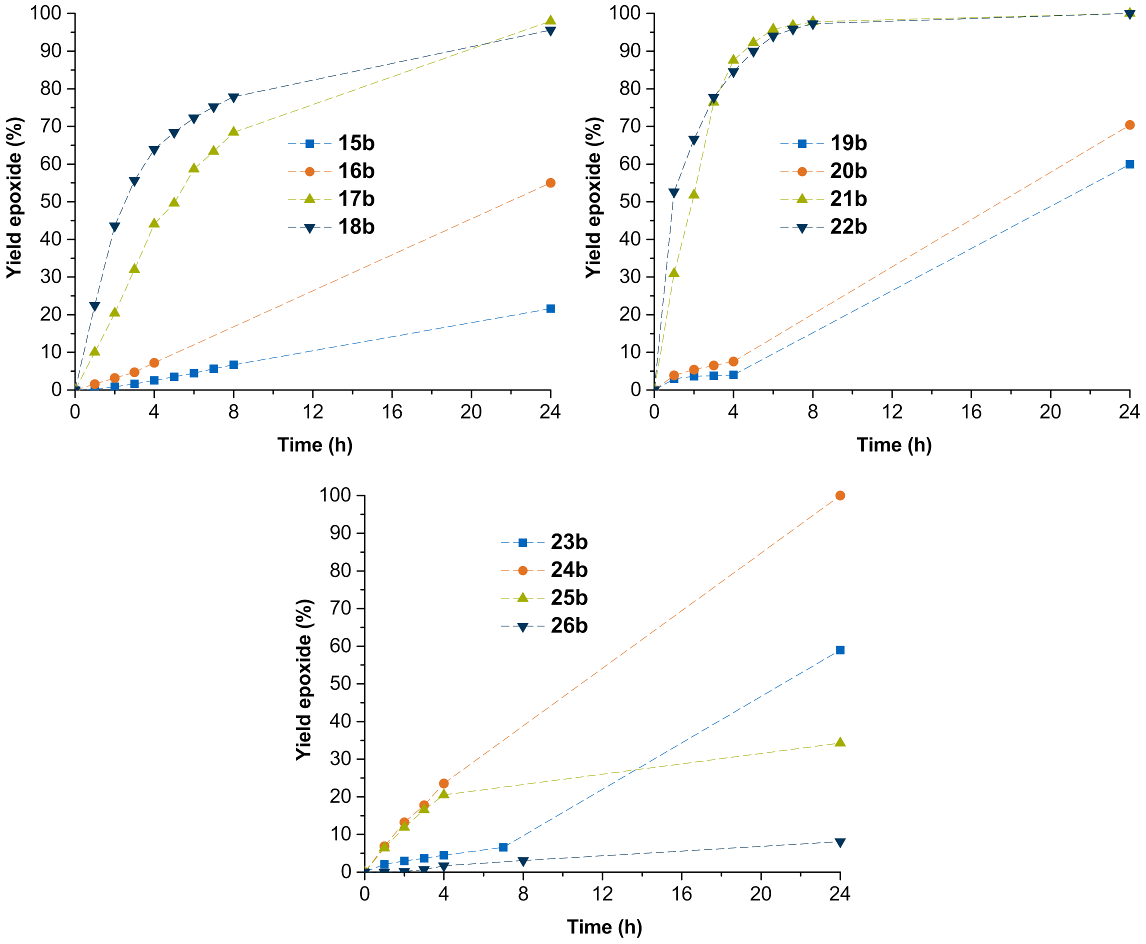

Figure 8.7: Comparison of the kinetic curves of imidazolium perrhenates with varying substituents in the second N-wingtip position.

Therefore, quantitative solubilities of catalysts **17b**, **21b** and **25b** in *cis*-cyclooctene, water, and aqueous H_2O_2 were determined by Johannes Schäffer at the University of Bayreuth. All three imidazolium perrhenates are practically insoluble in *cis*-cyclooctene (<100 ppm) and barely soluble (**17b** and **21b**) or insoluble (**25b**) in water. Surprisingly, in H_2O_2 (50 wt.% in water) **17b** is perfectly soluble and **21b** still exhibits a solubility of 25 wt.% (Figure 8.8 a). Thus, both ILs are

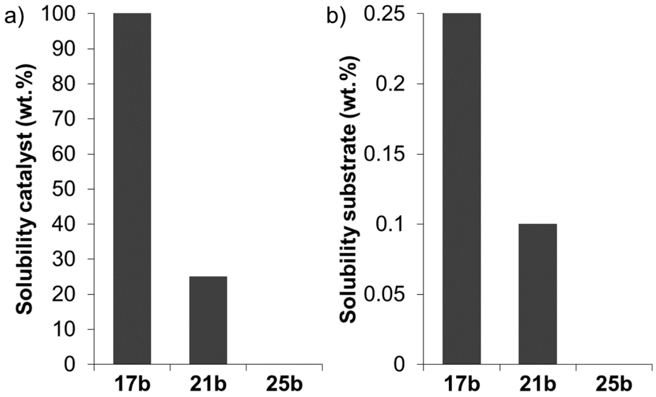

Figure 8.8: Relative Solubilities of a) IL catalysts in a solution of 50 wt.% H_2O_2 in water and b) *cis*-cyclooctene in a solution of 0.5 mmol catalyst and 25 mmol of H_2O_2 (50 wt.% in water).

entirely dissolved in the aqueous phase under catalytic conditions, whereas **25b** is insoluble in a solution of 50 wt.% H_2O_2 in water. These results suggest that the catalytic reaction is taking place in the aqueous phase. The hydrophobicity derived from the longer alkyl chains therefore must have a different effect than making the catalyst soluble in the substrate. Indeed, under catalytic conditions when 0.5 mmol of **17b** or **21b** are added to a mixture of 10 mmol *cis*-cyclooctene and 25 mmol H_2O_2 (50 wt.% in water) the solubility of *cis*-cyclooctene in the aqueous phase is dramatically increased (Figure 8.8 b). Note that solubility of *cis*-cyclooctene in a solution of 50 wt.% H_2O_2 in water is only 50 ppm and does not increase when **25b** is added. These results show that the most active catalyst **21b** is able to transfer *cis*-cyclooctene to the aqueous phase very efficiently. The lower activity of compound **17b**, which is also showing the phase transfer capabilities, is most probably caused by the strong ion contacts resulting from the unsubstituted C2 position. Catalyst **25b** is almost insoluble in aqueous H_2O_2, which resulted in a three-phase system, and is therefore not able to transfer the substrate. This might derive from its increased hydrophobicity compared to **17b** and **21b** originating from the *n*-butyl chains in C2 position. Another explanation might be that the phase transfer is enabled by micelle formation of the imidazolium perrhenates, which can be suppressed by the bulky *n*-butyl chains.

8.4 Recycling of the Catalyst

Stability and reusability of the imidazolium perrhenate were studied by recycling experiments with catalysts **17b** and **21b** and *cis*-cyclooctene as model substrate. A series of ten subsequent catalytic runs was performed. After four hours the reaction was stopped by adding *n*-hexane to remove cyclooctene oxide and residual *cis*-cyclooctene. This extraction procedure was repeated once before residual solvent, water, and hydrogen peroxide were subsequently removed under reduced pressure at 70 °C for of 4 h. After this cleaning procedure the next catalytic run was started by adding 10 mmol *cis*-cyclooctene and 25 mmol aqueous hydrogen peroxide. Both catalysts exhibited constant yields over all ten runs (Figure 8.9), showing the reusability and stability of the system and therefore minimal loss of the expensive metal.

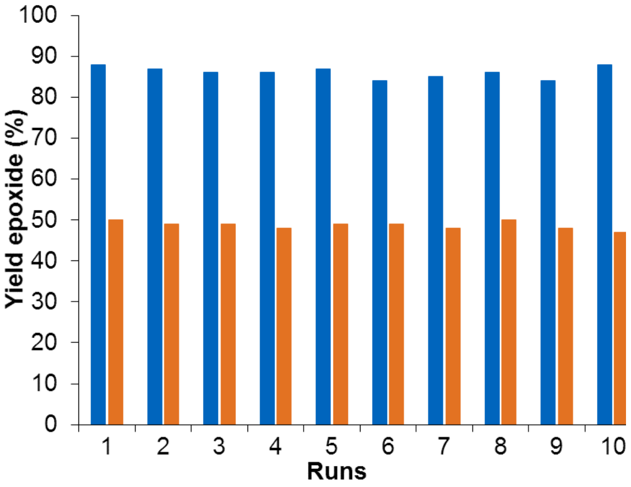

Figure 8.9: Recycling of catalysts **17b** (blue) and **21b** (orange) in epoxidation reaction with *cis*-cyclooctene.

9 Imidazolium Nitrate based Ionic Liquids

9.1 Synthesis

The imidazolium nitrates were prepared similar to the perrhenate containing ionic liquids (chapter 8.1)[137] using ammonium nitrate instead of perrhenate. Most compounds were received in high purities and yields (76-97 %). A complete list of all synthesized imidazolium cations used in oxidation catalysis is given in Figure 9.1.

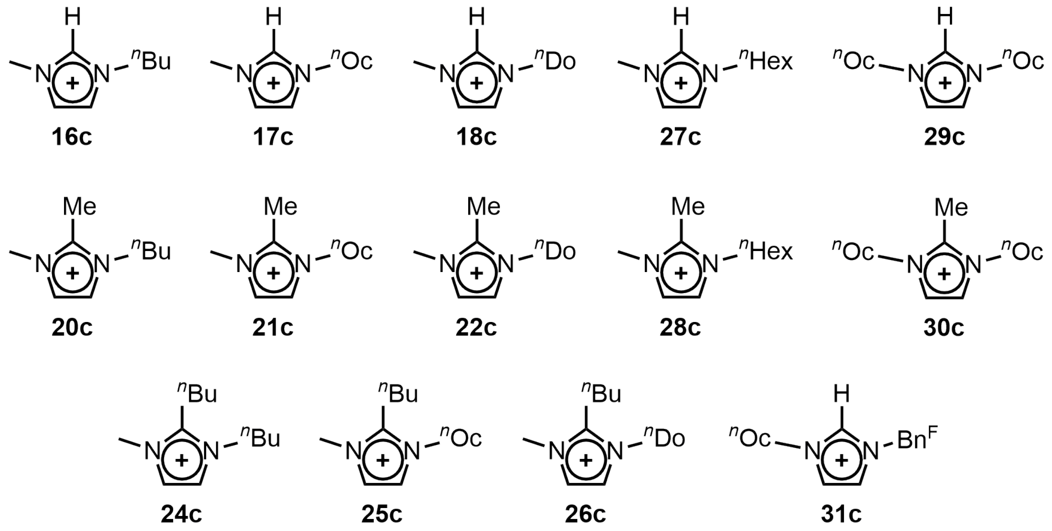

Figure 9.1: Illustration of imidazolium cations used in this study (Me = methyl, ^{n}Bu = *n*-butyl, ^{n}Oc = *n*-octyl, ^{n}Do = *n*-dodecyl, ^{n}Hex = *n*-hexadecyl, Bn^F = 2',3',4',5',6'-pentafluorobenzyl) and numbering for the resulting nitrates.

Furthermore, in order to obtain crystals for the determination of the molecular structure by single crystal X-ray diffraction, 1-benzyl-2,3-dimethylimidazolium (**32c**) and 1,2-dimethyl-3-pentafluorobenzylimidazolium nitrate (**33c**) were prepared. **32c** was crystallized by diethyl ether diffusing into a solution of the compound in dichloromethane. Crystals of **33c** grew directly out of the pure substance.

9.2 Characterization

All synthesized compounds were, like the perrhenates, characterized by means of ^{1}H- and ^{13}C-NMR spectroscopy as well as by elemental analysis and melting point determinations to confirm their purity. NMR spectroscopy results are discussed exemplarily for 1-methyl-3-octylimidazolium nitrate (**17c**), full listings for all compounds can be found in the experimental part.

In some cases residual water could not be removed completely (**16c**, **20c**, **24c**, **25c**, **27c**-**31c**), and therefore had to be considered when molecular masses and elemental analysis data were calculated. Furthermore, some of the imidazolium nitrates (**18c**, **21c**, **25c**-**28c**) were too hygroscopic to determine their melting points. When the waxy compounds were removed from the Schlenk tubes and thereby subjected to moisture they immediately liquefied.

9.2.1 NMR Spectroscopy

When measured in chloroform, one of the ^{1}H backbone imidazolium peaks was overlapping with the solvent signal. Therefore, only qualitative comparisons with the perrhenates can be made. A significant upfield shift for the C2 proton from 10.40 ppm in the bromide IL to 9.23 ppm in the nitrate compound can nevertheless be observed.

9.2.2 Single Crystal X-ray Diffraction and Hirshfeld Surface Analysis

The structures and Hirshfeld analyses presented here have previously been described by Christine Hutterer over the course of her master's thesis.[158]

Compound **32c** crystallizes in the $P2_12_12_1$ space group, **33c** in the $P2_1/c$ space group. The crystal structures allow discussion of the nitrate anion's position relative to the imidazolium cation in the solid state (shortest O–H contacts). Furthermore, the nature and strength of the contacts can be quantified by Hirshfeld surface analysis via calculated contracted hydrogen atom density.[159] Both relative position and contact strength have been reported for the respective im-

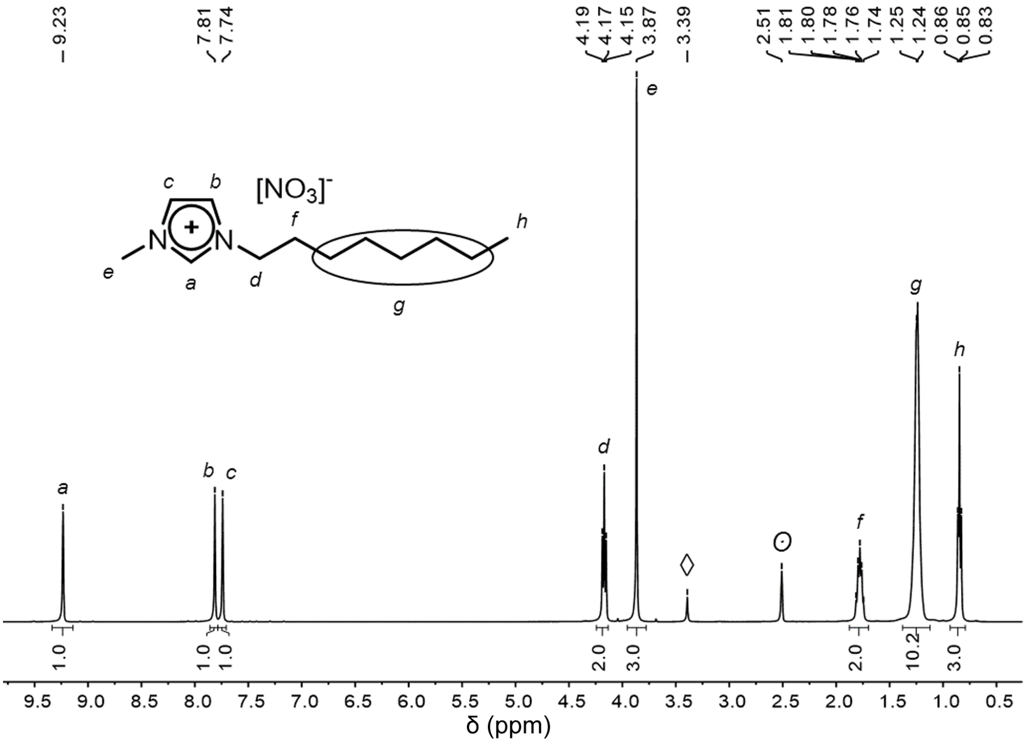

Figure 9.2: ^{1}H-NMR spectrum of **17c** (⊙ = DMSO, ◊ = H_2O).

idazolium perrhenates by Cokoja, Kühn and co-workers, making a comparison possible.[160]

In **32c** (Figure 9.3) the nitrate anion is located near the backbone protons and the methylene bridge of the imidazolium moiety (H2, H3 and H4B). The Hirshfeld surface analysis for **32c** (Figure 9.5 a) shows the strong contact areas (red areas) in exactly these positions. The methyl groups in C2 position are facing away from the anion. The shortest OH contact of 2.314 Å is formed via the protons of the methylene bridge. A similar contact length (2.373 Å) is found in the analogous imidazolium perrhenate, however it is located between a perrhenate oxygen and the methyl group in C2 position. The O–N–O bond angles of 119.3°, 120.1° and 120.7° differ only slightly from the theoretical angles of 120° in a planar nitrate molecule.

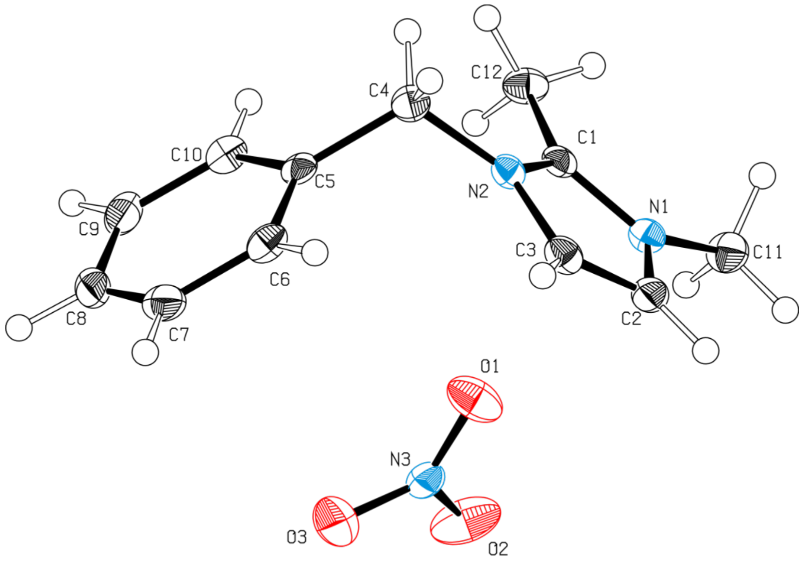
C12
C4
C10
C5
C1
N2
N1
C9
C3
C11
C6
C8
C7
C2
O1
N3
O3
O2

Figure 9.3: ORTEP style drawing of **32c** in the solid state. Thermal ellipsoids are drawn at the 50 % probability level. Selected bond lengths [Å] and bond angles [°]: O1–N3 1.242(2), O2–N3 1.241(2), O3–N3 1.241(3), O2–N3–O1 120.1(1), O2–N3–O3 119.3(2), O3–N3–O1 120.7(2).

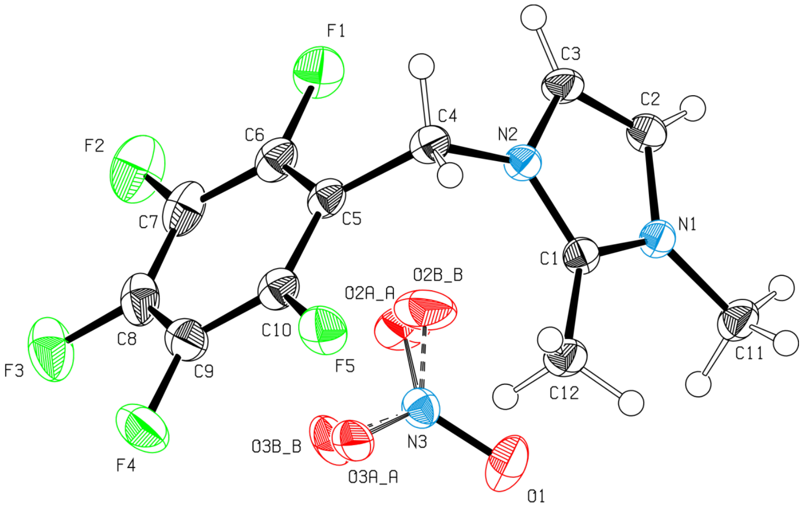
F1
C3
C2
C4
N2
C6
F2
C7
C5
N1
C1
O2B_B
O2A_A
C10
F5
C8
C9
C11
F3
C12
O3B_B
N3
F4
O3A_A
O1

Figure 9.4: ORTEP style drawing of **33c** in the solid state. Thermal ellipsoids are drawn at the 50 % probability level. Selected bond lengths [Å] and bond angles [°] :O1–N3 1.244(1), N3–O3A_a 1.233(9), N3–O2B_b 1.293(14), N3–O2A_a 1.204(10), N3–O3B_b 1.260(13), O2A_a–N3–O3A_a 120.8(7), O3A_a–N3–O1 115.6(4), O2A_a–N3–O1 123.6(6), O1–N3–O3B_b 125.9(10), O1–N3–O2B_b 115.6(9), O3B_ b–N3–O2B_b 118.5(10).

When a fluorinated benzyl group is introduced (**33c**, Figure 9.4), the acidity of the methyl group in C2 position is enhanced. Figure 9.5 b shows that the strongest interactions (red areas) in **33c** are formed by hydrogen bonds between nitrate oxygen atoms with hydrogen atoms of the methyl and methylene groups. Discussion of OH contact length and bond angles can only be made qualitatively, since the nitrate moiety is disordered. The shortest OH contact, between the methyl hydrogen atom H11C and O2B with a length of 2.250 Å, is shorter than in **32c**. This effect suggests that higher acidity due to the fluorinated residue leads to stronger anion-cation interactions. The stronger interaction can also be found in the fluorinated perrhenate compound. However, the shortest OH contact (2.262 Å) is again located in a different position (methylene bridge) probably due to the Lewis acidic pentafluorobenzyl group. This effect was also mentioned previously by our group with perrhenate as anion.[160]

The O–N–O bond angles differ significantly more from the theoretical angles of 120 °, hinting to a stronger cation–anion interaction.

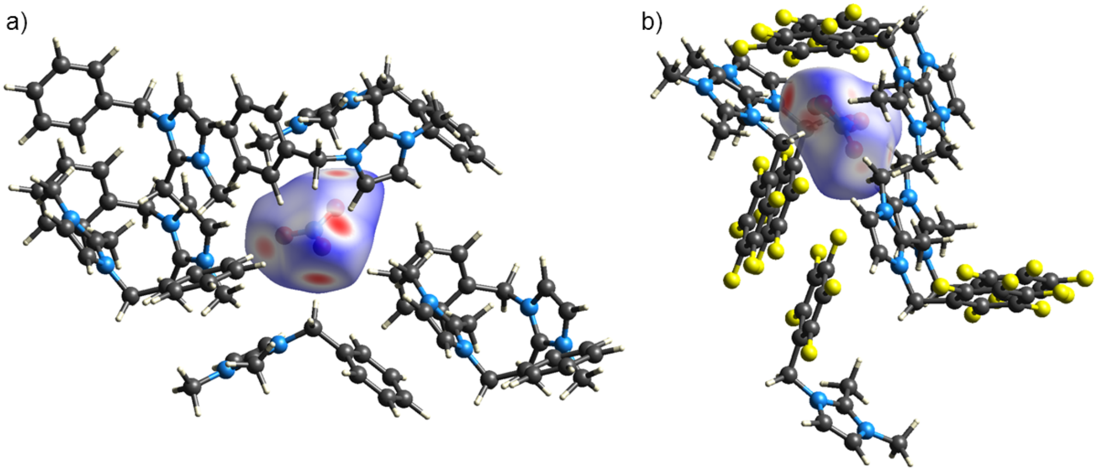

Figure 9.5: Hirshfeld surface analysis of a) **32c** and b) **33c**.

9.2.3 Solubility tests

The prominent influence of imidazolium perrhenate solubilities in different reaction mixture phases on their catalytic activity has been shown in chapter 8. Some imidazolium nitrates were thus qualitatively tested for their solubility behavior. The results are summarized in Table 9.1.

Table 9.1: Empirical solubility of imidazolium nitrates **16c**-**25c**, **27c** and **28c** in *cis*-cyclooctene (*cis*-CO), water, and H_2O_2 (50 wt.% in water) at 80 ℃ (+: solution, –: biphasic system, ±: emulsion).

Entry	Compound	Water	H_2O_2	*cis*-CO
1	**16c**	+	+	-
2	**17c**	+	+	±
3	**18c**	+	+	±
4	**20c**	+	+	-
5	**21c**	+	+	-
6	**22c**	+	+	±
7	**24c**	+	+	-
8	**25c**	+	+	-
9	**27c**	+	+	-
10	**28c**	+	+	-

All tested imidazolium nitrates exhibit much higher solubility in water and aqueous H_2O_2 than their perrhenate analogues. Most nitrate ILs show no obvious solubility in *cis*-cyclooctene, but **17c**, **18c** and **22c** formed emulsions (Table 9.1, entries 2, 3 and 6) and phase separation could not be observed even after 8 h without stirring (at room temperature). However, with these test it is not possible to determine the increased solubility of *cis*-cyclooctene in the aqueous phase when an imidazolium nitrate is added.

9.3 Catalytic Epoxidation of Olefins

9.3.1 Influence of Stirring

The catalytic activity in biphasic systems of catalyst and oxidant in the aqueous phase, and *cis*-cyclooctene in the organic phase is highly dependent on sufficient mixing. Therefore, three different magnetic stir bars were tested with **22c** as catalyst to ensure optimal and reproducible conditions for comparative catalysis runs with different nitrates. Each of the stir bars was tested under the same conditions (80 ℃, 24 h, 10 mol% catalyst) at medium stirring speed. The best results were achieved with a cross-shaped bar (Table 9.2, entry 2). However, when the same bar was used at higher speeds, it stopped stirring entirely and the yield dropped to 16 %. With the octagonal shaped bar (Table 9.2, entry 3) the yields could be maintained at higher stirring rates (31 %). All following catalysis experiments were therefore performed with octagonal stir bars at maximum stirring rate.

Table 9.2: Cyclooctene oxide yield for the different stir bars used.

Entry	Stir bar shape	Yield (%)
1	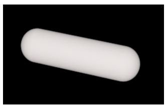	27
2	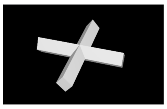	32
3	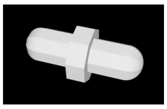	30

9.3.2 Catalyst Comparison

First, imidazolium nitrates **16c**-**26c** were tested in epoxidation catalysis using *cis*-cyclooctene as model substrate. The reactions were carried out at 80 ℃ using aqueous H_2O_2 as oxidant and a catalyst loading of 10 mol%, since these conditions had achieved the best results in previous studies.[161] As with the perrhenate ILs (chapter 8), no additional solvent was added to the reaction mixture.

Table 9.3: Yield of cyclooctene oxide after 8 and 24h reaction time.

Entry	Catalyst	Yield after 8h (%)	Yield after 24h (%)
1	**16c**	9	21
2	**17c**	16	50
3	**18c**	19	22
4	**20c**	n.a.	23
5	**21c**	6	19
6	**22c**	9	31
7	**24c**	6	22
8	**25c**	1	2
9	**26c**	n.a.	28
10	**27c**	n.a.	n.a.
11	**28c**	n.a.	n.a.
12	**29c**	12	31
13	**30c**	10	34
14	**31c**	11	36

Reaction conditions: 1 mmol catalyst (10 mol%), 10 mmol *cis*-cyclooctene, 25 mmol oxidant, 80 ℃.

The results obtained with samples taken after 8 and 24 h are summarized in Table 9.3 (entries 1-9). When the same reaction was carried out using $NaNO_3$ instead of imidazolium nitrate, no conversion was observed. Despite the higher reaction temperature and catalyst loadings much lower yields are observed than with the imidazolium perrhenates. This might be due to the increased solubility of the nitrate ILs in the aqueous phase. Therefore, additional imidazolium nitrates with more hydrophobic groups (**27c**-**31c**, Table 9.3, entries 10-14) were synthesized and applied in catalysis. Immediate decomposition of H_2O_2 (gas evolution) was observed with **27c** and **28c** (Table 9.3, entries 10 and 11), excluding those species from further catalytic experiments. For all other catalysts cyclooctene oxide yield over time at the standard conditions mentioned above was analyzed to further investigate their activity (Figure 9.6).

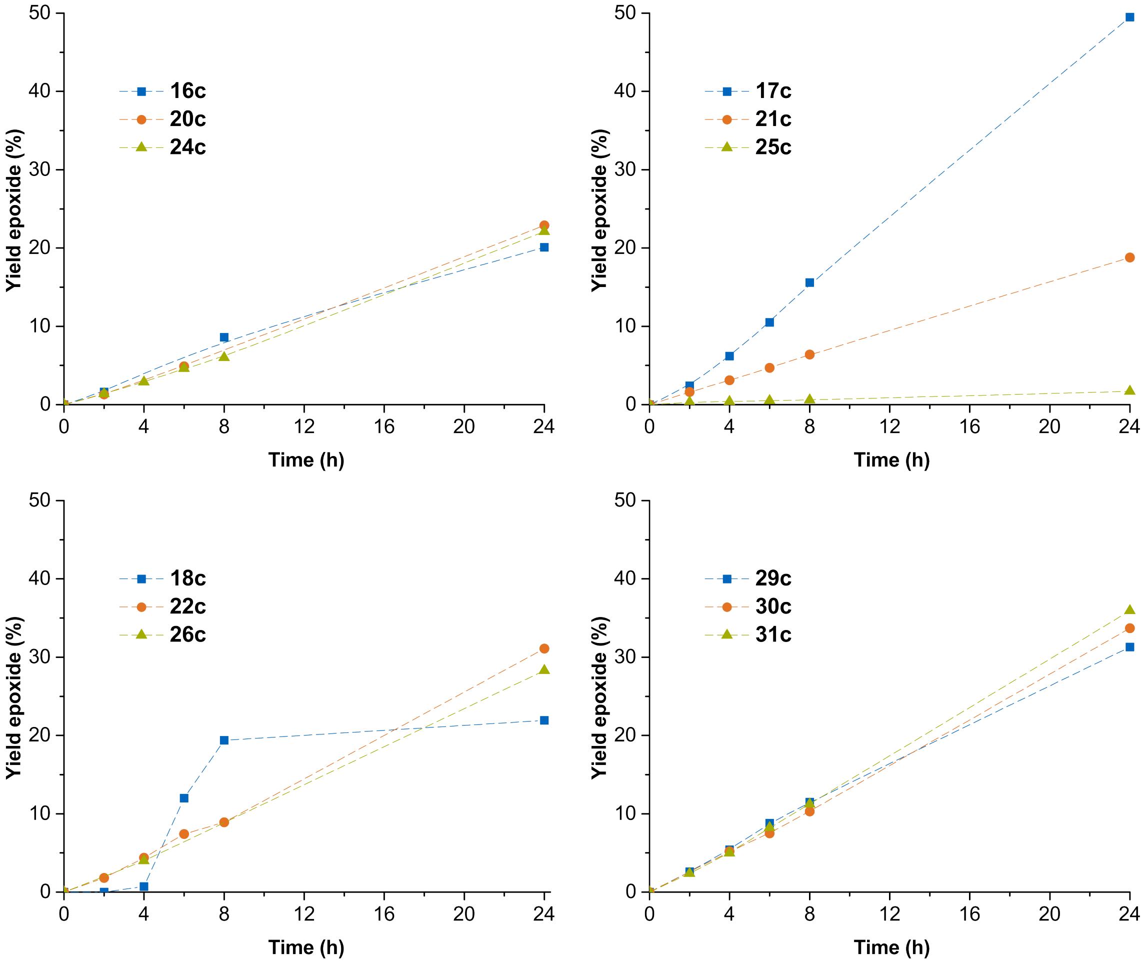

Figure 9.6: Comparison of the kinetic curves of imidazolium nitrates with varying substituents.

In contrast to the imidazolium perrhenates no clear trend is observable. All catalysts, except for **25c**, give the epoxide in a comparable yield after 24 h. Furthermore, depending on which catalyst batch was used in catalysis, the yields after 24 h differed, i.e. using **17c** from 28 to 50 %, **18c** from 22 to 60 % and **29c** from 31 to 75 %. However, with repeated runs of all three catalysts, **17c** was found to be more active than **18c** and **29c**, and is therefore noted as such in Table 9.3 and Figure 9.6. It is not fully understood what causes this effect, since for both compounds elemental analysis and ^{1}H NMR spectra never showed impurities. The only noticeable difference were yellow discolorations.

Conclusions and Outlook

10 Metal-organic Frameworks

In this work, a series of MOF materials containing a molecular molybdenum complex anchored to organic linkers has been synthesized. The frameworks were characterized by means of PXRD, ^{13}C-MAS-NMR, BET surface analysis and XPS. For UiO-67-NH_2 single crystals could be obtained and investigated by SC-XRD. They have been applied in oxidation catalysis, where it was found that most of the frameworks of UiO-type MOFs, in contrast to IRMOF-3, are very stable towards oxidative conditions. Additionally, the immobilization of the molybdenum complex via a Schiff base ligand provided a stable catalyst anchor, as no leaching was observed.

The use of different linker molecules gave rise to materials with various pore sizes. To compare the activities of the MOF materials to the homogeneous molecular analogue, [MoO_2(acac)(PhN=C-PhO)] was prepared and applied in epoxidation catalysis of *cis*-cyclooctene. Therefore, diffusion limitations of the MOF series could be observed and a strong dependence of catalytic activity on the effective pore size of the carrier material was found. The Mo@MOF catalyst with the highest effective pore size, Mo@UiO-67 mixed, can be efficiently recycled several times without notable loss of activity, showing the viability of this material for heterogeneous epoxidation catalysis of various olefins. However, smaller frameworks show a significant decrease in activity with every recycling step hinting to a blockage of the pores by the reactants and products formed. Further studies should be conducted with even lower functionalization of UiO-67 mixed as a possibility to further enhance its activity in oxidation catalysis. Another option to yield frameworks with enhanced pore size and therefore activity might be an improved synthesis of an UiO-68 MOF containing amino groups. The possibility of immobilizing different molecular catalysts could be investigated and different metal centers and ligands, including chiral compounds for enantioselective catalysis, should be considered.

11 Imidazolium Based Ionic Liquids

In summary, the catalytic properties of imidazolium based ionic liquids using perrhenate and nitrate anions in epoxidation catalysis were explored. The substituents at the imidazolium cation were varied to investigate their influence on catalytic performance.

11.1 Imidazolium Perrhenates

A catalogue of 12 different imidazolium based ILs bearing a perrhenate anion able to act as hydrogen bond acceptor were synthesized and characterized by means of NMR and IR spectroscopy, elemental analysis and melting point determinations. The compounds were tested in heterogeneous epoxidation catalysis using *cis*-cyclooctene as model substrate and aqueous hydrogen peroxide as oxidant. The different substitution patterns at the imidazolium moiety yielded materials with varying catalytic activity. The most active catalyst (**21b**) reached 100 % cyclooctene oxide yield within 24 h at 70 °C and 5 mol% catalyst loading whereas with **12b** almost no epoxide was formed. The compounds **17b** and **21b** could also be recycled for at least ten runs without any loss in activity. To investigate the reason for the different activities, solubilities of the ionic liquids in the aqueous and organic phase were determined. It was found that the solubility of *cis*-cyclooctene in the aqueous phase is increased dramatically in the presence of the catalysts. These results suggest that the ILs act as phase transfer agents for the olefin into the aqueous phase. Substitution of the C2 position with a methyl group enhanced catalytic activity, possibly due to reduction of the interionic Coulomb attractions such that activation of H_2O_2 by $[ReO_4]^-$ is facilitated. The high degree of hydrogen bonds formed by the anion also renders the IL soluble in aqueous H_2O_2. Introduction of alkyl chains in the wingtip position might enable the imidazolium perrhenates to form micelles, through which the substrate can be transferred into the aqueous phase. Longer alkyl chains in C2 position are found to decrease the activity of the catalyst. This might be attributed to steric effects preventing micelle formation and thereby also phase transfer of the substrate into the aqueous phase.

Future studies should focus on the adaption of the investigated ILs for various other substrates with respect to their relative solubilities in the multiphase catalysis system. Further improvement of the imidazolium systems could be achieved by introduction of functionalized groups at the cation. Other cations able to form micelles under the reaction conditions might be a suitable alternative to the imidazolium moieties. Immobilization of the ILs on solid supports to get SILPs (supported ionic liquid phases) might make catalyst recycling even simpler.

11.2 Imidazolium Nitrates

As less expensive anions than perrhenate could improve the relevance of IL catalysts, the nitrate anion was investigated as a possible alternative. The imidazolium counter ions were synthesized with similar substitution patterns to the $[ReO_4]^-$ counterparts and equally characterized. Additionally, two benzylated compounds were synthesized and crystallized. The obtained crystal structures were used for Hirshfeld surface analysis, showing that the Lewis acidity of the imidazolium moiety greatly influences the degree of ion contacts between cation and anion.

Catalytic tests using *cis*-cyclooctene as model substrate have shown that nitrates can indeed activate H_2O_2 and function as epoxidation catalysts. However, the obtained catalysts were far less active than the imidazolium perrhenates, even at elevated temperatures and higher catalyst loadings. The most active compound (**17c**) reached an epoxide yield of 50 % after 24 h at 80 °C, when 10 mol% catalyst were used. The lowered activities might be attributed to the increased solubility of the nitrate ILs in the aqueous phase and therefore lowered phase transfer abilities. Therefore, some additional, more hydrophobic cations (**27c**-**31c**) were investigated, but the expected increase in catalytic activity was not observed. In the cases of **27c** and **28c** decomposition of H_2O_2 was observed, preventing a thorough investigation of the catalytic properties of the compounds.

Furthermore, the reproducibility of the results is challenging and in some cases not possible. This issue and the solubilities of different imidazolium nitrates have to be investigated in more detail in future works.

Furthermore, mechanistic investigations by Raman spectroscopy and DFT calculations similar to the ones reported for perrhenates should be conducted to get an insight in the proper design of suitable imidazolium nitrates which might be active in epoxidation catalysis.

A follow-up study investigating other cations and other oxygen-containing anions, such as sulfates or phosphates, should be also considered. More hydrophobic counter ions, enabling micelle formation, should have a positive effect on the activity of nitrate ILs. Additionally, the SIPs described by Cokoja, Kühn, Love and co-workers[140] can be used as counter ions for nitrate, since they would be able to transfer the catalytic reaction from the aqueous into the organic phase. This might be a possibility to obtain more active catalysts and reproducible results, since the contact of the hygroscopic nitrate to water is suppressed.

Experimental Part

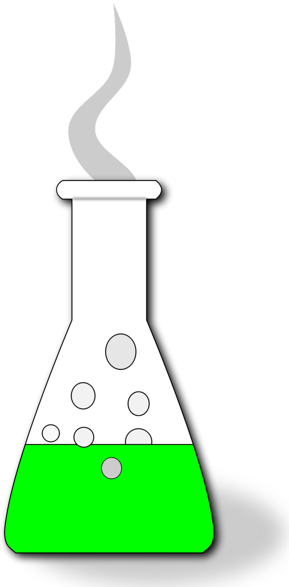

12 General Remarks

All chemicals were obtained commercially (Sigma-Aldrich, Acros) and used without further purification. Preparations of compounds **8**, **10** and **14**, the modifications of the MOF materials and the catalytic evaluation with Mo@MOFs were performed under Argon using Schlenk techniques. Argon 5.0 (purity 99.999 %) was bought from Westfalen AG. Catalytic runs with imidazolium salts were performed on a “Carousel 12 plus” from *Radleys*.

Melting points of the imidazolium salts were determined with a MPH-H2 melting point meter from *Schorpp Gerätetechnik*.

13 Analytical Methods

NMR Spectroscopy

Liquid NMR spectra were recorded at room temperature on a Bruker Avance DPX 400 and a Bruker DRX 400. Chemical shifts are given in parts per million (ppm) and the spectra were referenced by using the residual solvent shifts as internal standards. Solid-state ^{13}C NMR spectra were recorded on a Bruker Avance 300 spectrometer equipped with a 4 mm BBMAS probe head and referenced to adamantane as an external standard at 298 K.

BET Sorption Measurements

Specific surface area, pore diameters and pore size distributions were determined by physisorption of N_2. Measurements were carried out using a PMI automatic BET-Sorptometer operating at liquid nitrogen temperature (77 K), after degassing under vacuum. The results were calculated using the weight after degassing. Prior to analysis the samples were degassed to 20 microns vacuum at 250 °C.

Elemental Analysis

Elemental analysis was obtained from the microanalytical laboratory of the Technische Universität München.

GC-MS Measurements

GC methods to monitor conversion in catalytic experiments were performed on a *Hewlett-Packard* HP 5890 Series II instrument equipped with a FID, *Superlco* column Alphadex 120 and a *Hewlett-Packard* integration unit HP 3396 Series II.

X-ray Powder Diffraction

X-ray powder diffraction was carried out using a *Stoe* Stadi P diffractometer operated with CuKα_1 radiation (λ = 1.5406 Å) and a Ge(111) monochromator in transmission mode.

X-ray Single Crystal Diffraction

X-ray single crystal diffraction data were collected on an X-ray single crystal diffractometer equipped with a CCD detector (APEX II, κ-CCD), a rotating anode FR591 equipped with a Montel mirror optic (UiO-67-NH_2, **32c** and **33c**) or a fine focused sealed tube equipped with a graphite monochromator (in the case of [MoO_2(acac)(PhN=C-PhO)]) by using the APEXII software package.[162] The measurements were performed on single crystals coated with perfluorinated ether. The crystals were fixed on top of a glass fiber and transferred to the diffractometer. Crystals were frozen under a stream of cold nitrogen. A matrix scan was used to determine the initial lattice parameters. Reflections were merged and corrected for Lorenz and polarisation effects, scan speed, and background using SAINT.[163] Absorption corrections, including odd and even ordered spherical harmonics were performed using SADABS.[163] Space group assignments were based upon systematic absences, *E* statistics, and successful refinement of the structures. Structures were solved by direct methods with the aid of successive difference Fourier maps,[164] and were refined against all data using the APEX 2 software[162] in conjunction with SHELXL[164,165] and SHELXLE.[166] Methyl hydrogen atoms were refined as part of rigid rotating groups, with a C–H distance of 0.98 Å and $U_{iso(H)} = 1.5 \cdot U_{eq(C)}$. Other H atoms were placed in calculated positions and refined using a riding model, with methylene and aromatic C–H distances of 0.99 and 0.95 Å, respectively, and $U_{iso(H)} = 1.2 \cdot U_{eq(C)}$. Hydrogen atoms bond to nitrogen were not refined. Non-hydrogen atoms were refined with anisotropic displacement parameters. Full-matrix least-squares refinements were carried out by minimizing $\Sigma w(F_o^2-F_c^2)^2$ with SHELXL-97 weighting scheme.[164,165] Neutral atom scattering factors for all atoms and anomalous dispersion corrections for the non-hydrogen atoms were taken from the *International Tables for Crystallography*.[167] Images of the UiO-67-NH_2 crystal structures were generated by *Diamond*,[168] for **14**, **32c** and **33c** by PLATON.[169] The crystallographic data is summarized in Table 13.1.

Hirshfeld surface analyses were carried out using *CrystalExplorer*[170] and hydrogen bond lengths were characterized using *Mercury*.[171]

X-ray Photoelectron Spectroscopy

XPS data were acquired from a compacted sample in a UHV chamber at a base pressure of $5 \cdot 10^{-10}$ mbar while the sample was cooled to approx. 77 K. A non-monochromatic Mg anode source ($\hbar\omega$= 1253.6 eV) was used at magic angle incidence and normal emission. Electron energy spectra were measured with a hemispherical electron energy analyser (100 mm radius) set at a pass energy of 20 eV. Raw data were analyzed using the *IGOR Pro* software suit with custom-written analysis procedures. A Shirley-type background was subtracted from the Mo3d spectra while the energy binding scale was calibrated against the C1s line at 284.8 eV. A Voigt-type line slope was then used to fit the resulting peaks with no constraints regarding peak splitting or area ratios.

Table 13.1: Crystallographic data for compounds UiO-67-NH_2, **14**, **32c** and **33c**.

	UiO-67-NH_2	**14**	**32c**	**33c**
Formula	$C_{42}H_{24}N_3O_{16}Zr_3$	$C_{18}H_{17}MoNO_5$	$C_{12}H_{15}N_3O_3$	$C_{12}H_{10}F_5N_3O_3$
fw	1100.32	423.27	249.27	339.23
Colour/habit	yellow prism	yellow block	pale yellow prism	yellow fragment
Cryst. dimensions, mm^3	0.25 x 0.29 x 0.35	0.25 x 0.31 x 0.31	0.16 x 0.22 x 0.59	0.28 x 0.38 x 0.73
Crystal system	cubic	triclinic	orthorhombic	monoclinic
Space group	$Fm\bar{3}m$	$P\bar{1}$	$P2_12_12_1$	$P2_1/n$
a, Å	26.7882(6)	7.0807(1)	8.5838(4)	7.2191(3)
b, Å	26.7882(6)	9.4110(1)	10.3031(4)	15.6308(6)
c, Å	26.7882(6)	14.0768(2)	13.6630(7)	12.0351(5)
α, deg	90	93.622(1)	90	90
β, deg	90	99.297(1)	90	92.534(2)
γ, deg	90	111.590(1)	90	90
V, Å^3	19223.4(13)	853.04(2)	1208.35(10)	1356.72(10)
Z	8	2	4	4
T, K	123(2)	123	123	123
D_{calcd}, g cm^{-3}	0.760	1.648	1.370	1.661
μ, mm^{-1}	0.353	0.797	0.101	0.165
$F(000)$	4360	428	528	688
θ range, deg	1.32 – 25.38	2.35 – 25.44	2.48 – 25.02	2.14 – 25.41
Index ranges (h, k, l)	-32 – 31, ± 32, ± 32	± 8, ± 11, ± 16	± 10, ± 12, ± 16	± 8, ± 18, ± 14
No. of rflns collected	160563	24703	34284	39725
No. of independent rflns/R_{int}	951/0.0344	3145/0.0258	2135/0.0443	2501/0.0302
No. of observed rflns ($I>2\sigma(I)$)	914	3020	1978	2210
No. of data/restraints/parameters	951/26/52	3145/0/228	2135/0/223	2501/0/267
R1/wR2 $I>2\sigma(I)$)$^{(a)}$	0.0481/0.1378	0.0166/0.0421	0.0280/0.0626	0.0292/0.0750
R1/wR2 (all data)$^{(a)}$	0.0495/0.1396	0.0176/0.0426	0.0336/0.0660	0.0342/0.0784
GOF (on F^2)$^{(a)}$	1.237	1.083	1.097	1.053
Largest diff peak and hole (e·Å^{-3})	0.919/-0.885	+0.255/-0.298	0.171/-0.165	0.172/-0.240

(a) $R1 = \Sigma(||F_o|-|F_c||)/\Sigma|F_o|$; $wR2 = \{\Sigma[w(F_o^2-F_c^2)^2]/\Sigma[w(F_o^2)^2]\}^{1/2}$; $GOF = \{\Sigma[w(F_o^2-F_c^2)^2]/(n-p)\}^{1/2}$

14 Metal-organic Frameworks

14.1 Linker Preparation

Dimethyl-2-nitrobiphenyl-4,4'-dicarboxylate (5).

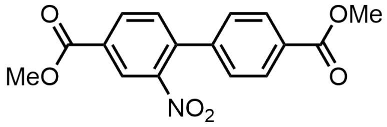

The compound was prepared similar to the procedure known from literature.[141] A mixture of nitric acid (56%, 1.3 mL, 74 mmol) and concentrated sulfuric acid (1.6 mL) was added dropwise to a solution of dimethylbiphenyl-4,4'-dicarboxylate (5 g, 74 mmol) in 50 mL of concentrated sulfuric acid at 0 ℃ under intense stirring. The reaction mixture was maintained at 0-5 ℃ for 1 h and at 10-15 ℃ for 4 h before being poured on crushed ice. The precipitated solids were separated by filtration, washed with water and recrystallized from isopropanol.

Yield: 4.12 g (71 %) of colorless powder.

^{1}H-NMR (400 MHz, DMSO-d$_6$, ppm) δ = 3.89 (s, 3H, -CH_3), 3.94 (s, 3H, -CH_3), 7.56 (d, ^3J(H,H) = 8 Hz, 2H, 3',5'/2',6'-Ar), 7.76 (d, ^3J(H,H) = 8 Hz, 1H, 6-Ar(NO$_2$)), 8.06 (d, ^3J(H,H) = 8 Hz, 2H, 3',5'/2',6'-Ar), 8.31 (dd, ^3J(H,H) = 8 Hz, ^4J(H,H) = 2 Hz, 1H, 5-Ar(NO$_2$)), 8.51 (d, ^3J = 2 Hz, 1H, 3-Ar(NO$_2$));

^{13}C-NMR (101 MHz, DMSO-d$_6$, ppm) δ = 52.8, 53.4, 125.4, 128.8, 130.0, 130.3, 130.9, 133.2, 133.7, 138.9, 141.4, 148.9, 164.8, 166.2.

Other data matched those previously reported for this compound.

Dimethyl-2-aminobiphenyl-4,4'-dicarboxylate (6).[142]

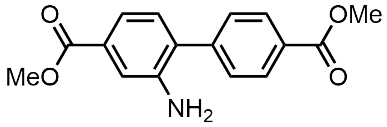

To a stirred solution of dimethyl-2-nitrobiphenyl-4,4'-dicarboxylate (**5**, 2.9 g, 9.19 mmol) in 115 mL methanol, tin powder (6.45 g) and 40 mL of an aqueous

1 M HCl solution were added. The suspension was heated to reflux for 2 h under intense stirring before being poured on to crushed ice. The solution was then basified with aq. 1 M NaOH solution and the precipitated solids were separated by filtration. The crude product was extracted with warm ethyl acetate. Any remaining insoluble by-products were removed by filtration over Celite. The solvent was removed under vacuum and crude product was purified by flash chromatography (ethyl acetate/dichloromethane: 10 %).

Yield: 2.18 g (92 %) of light yellow powder.

^{1}H-NMR (400 MHz, DMSO-d$_6$, ppm) δ = 3.83 (s, 3H, -C*H*$_3$), 3.88 (s, 3H, -C*H*$_3$), 5.23 (s, 2H, -N*H*$_2$), 7.14 (d, ^3J(H,H) = 8 Hz, 1H, 6-Ar(NH$_2$)), 7.22 (dd, ^3J(H,H) = 8, ^4J(H,H) = 2 Hz, 1H, 5-Ar(NH$_2$)), 7.44 (d, ^3J(H,H) = 2 Hz, 1H, 3-Ar(NH$_2$)), 7.61 (d, ^3J(H,H) = 8 Hz, 2H, 3',5'/2',6'-Ar), 8.04 (d, ^3J(H,H) = 8 Hz, 2H, 3',5'/2',6'-Ar); **^{13}C-NMR** (101 MHz, DMSO-d$_6$, ppm) δ = 52.0, 52.2, 116.0, 117.1, 128.3, 128.5, 128.9, 129.7, 129.9, 130.4, 143.7, 145.6, 166.1, 166.5.

Other data matched those previously reported for this compound.

2-Aminobiphenyl-4,4'-dicarboxylic acid (7).[142]

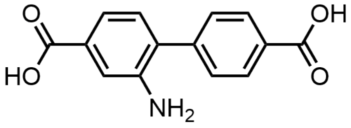

A mixture of dimethyl-2-aminobiphenyl-4,4'-dicarboxylate (**6**, 0.68 g, 2.4 mmol, 1 equiv.), 13 mL THF, and 13.2 mL of an aqueous 1M KOH solution was heated to reflux for 16 h. After cooling to room temperature in air THF was removed under vacuum and the solution was acidified with aq. 1M HCl. The resulting precipitate was separated by filtration, washed with water, then washed with methanol, and air-dried.

Yield: 0.585 g (95 %) of yellow powder.

^{1}H-NMR (400 MHz, DMSO-d$_6$, ppm) δ = 5.15 (s, 2H, -N*H*$_2$), 7.12 (d, ^3J(H,H) = 8 Hz, 1H, 6-Ar(NH$_2$)), 7.21 (dd, ^3J(H,H) = 8 Hz, ^3J(H,H) = 2 Hz, 1H, 5-Ar(NH$_2$)), 7.41 (d, ^3J(H,H) = 2 Hz, 1H, 3-Ar(NH_2)), 7.58 (d, ^3J(H,H) = 8 Hz, 2H, 3',5'/2',6'-Ar), 8.02 (d, ^3J(H,H) = 8 Hz, 2H, 3',5'/2',6'-Ar), 12.83 (bs, 2H, -CO_2H);

^{13}C-NMR (101 MHz, DMSO-d_6, ppm) δ = 116.7, 117.8, 128.8, 129.2, 129.9, 130.3, 130.7, 131.4, 143.8, 145.9, 167.6, 168.0.

Other data matched those previously reported for this compound.

Dimethyl 2'-amino-1,1':4',1''-terphenyl-4,4''-dicarboxylate (8).[99]

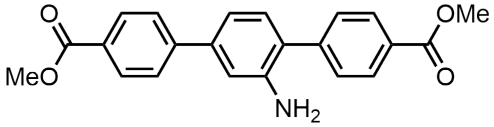

4-(methoxycarbonyl)phenylboronic acid (2.22 g, 12.2 mmol), 2,5-dibromoaniline (491 mg, 1.96 mmol) and potassium fluoride (2.36 g, 40.6 mmol) together with $Pd_2(dba)_3$ (270 mg, 0.29 mmol) were suspended in dry, degassed THF (20 mL). A 0.68 g/mL $PtBu_3$ solution in toluene (2.5 mL, 0.82 mmol) was added to the reaction mixture. While stirring at 50 °C for 24 h, a voluminous brownish precipitate formed. After cooling to room temperature, the mixture was poured into water (25 mL). The aqueous phase was extracted with DCM. The combined organic phases were mixed with 4.5 g of silica gel. After evaporation of the solvent the obtained powder was transferred to a silica column. After elution with DCM/EtOAc (25:1), the solvent was removed and the obtained powder dried in vacuo.

Yield: 1.03 g (69 %) of pale yellow powder.

^{1}H-NMR (400 MHz, DMSO-d_6, ppm) δ = 8.04 (2 AA' parts of 2 AA'XX' spin systems, 2H each, H-3, H-5, H-3'', H-5''), 7.77 and 7,64 (2 XX' parts of 2 AA'XX'' spin systems, 2H each, H-2, H-6, H-2'', H-6''), 7.20-7.14 (m, 2H, H-3', H-6'), 7.02 (dd, ^3J(H,H) = 8 Hz, ^4J(H,H) = 2 Hz, 1H, H-5'), 5.13 (s, 2H, -NH_2), 3.88 (s, 3H, -CH_3) 3.88 (s, 3H, -CH_3).

Other data matched those previously reported for this compound.

2'-Amino-1,1':4',1"-terphenyl-4,4"-dicarboxylic acid (9).

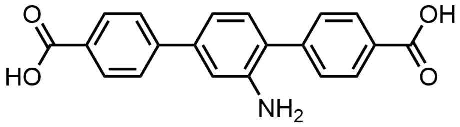

To a solution of Dimethyl-2'-amino-1,1':4',1"-terphenyl-4,4"-dicarboxylate (**8**, 273 mg, 0.76 mmol) in ethanol (300 mL) a solution of potassium hydroxide (2.44 g, 43.5 mmol) in water (52 mL) was added, and the reaction mixture was refluxed for 24 h. After cooling to room temperature, ethanol was removed in vacuo. The resulting solid was completely dissolved in water (80 mL). After acidification to pH$\sim$2 with HCl a yellow, light solid precipitated, was filtered, and dried in vacuo.

Yield: 1.19 g (98 %) of yellow powder.

^{1}H-NMR (400 MHz, DMSO-d_6, ppm) δ = 12.97 (bs, 2H, -COO*H*), 8.02 (2 AA' parts of 2 AA'XX' spin systems, 2 H each, H-3, H-5, H-3", H-5"), 7.74 and 7,61 (2XX' parts of 2 2AA'XX' spin systems, 2H each, H-2, H-6, H-2", H-6"), 7.24 – 7.11 (m, 2H, H-3', H-6'), 7.01 (dd, ^3J(H,H) = 8, ^4J(H,H) = 2 Hz, 1H, H-5'), 5.10 (s, 2H, -NH_2).

Other data matched those previously reported for this compound.

Dimethyl 1,1':4',1"-terphenyl-4,4"-dicarboxylate (10).

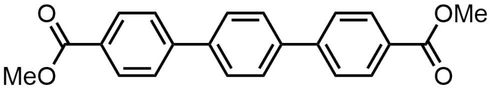

Dimethyl 1,1':4',1"-terphenyl-4,4"-dicarboxylate (**10**) was prepared similarly to **8** using 1,4-dibromobenzene (462 mg, 1.96 mmol) and 4-(methoxycarbonyl)phenylboronic acid (2.22 g, 12.2 mmol) as starting materials. The reaction time was extended to 5 days and a mixture of ethyl acetate and hexane (2:1) was used as eluent.

Yield: 1.02 g, 72 % of colorless solid.

^{1}H-NMR (400 MHz, DMSO-d_6, ppm) δ = 8.29 (s, 4H, H-3, H-5, H-3", H-5"), 7.94-7.89 (m, 8H, H-2, H-6, H-2', H-3', H-5', H-6', H-2", H-6"), 3.86 (s, 6H, -CH_3).

Other data matched those previously reported for this compound.

1,1':4',1"-Terphenyl-4,4"-dicarboxylic acid (11).

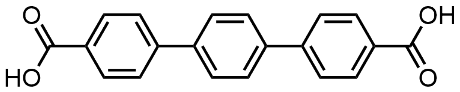

The deprotection of **10** (1.02 g, 2.95 mmol) was achieved analogous to the synthesis of **9**, using the same excess of KOH.

Yield: 398 mg, 42 % of colorless powder.

^{1}H-NMR (400 MHz, DMSO-d_6, ppm) $\delta = 12.95$ (bs, 2H, -COO*H*), 8.27 (s, 4H, H-3, H-5, H-", H-5"), 7.91-7.87 (m, 8H, H-2, H-6, H-2', H-3', H-5', H-6', H-2", H-6").

Other data matched those previously reported for this compound.

14.2 Catalyst Preparation

Preparation of UiO-MOFs.[96]

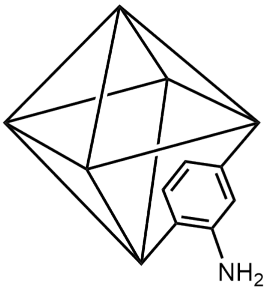

All preparations were performed in 100 mL screw thread glass vials. $ZrCl_4$ (650 mg, 2.73 mmol) and the linker (500 mg, 2.73 mmol 2-aminotherephthalic acid for UiO-66-NH_2; 83 mg, 0.45 mmol 2-aminoterephthalic acid and 382 mg, 2.28 mmol terephthalic acid for UiO-66 mixed; 703 mg, 2.73 mmol **7** for UiO-67-NH_2; 117 mg, 0.45 mmol **7** and 569 mg, 2.28 mmol biphenyl-4,4'-dicarboxylic acid for UiO-67 mixed) were dissolved in 64 mL DMF and water (0.2 mL, 11.1 mmol). The resulting mixture was placed in a preheated oven at 80 °C for 12 h and then held at 100 °C for 24 h. After cooling to room temperature in air, the liquid was decanted and the resulting solid was washed with 30 mL of absolute ethanol three times for 24 h at 60 °C. The resulting powder was dried under vacuum for 16 h.

UiO-68 mixed was prepared similar to the other mixed UiO MOFs using $ZrCl_4$ (330 mg, 2.75 mmol, 6 equiv.), 2'-amino-1,1':4',1"-terphenyl-4,4"-dicarboxylic acid (**9**, 153 mg, 0.46 mmol, 1 equiv.) and 1,1':4',1"-terphenyl-4,4"-dicarboxylic acid (**11**, 729 mg, 2.29 mmol, 5 equiv.) as starting materials dissolved in 31 mL DMF. 30 equiv. of benzoic acid (1.68 g, 13.75 mmol) and 4 equiv. of H_2O (33 µL, 1.83 mmol) were added to the reaction mixture prior to heating.

UiO-66: ^{13}C MAS-NMR: δ = 116.2, 132.5, 138.6, 152.4, 170.7, 172.5;

UiO-66 mixed: ^{13}C MAS-NMR: δ = 118.0, 129.4, 138.1, 148.0, 170.9;

UiO-67: ^{13}C MAS-NMR: δ = 119.6, 127.2, 128.6, 130.3, 136.2, 137.9, 142.8, 144.2, 171.9, 172.5;

UiO-67 mixed: ^{13}C MAS-NMR: δ = 124.9, 130.1, 134.9, 143.4, 172.3.

UiO-68 mixed: ^{13}C MAS-NMR was not performed, since the framework decomposed when modified with $MoO_2(acac)_2$.

Single-crystals of UiO-67-NH_2 were obtained when $ZrCl_4$ (108 mg, 0.42 mmol), **7** (100 mg, 0.42 mmol) and benzoic acid (1.54 g, 12.6 mmol) were dissolved in 12 mL DMF. The resulting mixture was placed in a preheated oven at 35 °C and slowly heated to 120 °C over a time period of five days and left at that temperature for 12 days.[99]

Preparation of IRMOF-3.[144]

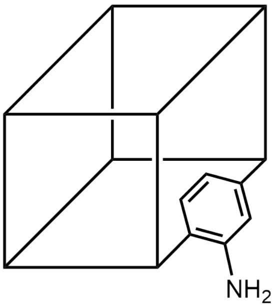

$Zn(NO_3)_2 \cdot 4H_2O$ (6 g, 23 mmol) and 2-aminotherephthalic acid (1.5 g, 8.3 mmol) were dissolved in DMF (200 mL). The solution was divided into 10 mL portions and filled into 20 mL screw thread glass vials. The vials were placed in a sand bath, and the bath was transferred to an oven. The temperature was raised to

100 ℃ over 2 h and held for 18 h. Then, the oven was turned off and the vials left in the sandbath until a final temperature of 35 ℃ was reached. Amber crystals of IRMOF-3 formed. The remaining solution from each vial was decanted, and the crystals were washed three times with dry DMF (3 × 12 mL) followed by one rinse with $CHCl_3$. The crystals were then soaked in 15 mL of $CHCl_3$ for 3 days, while the $CHCl_3$ was exchanged every 24 h.

^{13}C MAS-NMR: δ = 116.6, 132.6, 137.9, 150.8, 175.7, 177.5.

Modification with salicylaldehyde.

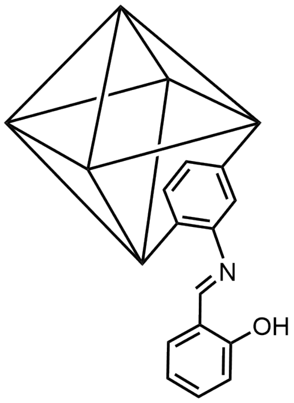

UiO-SI MOFs were prepared using a vapor diffusion method reported previously.[100] Salicylaldehyde (50 µL, 0.48 mmol, 2 equiv.) was introduced into a Schlenk tube and the MOFs (1 equiv. of amino groups; 70 mg, 0.04 mmol UiO-66-NH_2; 400 mg, 0.24 mmol UiO-66 mixed; 88 mg, 0.04 mmol UiO-67-NH_2; 508 mg, 0.24 mmol UiO-67 mixed; 622 mg, 0.24 mmol UiO-68 mixed; 33 mg, 0.04 mmol IRMOF-3) were weighed into a conical filter paper and fixed in the Schlenk tube, not touching the liquid. The system was evacuated and heated overnight at 100 ℃ under static vacuum. The products were washed with dichloromethane three times for 24 h and dried under vacuum for 16 h.

UiO-66-SI: ^{13}C MAS-NMR: δ = 116.8, 132.3, 138.8, 151.9, 171.5, 172.9;

UiO-66-SI mixed: ^{13}C MAS-NMR: δ = 115.9, 133.0, 138.3, 152.0, 170.4;

UiO-67-SI: ^{13}C MAS-NMR: δ = 117.0, 119.8, 127.7, 128.8, 129.6, 134.3, 135.9, 143.3, 173.1, 173.7;

UiO-67-SI mixed: ^{13}C MAS-NMR: δ = 119.7, 130.4, 134.1, 143.3, 172.2.

UiO-68-SI mixed: ^{13}C MAS-NMR was not performed, since the framework decomposed when modified with $MoO_2(acac)_2$.

IRMOF-3-SI: ^{13}C MAS-NMR: δ = 116.6, 119.0, 120.5, 128.4, 132.7, 137.9, 150.8, 175.7, 177.5.

Modification with $[MoO_2(acac)_2]$.

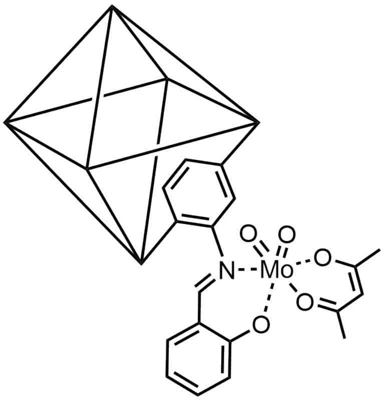

Dried MOFs (1 equiv. of imide groups; 61 mg, 0.03 mmol UiO-66-NH_2-SI; 182 mg, 0.1 mmol UiO-66-SI mixed; 72 mg, 0.03 mmol UiO-67-NH_2-SI; 229 mg, 0.1 mmol UiO-67-SI mixed; 270 mg, 0.1 mmol UiO-68-SI mixed; 34 mg, 0.03 mmol IRMOF-3-SI) were reacted with $MoO_2(acac)_2$ (100 mg, 0.31 mmol) in dichloromethane over four days under inert atmosphere. The products were washed with dichloromethane three times for 24h and dried under vacuum for 16 h.

Mo@UiO-66: ^{13}C MAS-NMR: δ = 25.0, 118.5, 133.1, 138.8, 150.9, 171.8; elemental analysis (%): calcd.: C 38.59, H 2.54, N 2.25, Mo 15.41; found: C 22.06, H 3.93, N 3.78, Mo 8.48;

Mo@UiO-66 mixed: ^{13}C MAS-NMR: δ = 25.9, 118.2, 129.6, 137.4, 163.3, 171.6; elemental analysis (%): calcd.: C 35.87, H 1.96, N 0.70, Mo 4.60; found: C 26.74, H 3.1, N 1.38, Mo 5.69;

Mo@UiO-67: ^{13}C MAS-NMR: δ = 24.4, 116.8, 119.4, 128.7, 129.8, 134.3, 137.9, 143.1, 172.2; elemental analysis (%): calcd.: C 44.70, H 2.84, N 2.00, Mo 13.74; found: C 46.27, H 2.85, N 3.02, Mo 3.23;

Mo@UiO-67 mixed: ^{13}C MAS-NMR: δ = 24.6, 125.0, 130.3, 135.0, 143.4, 172.2; elemental analysis (%): calcd.: C 46.76, H 2.58, N 0.57, Mo 3.78; found: C 44.20, H 2.59, N 0.58, Mo 2.43

Mo@UiO-68 mixed: not analyzed, since PXRD showed decomposition

Mo@IRMOF-3: ^{13}C MAS-NMR: δ = 25.0, 116.6, 118.9, 132.7, 137.9, 150.9, 175.8, 177.6; elemental analysis (%): calcd.: C 39.46, H 2.13, N 4.23, Mo 3.22; found: C 38.98, H 2.21, N 4.36, Mo 3.03.

(Mo values calcd. for complete modification of all possible sites in the MOFs).

Preparation of PhN=C-PhO (13).[145]

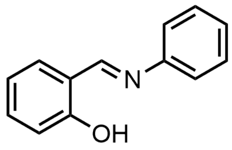

To a Schlenk tube containing salicylaldehyde (1.25 mL, 12 mmol), and formic acid (0.5 mL) in methanol (15 mL), aniline (1.5 g, 16 mmol) was added. The resulting orange-brown reaction mixture was stirred at room temperature for 16 h. The precipitated yellow solid was filtered, washed with cold methanol, and dried under vacuum.

Yield: 1.8 g (76 %) of yellow powder.[146]

^{1}H-NMR (400 MHz, $CDCl_3$, ppm) δ = 13.22 (s, 1H, O*H*), 8.59 (s, 1H, N=C*H*), 7.42-7.19 (m, 7H, Ar), 7.05-6.81 (m, 2H, Ar).

Other data matched those previously reported for this compound.

Preparation of [MoO_2(acac)(PhN=C-PhO)] (14).[147]

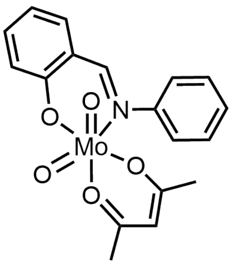

A solution of **13** (292 mg, 1.48 mmol) in dichloromethane (5 mL) was added to a solution of [$MoO_2(acac)_2$] (483 mg, 1.48 mmol) in dichloromethane (15 mL). The reaction mixture was stirred at room temperature overnight, and the resulting yellow mixture was filtered via a cannula. The solvent was removed under vacuum and the yellow oily residue suspended in Et_2O (10 mL). The solution was filtered and left overnight to give yellow crystals. No yield was determined, since only a few crystals were obtained.[146]

^{1}H-NMR (400 MHz, CD_2Cl_2, ppm) δ = 8.25 (s, 1H, N=C*H*), 7.58 (m, 1H, 5-Ar), 7.47 (m, 1H, 3-Ar), 7.35 (m, 2H, 3,5-Ar(-N)), 7.27 (m, 1H, 4-Ar(-N)), 7.16 (m, 2H, 2,6-Ar(-N)), 7.10 (m, 1H, 9-Ar), 7.07 (m, 1H, 11-Ar), 5.46 (s, 1H, acac), 2.00 (s, 3H, Me), 1.47 (s, 3H, -CH_3);

^{13}C-NMR (101 MHz, CD_2Cl_2, ppm) δ = 196.5, 186.5, 166.4, 161.6, 151.9, 136.1, 135.2, 129.1, 127.2, 123.7, 122.3, 121.7, 120.2, 104.5, 28.0, 25.4;

^{95}Mo-NMR (26 MHz, CD_2Cl_2, ppm) δ = -25.2.

14.3 Catalytic Epoxidation Experiments

Epoxidation of olefins with MOF catalysts.

All four Mo@UiO composites (0.03 mmol; 34 mg for UiO-66, 51 mg for UiO-66 mixed, 89 mg for UiO-67 and 119 mg for UiO-67 mixed) were examined as catalysts for the epoxidation of *cis*-cyclooctene (3 mmol; 414 µL) and Mo@UiO-67 mixed additionally for styrene and 1-octene (3 mmol; 344 µL styrene, 471 µL 1-octene) in neat *tert*-butyl hydroperoxide (4.5 mmol; 818 µL, 5.5 M solution in decane) at 50 °C. Samples were taken after 4 h and analysed by ^{1}H NMR spectroscopy in $CDCl_3$.

Epoxidation of propylene with Mo@UiO-67 mixed.

Mo@UiO-67 mixed (0.1 mmol, 480 mg) was examined as catalyst for the epoxidation of propylene (10 mmol) in neat *tert*-butyl hydroperoxide (15 mmol, 2.73 mL, 5.5 M solution in decane) at 50 ℃. Samples were taken after 4 h and analysed by ^{1}H NMR spectroscopy in $CDCl_3$.

Kinetic study for Mo@UiO-67 mixed.

The reaction for the kinetic study was performed as described above. The resulting graph is displayed in Figure 7.11. TOF was determined for the sample taken after 15 min.

Kinetic study of the homogeneous catalyst [MoO_2(acac)(PhN=C-PhO)].[146]

Complex **14** (0.012 mmol, 5 mg) was examined as catalyst for the epoxidation of *cis*-cyclooctene (1.18 mmol, 154 µL) in neat *tert*-butyl hydroperoxide (2.36 mmol, 430 µL, 5.5 M solution in decane) at room temperature. The resulting graph is also displayed in Figure 7.11. TOF was determined for the sample taken after 5 minutes.

Leaching test for Mo@UiO-67.

Mo@UiO-67 (0.01 mmol) was examined for leaching by performing a catalytic reaction with *cis*-cyclooctene (1 mmol; 130 µL) in neat *tert*-butyl hydroperoxide (1.5 mmol, 273 µL, 5.5 M solution in decane) at 50 ℃. Samples were taken after 5 and 30 min. After that the solid catalyst was removed by filtration, the reaction mixture was kept at 50 ℃ for four more hours, a last sample was taken and analysed by ^{1}H NMR spectroscopy in $CDCl_3$.

15 Imidazolium Bromides

15.1 Synthesis

The imidazolium bromides and iodides (for **15a**, **19a** and **23a**) were synthesized according to literature procedures.[149–154,172] Sufficient purity of all compounds was verified with ^{1}H-, ^{13}C-NMR spectroscopy, and elemental analysis prior to conversion to imidazolium perrhenates or nitrates.

16 Imidazolium Perrhenates

16.1 Synthesis

The imidazolium perrhenates were prepared as described in literature.[137] The previously synthesized imidazolium bromides were transformed to the corresponding hydroxide analogues through an anion exchange resin and subsequently treated with 1.1 equiv. of NH_4ReO_4 at 70 °C for 24 h leading to water and ammonia as only by-products. Afterwards, all volatiles were removed in high vacuum at elevated temperatures and dichloromethane was added to the resulting residue of imidazolium perrhenate and excess of NH_4ReO_4. The insoluble NH_4ReO_4 was filtered off and the target compound was received after removing the volatiles in vacuo. All synthesized compounds were characterized by means of ^{1}H-, ^{13}C-NMR and IR spectroscopy, as well as elemental analysis, and melting point determination.

16.2 Analysis

1,3-Dimethylimidazolium perrhenate (15b):

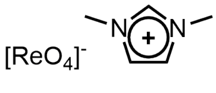

$C_5H_9N_2O_4Re$ (347.34 g/mol); 89 % yield of colorless powder; m.p.: 90 °C;

^{1}H-NMR (400 MHz, DMSO-d$_6$, ppm) δ = 9.02 (s, 1H, C*H*), 7.67 (d, ^3J(H,H) = 2 Hz, 2H, C*H*), 3.84 (s, 6H, CH_3);

^{13}C-NMR (101 MHz, $CDCl_3$, ppm) δ = 137.0, 123.5, 35.7;

IR (ATR, diamond crystal, neat, cm^{-1}) ν = 905 (Re=O asymmetric);

Elemental analysis (%) calcd.: C 17.29, H 2.61, N 8.07, O 18.42, Re 53.61; found: C 17.77, H 2.70, N 8.15, Re 52.75

1-Butyl-3-methylimidazolium perrhenate (16b):

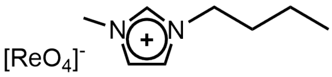

$C_8H_{15}N_2O_4Re$ (389.42 g/mol); 86 % yield of yellow liquid;

^{1}H-NMR (400 MHz, $CDCl_3$, ppm) δ = 8.92 (s, 1H, C*H*), 7.39 (s, 1H, C*H*), 7.36 (s, 1H, C*H*), 4.24 (t, ^3J(H,H) = 8 Hz, 2H, CH_2), 4.02 (s, 3H, CH_3), 1.89-1.81 (m, 2H, CH_2), 1.39-1.30 (m, 2H, CH_2), 0.97 (t, ^3J(H,H) = 7 Hz, 3H, CH_3);

^{13}C-NMR (101 MHz, $CDCl_3$, ppm) δ = 136.5, 123.9, 122.5, 50.3, 36.7, 32.1, 19.6, 13.5;

IR (ATR, diamond crystal, neat, cm^{-1}) ν = 892 (Re=O asymmetric);

Elemental analysis (%) calcd.: C 24.67, H 3.88, N 7.19, O 16.43, Re 47.82; found: C 24.98, H 3.81, N 7.06, Re 43.38.

1-Methyl-3-octylimidazolium perrhenate (17b):

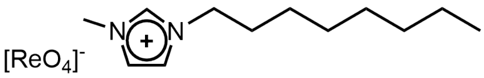

$C_{12}H_{23}N_2O_4Re$ (445.53 g/mol); 90 % yield of pale yellow liquid;

^{1}H-NMR (400 MHz, $CDCl_3$, ppm) δ = 8.85 (s, 1H, C*H*), 7.41 (s, 1H, C*H*), 7.36 (s, 1H, C*H*), 4.20 (t, ^3J(H,H) = 8 Hz, 2H, CH_2), 4.00 (s, 3H, CH_3), 1.89-1.79 (m, 2H, CH_2), 1.35-1.20 (m, 10H, CH_2), 0.84 (t, ^3J(H,H) = 8 Hz, 3H, CH_3);

^{13}C-NMR (101 MHz, $CDCl_3$, ppm) δ = 136.2, 124.0, 122.5, 50.5, 36.6, 31.7, 30.2, 29.0, 28.9, 26.3, 22.6, 14.1;

IR (ATR, diamond crystal, neat, cm^{-1}) ν = 895 (Re=O asymmetric);

Elemental analysis (%) calcd.: C 32.35, H 5.20, N 6.29, O 14.36, Re 41.79; found: C 32.60, H 5.30, N 6.31, Re 42.53.

1-Dodecyl-3-methylimidazolium perrhenate (18b):

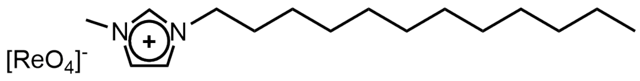

$C_{16}H_{31}N_2O_4Re$ (501.64 g/mol); 95 % yield of colorless powder; m.p.: 49 °C; **^{1}H-NMR** (400 MHz, $CDCl_3$, ppm) δ = 8.85 (s, 1H, C*H*), 7.40 (m, 1H, C*H*), 7.34 (m, 1H, C*H*), 4.21 (t, ${}^3J$(H,H) = 8 Hz, 2H, CH_2), 4.01 (s, 3H, CH_3), 1.89 (t, ${}^3J$(H,H) = 8 Hz, 2H, CH_2), 1.33–1.24 (m, 18H, CH_2), 0.86 (t, ${}^3J$(H,H) = 8 Hz, 3H, CH_3);
^{13}C-NMR (101 MHz, $CDCl_3$, ppm) δ = 136.4, 123.9, 122.4, 50.6, 36.7, 32.0, 30.3, 29.7, 29.7, 29.6, 29.5, 29,4, 29.1, 26.4, 22.8, 14.2;
IR (ATR, diamond crystal, neat, cm^{-1}) ν = 900 (Re=O asymmetric);
Elemental analysis (%) calcd.: C 38.31, H 6.23, N 5.58, O 12.76, Re 37.12; found: C 38.52, H 6.31, N 5.57, Re 37.14.

1,2,3-Trimethylimidazolium perrhenate (19b):

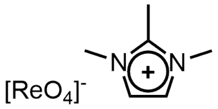

$C_6H_{11}N_2O_4Re$ (361.37 g/mol); 33 % yield of colorless powder; m.p.: 191 °C;
^{1}H-NMR (400 MHz, DMSO-d_6, ppm) δ = 7.24 (s, 2H, C*H*), 3.92 (s, 6H, CH_3), 2.76 (s, 3H, CH_3);
^{13}C-NMR (101 MHz, DMSO-d_6, ppm) δ = 144.8, 122.0, 34.8, 9.2;
IR (ATR, diamond crystal, neat, cm^{-1}) ν = 900 (Re=O asymmetric);
Elemental analysis (%) calcd.: C 19.94, H 3.07, N 7.75, O 17.71, Re 51.53; found: C 20.10, H 2.98, N 7.72, Re 51.63.

3-Butyl-1,2-dimethylimidazolium perrhenate (20b):

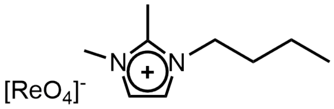

$C_9H_{17}N_2O_4Re$ (403.45 g/mol); 90 % yield of colorless powder; m.p.: 68 °C

^{1}H-NMR (400 MHz, $CDCl_3$, ppm) δ = 7.28 (d, ^3J(H,H) = 2 Hz, 1H, C*H*), 7.22 (d, ^3J(H,H) = 2 Hz, 1H, C*H*)), 4.12 (t, ^3J(H,H) = 8 Hz, 2H, CH_2), 3.89 (s, 3H, CH_3), 2.70 (s, 3H, CH_3), 1.84-1.76 (m, 2H, CH_2), 1.42-1.35 (m, 2H, CH_2), 1.00 (t, ^3J(H,H) = 7 Hz, 3H, CH_3);

^{13}C-NMR (101 MHz, $CDCl_3$, ppm) δ = 149.6, 122.8, 121.1, 48.9, 35.5, 31.7, 19.8, 13.7, 9.7;

IR (ATR, diamond crystal, neat, cm^{-1}) ν = 898 (Re=O asymmetric);

Elemental analysis (%) calcd.: C 26.79, H 4.25, N 6.94, O 15.86, Re 46.15; found: C 26.73, H 4.19, N 6.84, Re 46.90.

1,2-Dimethyl-3-octylimidazolium perrhenate (21b):

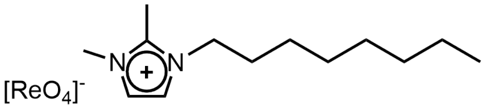

$C_{12}H_{25}N_2O_4Re$ (459.56 g/mol); 87 % yield of pale yellow oil;

^{1}H-NMR (400 MHz, $CDCl_3$, ppm) δ = 7.33 (d, ^3J(H,H) = 2 Hz, 1H, C*H*), 7.25 (d, ^3J(H,H) = 2 Hz, 1H, C*H*), 4.09 (t, ^3J(H,H) = 8 Hz, 2H, CH_2), 3.87 (s, 3H, CH_3), 2.67 (s, 3H, CH_3), 1.81-1.71 (m, 2H, CH_2), 1.40-1.20 (m, 10H, CH_2), 0.86 (t, ^3J(H,H) = 7 Hz, 3H, CH_3);

^{13}C-NMR (101 MHz, $CDCl_3$, ppm) δ = 143.7, 122.7, 120.9, 48.8, 35.3, 31.6, 29.6, 28.9, 26.3, 22.5, 14.0, 9.5;

IR (ATR, diamond crystal, neat, cm^{-1}) ν = 895 (Re=O asymmetric);

Elemental analysis (%) calcd.: C 33.98, H 5.48, N 6.10, O 13.93, Re 40.52; found: C 34.00, H 5.42, N 6.05, Re 40.50.

1,2-Dimethyl-3-dodecylimidazolium perrhenate (22b):

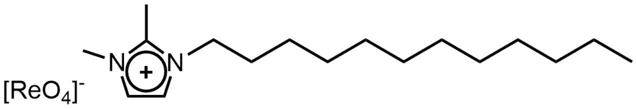

$C_{17}H_{33}N_2O_4Re$ (515.66); 90 % yield of colorless powder; m.p.: 50 °C;

^{1}H-NMR (400 MHz, $CDCl_3$, ppm) δ = 7.31 (d, ^3J(H,H) = 2 Hz, 1H, C*H*), 7.23 (d, ^3J(H,H) = 2 Hz, 1H, C*H*), 4.06 (t, ^3J(H,H) = 8 Hz, 2H, CH_2), 3.84 (s, 3H, CH_3), 2.64 (s, 3H, CH_3), 1.79-1.70 (m, 2H, CH_2), 1.30-1.20 (m, 18H, CH_2), 0.84 (t, ^3J(H,H) = 7 Hz, 3H, CH_3);

^{13}C-NMR (101 MHz, $CDCl_3$, ppm) δ = 143.8, 122.8, 121.0, 48.9, 35.3, 31.9, 29.8, 29.6, 29.6, 29.4, 29.3, 29.1, 26.4, 22.7, 14.2, 9.5;

IR (ATR, diamond crystal, neat, cm^{-1}) ν = 895 (Re=O asymmetric);

Elemental analysis (%) calcd.: C 39.60, H 6.45, N 5.43, O 12.41, Re 36.11; found: C 39.91, H 6.47, N 5.33, Re 36.44.

2-Butyl-1,3-dimethylimidazolium perrhenate (23b):

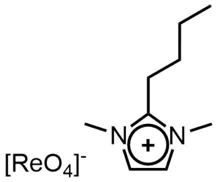

$C_9H_{17}N_2O_4Re$ (403.45 g/mol); 86 % yield of colorless powder; m.p.: 93 °C;

^{1}H NMR (400 MHz, DMSO-d_6, ppm) δ = 7.60 (s, 2H, C*H*), 3.79 (s, 6H, CH_3), 2.99 (t, ^3J(H,H) = 8 Hz, 2H, CH_2), 1.60-1.50 (m, 2H, CH_2), 1.42-1.30 (m, 2H, CH_2), 0.91 (t, ^3J(H,H) = 7 Hz, 3H, CH_3);

^{13}C-NMR (101 MHz, DMSO-d_6, ppm) δ = 144.8, 122.0, 34.8, 9.2;

IR (ATR, diamond crystal, neat, cm^{-1}) ν = 897 (Re=O asymmetric);

Elemental analysis (%) calcd.: C 26.79, H 4.25, N 6.94, O 15.86, Re 46.15; found: C 26.99, H 4.25, N 6.95, Re 45.92.

1,2-Dibutyl-3-methylimidazolium perrhenate (24b):

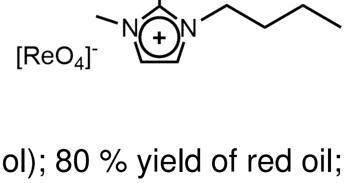

$C_{12}H_{23}N_2O_4Re$ (445.53 g/mol); 80 % yield of red oil;

^{1}H-NMR (400 MHz, $CDCl_3$, ppm) δ = 7.36 (s, 1H, C*H*), 7.31 (s, 1H, C*H*), 4.09 (t, ^3J(H,H) = 8 Hz, 2H, CH_2), 3.88 (s, 3H, CH_3), 3.00 (t, ^3J(H,H) = 8 Hz, 2H, CH_2), 1.83-1.75 (m, 2H, CH_2), 1.63-1.55 (m, 2H, CH_2), 1.50-1.35 (m, 4H, CH_2), 0.98 (t, ^3J(H,H) = 8 Hz, 6H, CH_3);

^{13}C-NMR (101 MHz, $CDCl_3$, ppm) δ = 146.9, 123.2, 121.1, 48.5, 35.3, 32.1, 29.2, 23.1, 22.6, 19.8, 13.7, 13.6;

IR (ATR, diamond crystal, neat, cm^{-1}) ν = 894 (Re=O asymmetric);

Elemental analysis (%) calcd.: C 32.50, H 4.77, N 6.32, O 14.43, Re 41.98; found: C 32.47, H 5.07, N 6.21, Re 41.89.

2-Butyl-1-methyl-3-octylimidazolium perrhenate (25b):

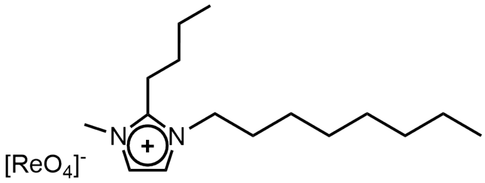

$C_{16}H_{31}N_2O_4Re$ (501.64 g/mol); 85 % yield of colorless powder; m.p.: 53 °C;

^{1}H-NMR (400 MHz, $CDCl_3$, ppm) δ = 7.33 (d, ^3J(H,H) = 2 Hz, 1H, C*H*), 7.28 (d, ^3J(H,H) = 2 Hz, 1H, C*H*), 4.04 (t, ^3J(H,H) = 8 Hz, 2H, CH_2), 3.84 (s, 3H, CH_3), 2.96 (t, ^3J(H,H) = 8 Hz, 2H, CH_2), 1.80-1.75 (m, 2H, CH_2), 1.63-1.55 (m, 2H, CH_2), 1.47-1.37 (m, 2H, CH_2), 1.31-1.21 (m, 10H, CH_2), 0.93 (t, ^3J(H,H) = 7 Hz, 3H, CH_3), 0.81 (t, ^3J(H,H) = 7 Hz, 3H, CH_3);

^{13}C-NMR (101 MHz, $CDCl_3$, ppm) δ = 146.6, 123.1, 120.9, 48.6, 35.2, 31.6, 30.0, 29.1, 28.9, 28.9, 26.4, 23.0, 22.5, 22.4, 14.0, 13.5;

IR (ATR, diamond crystal, neat, cm^{-1}) ν = 894 (Re=O asymmetric);

Elemental analysis (%) calcd.: C 38.31, H 6.23, N 5.58, O 12.76, Re 37.12; found: C 38.43, H 6.71, N 5.64, Re 36.41.

2-Butyl-1-dodecyl-3-methylimidazolium perrhenate (26b):

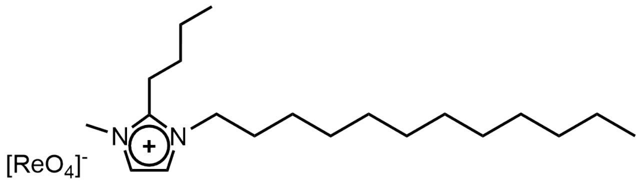

$C_{20}H_{39}N_2O_4Re$ (557.75 g/mol); 72 % yield of off-white powder; m.p.: 76 °C;

^{1}H-NMR (400 MHz, $CDCl_3$, ppm) δ = 7.38 (d, ^3J(H,H) = 2 Hz, 1H, C*H*), 7.28 (d, ^3J(H,H) = 2 Hz, 1H, C*H*), 4.07 (t, ^3J(H,H) = 8 Hz, 2H, CH_2), 3.90 (s, 3H, CH_3), 3.01 (t, ^3J(H,H) = 8 Hz, 2H, CH_2), 1.90-1.80 (m, 2H, CH_2), 1.68-1.58 (m, 2H, CH_2), 1.53-1.42 (m, 2H, CH_2), 1.40-1.20 (m, 18H, CH_2), 0.99 (t, ^3J(H,H) = 7 Hz, 3H, CH_3), 0.87 (t, ^3J(H,H) = 7 Hz, 3H, CH_3);

^{13}C-NMR (101 MHz, $CDCl_3$, ppm) δ = 146.9, 123.3, 121.0, 48.8, 35.4, 32.0, 30.2, 29.7,29.6, 29.5, 29.4, 29.2, 29.1, 26.6, 23.2, 22.6, 14.3, 13.7;

IR (ATR, diamond crystal, neat, cm^{-1}) ν = 902 (Re=O asymmetric);

Elemental analysis (%) calcd.: C 43.07, H 7.05, N 5.02, O 11.47, Re 33.39; found: C 43.45, H 7.17, N 5.06, Re 32.57.

16.3 Catalysis

Experimental Procedure for Catalytic Olefin Epoxidation

The corresponding catalyst (0.5 mmol) was placed in a glass tube equipped with a magnetic stir bar. Subsequently, the substrate (10.0 mmol) was added and the reaction mixture was heated to 70 °C. Finally, the oxidant (25.0 mmol) was added and the reaction mixture was kept at 70 °C for 4 and 24 hours. Continuous samples (0.1 mL) were taken from the top phase (substrate+product), mixed with an internal standard (1.0 mL) and isopropanol (0.9 mL), and analysed by GC.

17 Imidazolium Nitrates

17.1 Synthesis

The imidazolium nitrates were prepared as described in literature for the corresponding perrhenates.[137] The previously synthesized imidazolium bromides were transformed to the corresponding hydroxide analogues using an anion exchange resin and subsequently treated with 1.1 equiv. of NH_4NO_3 at 70 ℃ for 24 h, leading to water and ammonia as only by-products. Afterwards, all volatiles were removed in high vacuum at elevated temperatures and dichloromethane was added to the resulting residue of imidazolium perrhenate and excess of NH_4NO_3. The insoluble NH_4NO_3 was filtered off and the target compound received after removing the volatiles in vacuo. All synthesized compounds were characterized by means of ^{1}H- and ^{13}C-NMR as well as elemental analysis and melting point determination.

17.2 Analysis

1-Butyl-3-methylimidazolium nitrate (16c):

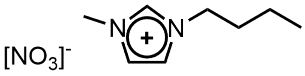

$C_8H_{15}N_3O_3$ (201.23 g/mol); 97 % yield of yellow liquid;

^{1}H-NMR (400 MHz, $CDCl_3$, ppm) δ = 9.93 (s, 1H, NC*H*N), 7.40 (t, ^{3}J(H,H) = 2 Hz, 1H, NC*H*), 7.33 (t, ^{3}J(H,H) = 2 Hz, 1H, NC*H*), 4.23 (t, ^{3}J(H,H) = 7 Hz, 2H, NCH_2), 4.01 (s, 3H, NCH_3), 1.93-1.80 (m, 2H, CH_2), 1.43-1.28 (m, 2H, CH_2), 0.95 (t, ^{3}J(H,H) = 7 Hz, 3H, $\mathrm{CH_2}$CH_3);

^{13}C-NMR (101 MHz, $CDCl_3$, ppm) δ = 138.36, 123.53, 122.02, 50.02, 36.48, 32.19, 19.56, 13.49;

Elemental analysis (%) calcd. (0.4 equiv. H_2O): C 46.10, H 7.64, N 20.16; found: C 45.77, H 7.25, N 20.85.

1-Octyl-3-methylimidazolium nitrate (17c):

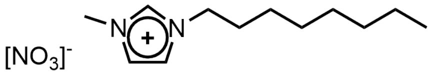

$C_{12}H_{23}N_3O_3$ (257.33 g/mol); 76 % yield of colorless liquid;

^{1}H-NMR (400 MHz, $CDCl_3$, ppm) δ = 10.05 (s, 1H,NC*H*N), 7.33 (t, ^3J(H,H) = 2 Hz, 1H, NC*H*), 7.26 (t, ^3J(H,H) = 2 Hz, 1H, NC*H*), 4.22 (t, ^3J(H,H) = 7.5 Hz, 2H, NCH_2), 4.02 (s, 3H, NCH_3), 1.93-1.84 (m, 2H, CH_2), 1.35-1.21 (m, 10H, CH_2), 0.87 (t, ^3J(H,H) = 7 Hz, 3H, CH_2CH_3);

^{13}C-NMR (101 MHz, $CDCl_3$, ppm) δ = 138.68, 123.36, 121.81, 50.37, 36.55, 31.79, 30.35, 29.13, 29.02, 26.37, 22.71, 14.19;

Elemental analysis (%) calcd.: C 56.01, H 9.01, N 16.33; found: C 55.20, H 9.00, N 16.22.

1-Dodecyl-3-methylimidazolium nitrate (18c):

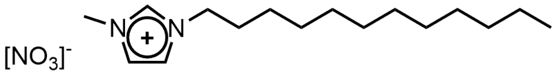

$C_{16}H_{31}N_3O_3$ (313.44 g/mol); 93 % yield of colorless solid;

^{1}H-NMR (400 MHz, $CDCl_3$, ppm) δ = 9.98 (s, 1H, NC*H*N), 7.40 (s, 1H, NC*H*), 7.31 (s, 1H, NC*H*), 4.24 (t, ^3J(H,H) = 7 Hz, 2H, NCH_2), 4.04 (s, 3H, NCH_3), 1.95-1.83 (m, 2H, CH_2), 1.38-1.22 (m, 18H, CH_2), 0.89 (t, ^3J(H,H) = 7 Hz, 3H, CH_2CH_3);

^{13}C-NMR (101 MHz, $CDCl_3$, ppm) δ = 123.01, 121.59, 50.48, 36.67, 32.05, 30.36, 29.73, 29.62, 29.49, 29.47, 29.08, 26.39, 22.83, 14.28;

Elemental analysis (%) calcd.: C 61.31, H 9.97, N 13.41; found: C 61.13, H 9.97, N 13.39.

1-Butyl-2,3-dimethylimidazolium nitrate (20c):

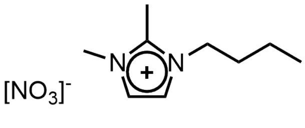

$C_9H_{17}N_3O_3$ (215.25 g/mol); 96 % yield of yellow liquid;

^{1}H-NMR (400 MHz, $CDCl_3$, ppm) δ = 7.47 (d, ^3J(H,H) = 2 Hz, 1H, NC*H*), 7.36 (d, ^3J(H,H) = 2 Hz, 1H, NC*H*), 4.11 (t, ^3J(H,H) = 7 Hz, 2H, NCH_2), 3.87 (s, 3H, NCH_3), 2.67 (s, 3H, CCH_3), 1.83-1.70 (m, 2H, CH_2), 1.42-1.30 (m, 2H, CH_2), 0.94 (t, ^3J(H,H) = 7 Hz, 3H, CH_2CH_3);

^{13}C-NMR (101 MHz, $CDCl_3$, ppm) δ = 143.92, 123.00, 121.16, 48.63, 35.45, 31.80, 19.70, 13.60, 9.76;

Elemental analysis (%) calcd. (0.67 equiv. H_2O): C 47.57, H 8.13, N 18.49; found: C 47.43, H 8.09, N 18.65.

1-Octyl-2,3-dimethylimidazolium nitrate (21c):

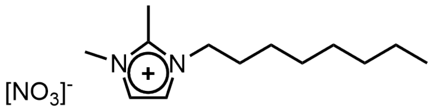

$C_{13}H_{25}N_3O_3$ (271.19 g/mol); 91 % yield of colorless solid;

^{1}H-NMR (400 MHz, $CDCl_3$, ppm) δ = 7.43 (d, ^3J(H,H) = 2 Hz, 1H, NC*H*), 7.26 (d, ^3J(H,H) = 2 Hz, 1H, NC*H*), 4.10 (t, ^3J(H,H) = 7 Hz, 2H, NCH_2), 3.91 (s, 3H, NCH_3), 2.70 (s, 3H, CCH_3), 1.85-1,77 (m, 2H, CH_2), 1.36-1.23 (m, 10H, CH_2), 0.87 (t, ^3J(H,H) = 7 Hz, 3H, CH_2CH_3);

^{13}C-NMR (101 MHz, $CDCl_3$, ppm) δ = 123.29, 121.26, 49.34, 35.96, 32.12, 30.18, 29.48, 29.42, 26.85, 23.03, 14.52, 10.28;

Elemental analysis (%) calcd.: C 57.54, H 9.29, N 15.49; found: C 56.96, H 9.24, N 15.30.

1-Dodecyl-2,3-dimethylimidazolium nitrate (22c):

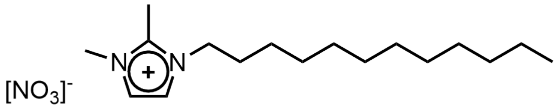

$C_{17}H_{33}N_3O_3$ (327.47 g/mol); 95 % yield of pale yellow solid; m.p.: 62 °C;

^{1}H-NMR (400 MHz, $CDCl_3$, ppm) δ = 7.42 (d, ^3J(H,H) = 2 Hz, 1H, NC*H*), 7.25 (d, ^3J(H,H) = 2 Hz, 1H, NC*H*), 4.10 (t, ^3J(H,H) = 7 Hz, 2H, NCH_2), 3.91 (s, 3H, NCH_3), 2.71 (s, 3H, CCH_3), 1.87-1.76 (m, 2H, CH_2), 1.39-1.20 (m, 18H, CH_2), 0.88 (t, ^3J(H,H) = 7 Hz, 3H, CH_2CH_3);

^{13}C-NMR (101 MHz, $CDCl_3$, ppm) δ = 122.97, 120.91, 49.05, 35.69, 32.04, 29.86, 29.72, 29.63, 29.51, 29.47, 29.15, 26.55, 22.83, 14.28, 10.02;

Elemental analysis (%) calcd.: C 62.35, H 10.16, N 12.83; found: C 62.53, H 10.32, N 12.81.

1,2-Dibutyl-3-methylimidazolium nitrate (24c):

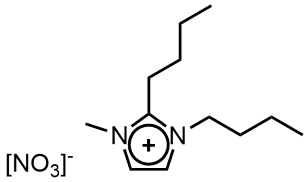

$C_{12}H_{23}N_3O_3$ (257.33 g/mol); 90 % yield of pale yellow liquid;

^{1}H-NMR (400 MHz, DMSO-d$_6$, ppm) δ = 7.73 (d, ^3J(H,H) = 2 Hz, 1H, NCH), 7.68 (d, ^3J(H,H) = 2 Hz, 1H, NCH), 4.12 (t, ^3J(H,H) = 7 Hz, 2H, NCH_2), 3.81 (s, 3H, NCH_3), 3.01 (t, ^3J(H,H) = 8 Hz, 2H, CCH_2), 1.77-1.67 (m, 2H, CH_2), 1.59-1.49 (m, 2H, CH_2), 1.44-1.34 (m, 2H, CH_2), 1.34-1.24 (m, 2H, CH_2), 0.91 (t, ^3J(H,H) = 7 Hz, 3H, CH_3), 0.90 (t, ^3J(H,H) = 7 Hz, 3H, CH_3);

^{13}C-NMR (101 MHz, DMSO-d$_6$, ppm) δ = 146.6, 122.9, 120.9, 47.1, 34.6, 31.6, 28.3, 22.0, 21.7, 18.9, 13.5, 13.4;

Elemental analysis (%) calcd. (1 equiv. H_2O): C 52.35, H 9.15, N 15.26; found: C 52.33, H 9.05, N 15.17.

1-Octyl-2-butyl-3-methylimidazolium nitrate (25c):

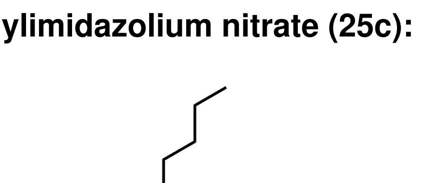

$C_{16}H_{31}N_3O_3$ (313.44 g/mol); 82 % yield of colorless solid;

^{1}H-NMR (400 MHz, $CDCl_3$, ppm) δ = 7.61 (d, ^3J(H,H) = 2 Hz, 1H, NC*H*), 7.38 (d, ^3J(H,H) = 2 Hz, 1H, NC*H*), 4.11 (t, ^3J(H,H) = 7 Hz, 2H, NCH_2), 3.96 (s, 3H, NCH_3), 3.05 (t, ^3J(H,H) = 7 Hz, 2H, CCH_2), 1.91-1.82 (m, 2H, CH_2), 1.69-1.59 (m, 2H, CH_2), 1.55-1.44 (m, 2H, CH_2), 1.42-1.23 (m, 10H, CH_2), 1.01 (t, ^3J(H,H) = 7 Hz, 3H, CH_2CH_3), 0.90 (t, ^3J(H,H) = 7 Hz, 3H, CH_2CH_3);

^{13}C-NMR (101 MHz, $CDCl_3$, ppm) δ = 123.61, 120.99, 48.73, 35.55, 31.80, 30.22, 29.32, 29.15, 29.11, 26.59, 23.32, 22.72, 22.64, 14.20, 13.71;

Elemental analysis (%) calcd. (0.5 equiv. H_2O): C 59.60, H 10.00, N 13.03; found: C 59.5, H 9.99, N 12.78.

2-Butyl-1-dodecyl-3-methylimidazolium nitrate (26c):

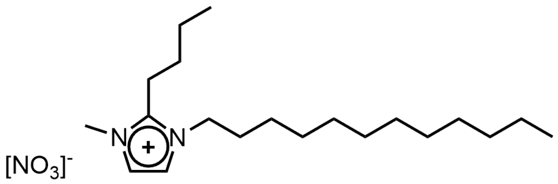

$C_{20}H_{39}N_3O_3$ (369.55 g/mol); 89 % yield of colorless solid;

^{1}H-NMR (400 MHz, DMSO-d_6, ppm) δ = 7.71 (d, ^3J(H,H) = 2 Hz, 1H, NC*H*), 7.66 (d, ^3J(H,H) = 2 Hz, 1H, NC*H*), 4.10 (t, ^3J(H,H) = 7.5 Hz, 2H, NCH_2), 3.80 (s, 3H, NCH_3), 3.06-2.94 (m, 2H, CH_2), 1.78-1.67 (m, 2H, CH_2), 1.59-1.48 (m, 2H, CH_2), 1.44-1.33 (m, 2H, CH_2), 1.31-1.19 (m, 18H, CH_2), 0.91 (t, ^3J(H,H) = 7 Hz, 3H, CH_3), 0.88-0.82 (m, 3H, CH_3);

^{13}C-NMR (101 MHz, DMSO-d_6, ppm) δ = 146.5, 122.9, 120.9, 47.3, 34.6, 31.3, 29.5, 29.0, 28.9, 28.8, 28.7, 28.5, 28.4, 25.6, 22.1, 22.0, 21.7, 13.9, 13.5;

Elemental analysis (%) calcd.: C 65.00, H 10.64, N 11.37; found: C 64.69, H 10.75, N 11.54.

1-Hexadecyl-3-methylimidazolium nitrate (27c):

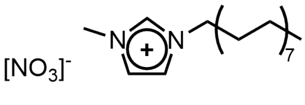

$C_{20}H_{39}N_3O_3$ (369.55 g/mol); 96 % yield of pale yellow solid;

^{1}H-NMR (400 MHz, $CDCl_3$, ppm) δ = 10.21 (s, 1H, NC*H*N), 7.26 (s, 1H, NC*H*), 7.23 (s, 1H, NC*H*), 4.26 (t, ^3J(H,H) = 7 Hz, 2H, NCH_2), 4.05 (s, 3H, NCH_3), 1.96-1.85 (m, 2H, CH_2), 1.38-1.20 (m, 26H, CH_2), 0.90 (t, ^3J(H,H) = 7 Hz, 3H, CH_2CH_3);

^{13}C-NMR (101 MHz, $CDCl_3$, ppm) δ = 139.11, 122.90, 121.47, 50.33, 36.50, 31.94, 30.22, 29.70, 29.67, 29.60, 29.50, 29.37, 28.95, 26.26, 22.71, 14.15;

Elemental analysis (%) calcd. (0.25 equiv. H_2O): C 64.22, H 10.64, N 11.23; found: C 64.76, H 10.68, N 11.16.

1-Hexadecyl-2,3-dimethylimidazolium nitrate (28c):

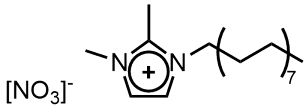

$C_{21}H_{41}N_3O_3$ (383.58 g/mol); 93 % yield of pale yellow solid;

^{1}H-NMR (400 MHz, DMSO-d_6, ppm) δ = 7.65 (d, ^3J(H,H) = 2 Hz, 1H, NC*H*), 7.62 (d, ^3J(H,H) = 2 Hz, 1H, NC*H*), 4.10 (t, ^3J(H,H) = 7 Hz, 2H, NCH_2), 3.75 (s, 3H, NCH_3), 2.58 (s, 3H, CCH_3), 1.75-1.64 (m, 2H, CH_2), 1.33-1.18 (m, 26H, CH_2), 0.86 (t, ^3J(H,H) = 7 Hz, 3H, CH_2CH_3);

^{13}C-NMR (101 MHz, DMSO-d_6, ppm) δ = 122.76, 121.32, 47.94, 35.13, 31.76, 29.65, 29.51, 29.47, 29.35, 29.17, 28.96, 26.06, 22.56, 14.43, 9.59;

Elemental analysis (%) calcd. (0.5 equiv. H_2O): C 64.25, H 10.78, N 10.70; found: C 64.22, H 10.75, N 10.46.

1,3-Dioctylimidazolium nitrate (29c):

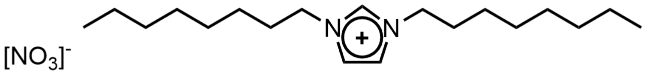

$C_{19}H_{37}N_3O_3$ (355.52 g/mol); yield: 82 % of yellow oil;

^{1}H-NMR (400 MHz, DMSO-d_6, ppm) δ = 9.28 (s, 1H, NC*H*N), 7.83 (s, 2H, NC*H*), 4.17 (t, ^3J(H,H) = 7 Hz, 4H, NCH_2), 1.85-1.74 (m, 4H, CH_2), 1.33-1.15 (m, 20H, CH_2), 0.85 (t, ^3J(H,H) = 7 Hz, 6H, CH_2CH_3);

^{13}C-NMR (101 MHz, $CDCl_3$, ppm) δ = 136.5, 122.9, 49.3, 31.6, 29.7, 29.0, 28.8, 25.9, 22.5, 14.4;

Elemental analysis (%) calcd. (0.5 equiv. H_2O): C 62.60, H 10.51, N 11.53; found: C 62.53, H 10.46, N 11.49.

1,3-Dioctyl-2-methylimidazolium nitrate (30c):

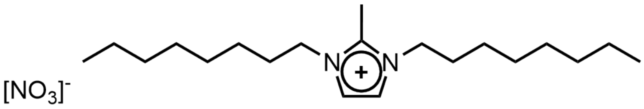

$C_{20}H_{39}N_3O_3$ (369.55 g/mol); 91 % yield of pale brown oil;

^{1}H-NMR (400 MHz, DMSO-d_6, ppm) δ = 7.72 (s, 2H, NC*H*), 4.11 (t, ^3J(H,H) = 7 Hz, 4H, NC*H*$_2$), 1.80-1.66 (m, 4H, C*H*$_2$), 1.36-1.16 (m, 20H, C*H*$_2$), 0.85 (t, ^3J(H,H) = 7 Hz, 6H, CH_2CH_3);

^{13}C-NMR (101 MHz, $CDCl_3$, ppm) δ = 144.1, 121.8, 47.9, 31.6, 29.5, 29.0, 28.9, 26.1, 22.5, 14.4, 9.6;

Elemental analysis (%) calcd. (1 equiv. H_2O): C 61.98, H 10.66, N 10.84; found: C 61.86, H 10.50, N 11.07.

1-(2,3,4,5,6-pentafluoro)benzyl-3-octylimidazolium nitrate (31c):

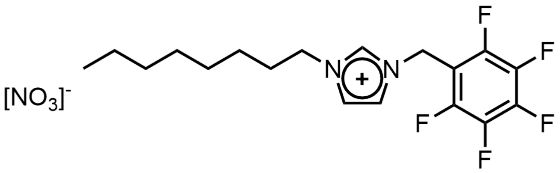

$C_{18}H_{22}F_5N_3O_3$ (423.16 g/mol); 93 % yield of colorless oil;

^{1}H-NMR (400 MHz, DMSO-d_6, ppm) δ = 9.34 (s, 1H, NC*H*N), 7.87 (s, 1H, NC*H*), 7.83 (s, 1H, NC*H*), 5.66 (m, 2H, C*H*$_2$), 4.18 (t, ^3J(H,H) = 7 Hz, 2H, NC*H*$_2$), 1.78 (p, ^3J(H,H) = 7 Hz, 2H, C*H*$_2$), 1.34-1.15 (m, 10H, C*H*$_2$), 0.86 (t, ^3J(H,H) = 7 Hz, 6H, CH_2CH_3);

^{13}C-NMR (101 MHz, DMSO-d_6, ppm) δ = 137.2, 123.3, 49.5, 31.6, 29.7, 29.0, 28.7, 25.9, 22.5, 14.4;

Elemental analysis (%) calcd. (0.5 equiv. H_2O): C 50.00, H 5.36, F 21.97, N 9.72; found: C 50.04, H 5.29, F 22.20, N 9.67.

1-Benzyl-2,3-dimethylimidazolium nitrate (32c):

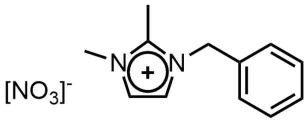

$C_{12}H_{15}N_3O_3$ (249.27 g/mol); 95 % yield of pale yellow solid; m.p.: 78 °C;

^{1}H-NMR (400 MHz, DMSO-d_6, ppm) δ = 7.71 (d, ^3J(H,H) = 2 Hz, 1H, NC*H*), 7.66 (d, ^3J(H,H) = 2 Hz, 1H, NC*H*), 7.44-7.31 (m, 5H, Ar), 5.41 (s, 2H, NCH_2), 3.76 (s, 3H, NCH_3), 2.95 (s, 3H, CCH_3);

^{13}C-NMR (101 MHz, DMSO-d_6, ppm) δ = 144.7, 134.6, 129.0, 128.5, 127.7, 122.7, 121.3, 50.6, 34.8, 9.5;

Elemental analysis (%) calcd.: C 57.82, H 6.07, N 16.86; found: C 57.08, H 6.00, N 16.50.

1,2-Dimethyl-3-pentafluorobenzylimidazolium nitrate (33c):

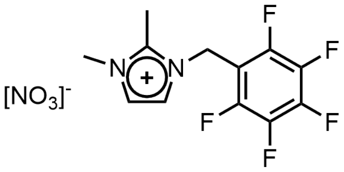

$C_{12}H_{10}F_5N_3O_3$ (339.22 g/mol); 88 % yield of colorless solid; m.p.: 121 °C;

^{1}H-NMR (400 MHz, DMSO-d_6, ppm) δ = 7.67 (d, ^3J(H,H) = 2 Hz, 1H, NC*H*), 7.63 (d, ^3J(H,H) = 2 Hz, 1H, NC*H*), 5.60 (s, 2H, NCH_2), 3.76 (s, 3H, NCH_3), 2.61 (s, 3H, CCH_3);

^{13}C-NMR (101 MHz, DMSO-d_6, ppm) δ = 145.3, 122.7, 121.3, 34.9, 9.27;

^{19}F-NMR (101 MHz, DMSO-d_6, ppm) δ = -140.8, -149.5, -159.1;

Elemental analysis (%) calcd.: C 42.49, H 2.97, N 12.39, F 28.00; found: C 41.91, H 2.83, N 12.35, F 28.30.

References

[1] F. Cavani and J. H. Teles, *ChemSusChem*, 2009, **2**, 508–534.

[2] T. A. Nijhuis, M. Makkee, J. A. Moulijn and B. M. Weckhuysen, *Ind. Eng. Chem. Res.*, 2006, **45**, 3447–3459.

[3] *Catalysts for Fine Chemical Synthesis*, ed. S. M. Roberts and J. Whittall, vol. 5.

[4] M. R. C. ltd, *World Propylene Oxide (PO) Market to See Sustained Growth in Years Ahead*, 2014.

[5] P. J. Carlberg, H. L. Crampton, A. Forlin, E. PEDERNERA and C. E. MEZA, 2013.

[6] W. F. Richey, in *Kirk-Othmer: Encyclopedia of Chemical Technology*, Kirk-Othmer, New York, 4th edn., 1994, vol. 6, p. 140.

[7] E. Bartholome, W. Koehler, A. May and G. Stoeckelmann, 1971.

[8] E. I. Korchak and M. Pell, 1965.

[9] W. S. Dubner and R. N. Cochran, 1993.

[10] J. J. Van Der Sluis, 1999.

[11] J. Kollar, 1966.

[12] E. T. Marquis, K. P. Keating, J. F. Knifton, W. A. Smith, J. R. Sanderson and J. Lustri, 1990.

[13] P. Bassler, H.-G. Göbbel and M. Weidenbach, *Chem. Eng. Trans.*, 2010, **21**, 571–576.

[14] P. Bassler, A. Berg, A. Rehfinger, N. Rieber, P. Rudolf and J. H. Teles, 2002.

[15] P. Bassler, W. Harder, P. Resch, N. Rieber, W. Ruppel, J. H. Teles, A. Walch, A. Wenzel and P. Zehner, 2002.

[16] R. Patrascu, S. Astori and M. M. Weidenbach, 2004.

[17] J. P. Dever, K. F. George, W. C. Hoffman and H. Soo, in *Kirk-Othmer: Encyclopedia of Chemical Technology*, Kirk-Othmer, New York, 4th edn., 1995, vol. 9, p. 915.

[18] S. Huber, M. Cokoja and F. E. Kühn, *J. Organomet. Chem.*, 2014, **751**, 25–32.

[19] S. A. Hauser, M. Cokoja and F. E. Kühn, *Catal. Sci. Technol.*, 2013, **3**, 552–561.

[20] J. W. Kück, A. Raba, I. I. E. Markovits, M. Cokoja and F. E. Kühn, *ChemCatChem*, 2014, **6**, 1882–1886.

[21] S. Krackl, A. Company, S. Enthaler and M. Driess, *ChemCatChem*, 2011, **3**, 1186–1192.

[22] D. Betz, A. Raith, M. Cokoja and F. E. Kühn, *ChemSusChem*, 2010, **3**, 559–562.

[23] P. Altmann, M. Cokoja and F. E. Kühn, *Eur. J. Inorg. Chem.*, 2012, **2012**, 3235–3239.

[24] A. Schmidt, N. Grover, T. K. Zimmermann, L. Graser, M. Cokoja, A. Pöthig and F. E. Kühn, *J. Catal.*, 2014, **319**, 119–126.

[25] W. A. Herrmann, R. M. Kratzer, H. Ding, W. R. Thiel and H. Glas, *J. Organomet. Chem.*, 1998, **555**, 293–295.

[26] I. R. Beattie and P. J. Jones, *Inorg. Chem.*, 1979, **18**, 2318–2319.

[27] W. A. Herrmann, J. G. Kuchler, J. K. Felixberger, E. Herdtweck and W. Wagner, *Angew. Chem. Int. Ed. Engl.*, 1988, **27**, 394–396.

[28] W. A. Herrmann, A. M. J. Rost, J. K. M. Mitterpleininger, N. Szesni, S. Sturm, R. W. Fischer and F. E. Kühn, *Angew. Chem. Int. Ed. Engl.*, 2007, **46**, 7301–7303.

[29] W. A. Herrmann, W. Wagner, U. N. Flessner, U. Volkhardt and H. Komber, *Angew. Chem. Int. Ed. Engl.*, 1991, **30**, 1636–1638.

[30] Z. Zhu and J. H. Espenson, *J. Org. Chem.*, 1996, **61**, 324–328.

[31] A. M. Santos, C. C. Romão and F. E. Kühn, *J. Am. Chem. Soc.*, 2003, **125**, 2414–2415.

[32] F. E. Kühn and A. M. Santos, *Mini-Rev. Org. Chem.*, 2004, **1**, 55–64.

[33] S. Vkuturi, G. Chapman, I. Ahmad and K. M. Nicholas, *Inorg. Chem.*, 2010, **49**, 4744–4746.

[34] I. Ahmad, G. Chapman and K. M. Nicholas, *Organometallics*, 2011, **30**, 2810–2818.

[35] P. Liu and K. M. Nicholas, *Organometallics*, 2013, **32**, 1821–1831.

[36] R. G. Harms, I. I. E. Markovits, M. Drees, W. A. Herrmann, M. Cokoja and F. E. Kühn, *ChemSusChem*, 2014, **7**, 429–434.

[37] F. E. Kühn, A. Scherbaum and W. A. Herrmann, *J. Organomet. Chem.*, 2004, **689**, 4149–4164.

[38] W. A. Herrmann, R. W. Fischer and D. W. Marz, *Angew. Chem. Int. Ed. Engl.*, 1991, **30**, 1638–1641.

[39] H.-J. Lee, T.-P. Shi, D. H. Busch and B. Subramaniam, *Chem. Eng. Sci.*, 2007, **62**, 7282–7289.

[40] I. I. E. Markovits, M. H. Anthofer, H. Kolding, M. Cokoja, A. Pöthig, A. Raba, W. A. Herrmann, R. Fehrmann and F. E. Kühn, *Catal. Sci. Technol.*, 2014, **4**, 3845–3849.

[41] H. Mimoun, I. Seree de Roch and L. Sajus, *Tetrahedron*, 1970, **26**, 37–50.

[42] K. B. Sharpless, J. M. Townsend and D. R. Williams, *J. Am. Chem. Soc.*, 1972, **94**, 295–296.

[43] W. R. Thiel and T. Priermeier, *Angew. Chem. Int. Ed. Engl.*, 1995, **34**, 1737–1738.

[44] W. R. Thiel, *J. Mol. Catal. A: Chem.*, 1997, **117**, 449–454.

[45] W. R. Thiel and J. Eppinger, *Chem. Eur. J.*, 1997, **3**, 696–705.

[46] A. Comas-Vives, A. Lledós and R. Poli, *Chem. Eur. J.*, 2010, **16**, 2147–2158.

[47] P. J. Costa, M. J. Calhorda and F. E. Kühn, *Organometallics*, 2010, **29**, 303–311.

[48] J. Morlot, N. Uyttebroeck, D. Agustin and R. Poli, *ChemCatChem*, 2013, **5**, 601–611.

[49] M. H. Valkenberg and W. F. Hölderich, *Catal. Rev.*, 2002, **44**, 321–374.

[50] R. K. Rana and B. Viswanathan, *Catal. Lett.*, 1998, **52**, 25–29.

[51] P. Ferreira, I. S. Gonçlves, F. E. Kühn, A. D. Lopes, M. A. Martins, M. Pillinger, A. Pina, J. a. Rocha, C. C. Romão, A. M. Santos, T. M. Santos and A. A. Valente, *Eur. J. Inorg. Chem.*, 2000, **2000**, 2263–2270.

[52] M. Jia and W. R. Thiel, *Chem. Commun.*, 2002, **0**, 2392–2393.

[53] A. Sakthivel, J. Zhao, M. Hanzlik and F. E. Kühn, *Dalton Trans.*, 2004, 3338–3341.

[54] A. Taguchi and F. Schüth, *Microporous Mesoporous Mater.*, 2005, **77**, 1–45.

[55] M. Masteri-Farahani, F. Farzaneh and M. Ghandi, *J. Mol. Catal. A: Chem.*, 2003, **192**, 103–111.

[56] P. Célestin Bakala, E. Briot, L. Salles and J.-M. Brégeault, *Appl. Catal., A*, 2006, **300**, 91–99.

[57] M. Bagherzadeh, M. Zare, T. Salemnoush, S. Özkar and S. Akbayrak, *Appl. Catal., A*, 2014, **475**, 55–62.

[58] J. Zhang, P. Jiang, Y. Shen, W. Zhang and X. Li, *Microporous Mesoporous Mater.*, 2015, **206**, 161–169.

[59] J. Sobczak and J. J. Ziólkowski, *J. Mol. Catal.*, 1977, **3**, 165–172.

[60] S. Ivanov, R. Boeva and S. Tanielyan, *J. Catal.*, 1979, **56**, 150–159.

[61] S. V. Kotov, S. Boneva and T. Kolev, *J. Mol. Catal. A: Chem.*, 2000, **154**, 121–129.

[62] K. G. Vassilev, D. K. Dimov, R. T. Stamenova, R. S. Boeva and C. B. Tsvetanov, *J. Polym. Sci. A Polym. Chem.*, 1986, **24**, 3541–3554.

[63] R. T. Stamenova, C. B. Tsvetanov, K. G. Vassilev, S. K. Tanielyan and S. K. Ivanov, *J. Appl. Polym. Sci.*, 1991, **42**, 807–812.

[64] Y. Kurusu and Y. Masuyama, *J. Macromol. Sci. Chem.*, 1989, **26**, 391–403.

[65] M. M. Miller and D. C. Sherrington, *J. Catal.*, 1995, **152**, 368–376.

[66] S. Tangestaninejad, M. H. Habibi, V. Mirkhani, M. Moghadam and G. Grivani, *Inorg. Chem. Commun.*, 2006, **9**, 575–578.

[67] R. Mbeleck, K. Ambroziak, B. Saha and D. C. Sherrington, *React. Funct. Polym.*, 2007, **67**, 1448–1457.

[68] M. Mohammadikish, M. Masteri-Farahani and S. Mahdavi, *J. Magn. Magn. Mater.*, 2014, **354**, 317–323.

[69] M. Moghadam, S. Tangestaninejad, V. Mirkhani, I. Mohammadpoor-Baltork, A. Mirjafari and N. S. Mirbagheri, *J. Mol. Catal. A: Chem.*, 2010, **329**, 44–49.

[70] K. R. Jain and F. E. Kühn, *Dalton Trans.*, 2008, 2221–2227.

[71] Y. Kinoshita, I. Matsubara, T. Higuchi and Y. Saito, *Bull. Chem. Soc. Jpn.*, 1959, **32**, 1221–1226.

[72] A. A. Berlin and N. G. Matveeva, *Russ. Chem. Rev.*, 1960, **29**, 119.

[73] D. B. Sowerby and L. F. Audrieth, *J. Chem. Educ.*, 1960, **37**, 134.

[74] E. A. Tomic, *J. Appl. Polym. Sci.*, 1965, **9**, 3745–3752.

[75] J. E. Bailar, in *Preparative Inorganic Reactions*, ed. W. Jolly, Interscience, New York, 1964, vol. 1, pp. 1–27.

[76] B. F. Hoskins and R. Robson, *J. Am. Chem. Soc.*, 1990, **112**, 1546–1554.

[77] S. R. Batten and R. Robson, *Angew. Chem. Int. Ed. Engl.*, 1998, **37**, 1460–1494.

[78] H. Li, M. Eddaoudi, M. O'Keeffe and O. M. Yaghi, *Nature*, 1999, **402**, 276–279.

[79] A. Corma, H. García and F. X. Llabrés i Xamena, *Chem. Rev.*, 2010, **110**, 4606–4655.

[80] J. L. C. Rowsell and O. M. Yaghi, *Microporous Mesoporous Mater.*, 2004, **73**, 3 – 14.

[81] S. Kitagawa and M. Kondo, *Bull. Chem. Soc. Jpn.*, 1998, **71**, 1739–1753.

[82] S. Kitagawa, R. Kitaura and S.-i. Noro, *Angew. Chem. Int. Ed. Engl.*, 2004, **43**, 2334–2375.

[83] M. J. Ingleson, J. P. Barrio, J.-B. Guilbaud, Y. Z. Khimyak and M. J. Rosseinsky, *Chem. Commun.*, 2008, 2680–2682.

[84] J. H. Cavka, S. Jakobsen, U. Olsbye, N. Guillou, C. Lamberti, S. Bordiga and K. P. Lillerud, *J. Am. Chem. Soc.*, 2008, **130**, 13850–13851.

[85] S. M. Hawxwell, G. M. Espallargas, D. Bradshaw, M. J. Rosseinsky, T. J. Prior, A. J. Florence, J. v. d. Streek and L. Brammer, *Chem. Commun.*, 2007, 1532–1534.

[86] C. A. Black, L. R. Hanton and M. D. Spicer, *Chem. Commun.*, 2007, 3171–3173.

[87] P. Ren, M.-L. Liu, J. Zhang, W. Shi, P. Cheng, D.-Z. Liao and S.-P. Yan, *Dalton Trans.*, 2008, 4711–4713.

[88] S.-H. Cho, B. Ma, S. T. Nguyen, J. T. Hupp and T. E. Albrecht-Schmitt, *Chem. Commun.*, 2006, 2563–2565.

[89] T. Bogaerts, A. V. Y.-D. Deyne, Y.-Y. Liu, F. Lynen, V. V. Speybroeck and P. V. D. Voort, *Chem. Commun.*, 2013, **49**, 8021–8023.

[90] A. M. Shultz, A. A. Sarjeant, O. K. Farha, J. T. Hupp and S. T. Nguyen, *J. Am. Chem. Soc.*, 2011, **133**, 13252–13255.

[91] S. Bhattacharjee, D.-A. Yang and W.-S. Ahn, *Chem. Commun.*, 2011, **47**, 3637–3639.

[92] K. Leus, G. Vanhaelewyn, T. Bogaerts, Y.-Y. Liu, D. Esquivel, F. Callens, G. B. Marin, V. Van Speybroeck, H. Vrielinck and P. Van Der Voort, *Catal. Today*, 2013, **208**, 97–105.

[93] K. Leus, Y.-Y. Liu, M. Meledina, S. Turner, G. Van Tendeloo and P. Van Der Voort, *J. Catal.*, 2014, **316**, 201–209.

[94] P. Neves, A. C. Gomes, T. R. Amarante, F. A. A. Paz, M. Pillinger, I. S. Gonçalves and A. A. Valente, *Microporous Mesoporous Mater.*, 2015, **202**, 106–114.

[95] M. Saito, T. Toyao, K. Ueda, T. Kamegawa, Y. Horiuchi and M. Matsuoka, *Dalton Trans.*, 2013, **42**, 9444–9447.

[96] M. Kandiah, M. H. Nilsen, S. Usseglio, S. Jakobsen, U. Olsbye, M. Tilset, C. Larabi, E. A. Quadrelli, F. Bonino and K. P. Lillerud, *Chem. Mater.*, 2010, **22**, 6632–6640.

[97] S. J. Garibay and S. M. Cohen, *Chem. Commun.*, 2010, **46**, 7700–7702.

[98] M. Puchberger, F. R. Kogler, M. Jupa, S. Gross, H. Fric, G. Kickelbick and U. Schubert, *Eur. J. Inorg. Chem.*, 2006, **2006**, 3283–3293.

[99] A. Schaate, P. Roy, A. Godt, J. Lippke, F. Waltz, M. Wiebcke and P. Behrens, *Chem. Eur. J.*, 2011, **17**, 6643–6651.

[100] M. Servalli, M. Ranocchiari and J. A. V. Bokhoven, *Chem. Commun.*, 2012, **48**, 1904–1906.

[101] X. Zhang, F. X. Llabrés i Xamena and A. Corma, *J. Catal.*, 2009, **265**, 155–160.

[102] J. Canivet, S. Aguado, Y. Schuurman and D. Farrusseng, *J. Am. Chem. Soc.*, 2013, **135**, 4195–4198.

[103] M. Pintado-Sierra, A. M. Rasero-Almansa, A. Corma, M. Iglesias and F. Sánchez, *J. Catal.*, 2013, **299**, 137–145.

[104] P. Walden, *Bull. Acad. Imper. Sci. St. Pétersbourg*, 1914, **8**, 405–422.

[105] J. S. Wilkes, J. A. Levisky, R. A. Wilson and C. L. Hussey, *Inorg. Chem.*, 1982, **21**, 1263–1264.

[106] J. S. Wilkes and M. J. Zaworotko, *J. Chem. Soc., Chem. Commun.*, 1992, 965–967.

[107] J. Ranke, S. Stolte, R. Störmann, J. Arning and B. Jastorff, *Chem. Rev.*, 2007, **107**, 2183–2206.

[108] S. Stolte, J. Arning, U. Bottin-Weber, M. Matzke, F. Stock, K. Thiele, M. Uerdingen, U. Welz-Biermann, B. Jastorff and J. Ranke, *Green Chem.*, 2006, **8**, 621–629.

[109] R. P. Swatloski, J. D. Holbrey and R. D. Rogers, *Green Chem.*, 2003, **5**, 361–363.

[110] J. G. Huddleston, A. E. Visser, W. M. Reichert, H. D. Willauer, G. A. Broker and R. D. Rogers, *Green Chem.*, 2001, **3**, 156–164.

[111] N. V. Plechkova and K. R. Seddon, *Chem. Soc. Rev.*, 2007, **37**, 123–150.

[112] J. A. Boon, J. A. Levisky, J. L. Pflug and J. S. Wilkes, *J. Org. Chem.*, 1986, **51**, 480–483.

[113] S. E. Fry and N. J. Pienta, *J. Am. Chem. Soc.*, 1985, **107**, 6399–6400.

[114] Y. Chauvin, B. Gilbert and I. Guibard, *J. Chem. Soc., Chem. Commun.*, 1990, 1715–1716.

[115] C. P. Mehnert, *Chem. Eur. J.*, 2005, **11**, 50–56.

[116] H.-P. Steinrück, J. Libuda, P. Wasserscheid, T. Cremer, C. Kolbeck, M. Laurin, F. Maier, M. Sobota, P. S. Schulz and M. Stark, *Adv. Mater.*, 2011, **23**, 2571–2587.

[117] V. I. Pârvulescu and C. Hardacre, *Chem. Rev.*, 2007, **107**, 2615–2665.

[118] J. G. Huddleston and R. D. Rogers, *Chem. Commun.*, 1998, 1765–1766.

[119] K. E. Gutowski, G. A. Broker, H. D. Willauer, J. G. Huddleston, R. P. Swatloski, J. D. Holbrey and R. D. Rogers, *J. Am. Chem. Soc.*, 2003, **125**, 6632–6633.

[120] M. J. Earle, P. B. McCormac and K. R. Seddon, *Green Chem.*, 1999, **1**, 23–25.

[121] M. J. Earle and K. R. Seddon, *Pure Appl. Chem*, 2000, **72**, 1391–1398.

[122] M. J. Earle, K. R. Seddon, C. J. Adams and G. Roberts, *Chem. Commun.*, 1998, 2097–2098.

[123] T. Welton, *Coord. Chem. Rev.*, 2004, **248**, 2459–2477.

[124] T. Welton, *Chem. Rev.*, 1999, **99**, 2071–2084.

[125] J. P. Hallett and T. Welton, *Chem. Rev.*, 2011, **111**, 3508–3576.

[126] P. Wasserscheid and W. Keim, *Angew. Chem. Int. Ed. Engl.*, 2000, **39**, 3772–3789.

[127] J. Dupont, R. F. de Souza and P. A. Z. Suarez, *Chem. Rev.*, 2002, **102**, 3667–3692.

[128] R. Sheldon, *Chem. Commun.*, 2001, 2399–2407.

[129] S. Liu and J. Xiao, *J. Mol. Catal. A: Chem.*, 2007, **270**, 1–43.

[130] Q. Zhang, S. Zhang and Y. Deng, *Green Chem.*, 2011, **13**, 2619–2637.

[131] R. D. Rogers and K. R. Seddon, *Science*, 2003, **302**, 792–793.

[132] M. Maase, K. Massonne, K. Halbritter, R. Noe, M. Bartsch, W. Siegel, V. Stegmann, M. Flores, O. Huttenloch and M. Becker, 2003.

[133] C. E. Song and E. J. Roh, *Chem. Commun.*, 2000, 837–838.

[134] D. Betz, P. Altmann, M. Cokoja, W. A. Herrmann and F. E. Kühn, *Coord. Chem. Rev.*, 2011, **255**, 1518–1540.

[135] M. Crucianelli, R. Saladino and F. De Angelis, *ChemSusChem*, 2010, **3**, 524–540.

[136] D. Betz, W. A. Herrmann and F. E. Kühn, *J. Organomet. Chem.*, 2009, **694**, 3320–3324.

[137] I. I. E. Markovits, W. A. Eger, S. Yue, M. Cokoja, C. J. Münchmeyer, B. Zhang, M.-D. Zhou, A. Genest, J. Mink, S.-L. Zang, N. Rösch and F. E. Kühn, *Chem. Eur. J.*, 2013, **19**, 5972–5979.

[138] L. Cammarata, S. G. Kazarian, P. A. Salter and T. Welton, *Phys. Chem. Chem. Phys.*, 2001, **3**, 5192–5200.

[139] W. A. Herrmann, R. W. Fischer, W. Scherer and M. U. Rauch, *Angew. Chem. Int. Ed. Engl.*, 1993, **32**, 1157–1160.

[140] M. Cokoja, I. I. E. Markovits, M. H. Anthofer, S. Poplata, A. Pöthig, D. S. Morris, P. A. Tasker, W. A. Herrmann, F. E. Kühn and J. B. Love, *Chem. Commun.*, 2015, **51**, 3399–3402.

[141] V. K. Olkhovik, D. A. Vasilevskii, A. A. Pap, G. V. Kalechyts, Y. V. Matveienko, A. G. Baran, N. A. Halinouski and V. G. Petushok, *ARKIVOC*, 2008, **9**, 69–93.

[142] R. K. Deshpande, J. L. Minnaar and S. G. Telfer, *Angew. Chem. Int. Ed. Engl.*, 2010, **49**, 4598–4602.

[143] M. Kim, J. F. Cahill, K. A. Prather and S. M. Cohen, *Chem. Commun.*, 2011, **47**, 7629–7631.

[144] K. K. Tanabe, Z. Wang and S. M. Cohen, *J. Am. Chem. Soc.*, 2008, **130**, 8508–8517.

[145] S. Bhunora, J. Mugo, A. Bhaw-Luximon, S. Mapolie, J. Van Wyk, J. Darkwa and E. Nordlander, *Appl. Organometal. Chem.*, 2011, **25**, 133–145.

[146] S. Hauser, private communication, 2014.

[147] G. Chahboun, J. A. Brito, B. Royo, M. A. El Amrani, E. Gómez-Bengoa, M. E. G. Mosquera, T. Cuenca and E. Royo, *Eur. J. Inorg. Chem.*, 2012, **2012**, 2940–2949.

[148] A. M. Rasero-Almansa, A. Corma, M. Iglesias and F. Sánchez, *ChemCatChem*, 2013, **5**, 3092–3100.

[149] M. E. Wilhelm, M. H. Anthofer, R. M. Reich, V. D'Elia, J.-M. Basset, W. A. Herrmann, M. Cokoja and F. E. Kühn, *Catal. Sci. Technol.*, 2014, **4**, 1638–1643.

[150] F. Gu, H. Dong, Y. Li, Z. Si and F. Yan, *Macromolecules*, 2014, **47**, 208–216.

[151] A. Füstner, M. Alcarazo, R. Goddard and C. W. Lehmann, *Angew. Chem. Int. Ed. Engl.*, 2008, **47**, 3210–3214.

[152] J. E. Schmidt, M. A. Deimund, D. Xie and M. E. Davis, *Chem. Mater.*, 2015, **27**, 3756–3762.

[153] N. L. Lancaster, P. A. Salter, T. Welton and G. B. Young, *J. Org. Chem.*, 2002, **67**, 8855–8861.

[154] C. Betti, D. Landini and A. Maia, *Tetrahedron*, 2008, **64**, 1689–1695.

[155] E. Ennis and S. T. Handy, *Molecules*, 2009, **14**, 2235–2245.

[156] C. Münchmeyer, private communication, 2014.

[157] R. Reich, private communication, 2014.

[158] C. Hutterer, *M.Sc. thesis*, Technische Universität München, 2014.

[159] M. A. Spackman and D. Jayatilaka, *CrystEngComm*, 2009, **11**, 19–32.

[160] R. M. Reich, M. Cokoja, I. I. E. Markovits, C. J. Münchmeyer, M. Kaposi, A. Pöthig, W. A. Herrmann and F. E. Kühn, *Dalton Trans.*, 2015, **44**, 8669–8677.

[161] M. Anthofer, private communication, 2014.

[162] *APEX suite of crystallographic software. APEX 2 Version 2008.4*, 2008.

[163] *SAINT, Version 7.56a and SADABS Version 2008/1*, 2008.

[164] G. M. Sheldrick, *"SHELXL-97", Program for Crystal Structure Solution*, 1998.

[165] G. M. Sheldrick, *"SHELXL-2014", Program for Crystal Structure Solution*, 2014.

[166] C. B. Hubschle, G. M. Sheldrick and B. Dittrich, *J. Appl. Crystallogr.*, 2011, **44**, 1281–1284.

[167] A. J. C. Wilson, in *International Tables for Crystallography*, Kluwer Academic Publishers, Dordrecht, The Netherlands, 1992, vol. C, pp. Tables 6.1.1.4 (pp. 500–502), 4.2.6.8 (pp. 219–222) and 4.2.4.2 (pp. 193–199).

[168] *Diamond - Crystal and Molecular Structure Visualization, Crystal Impact - Dr. H. Putz & Dr. K. Brandenburg GbR*.

[169] A. L. Spek, *“PLATON”, A Mulitpurpose Crystallographic Tool*, 2010.

[170] S. K. Wolff, D. J. Grimwood, J. J. McKinnon, M. J. Turner, D. Jayatilaka and M. A. Spackman, *CrystalExplorer*, 2012.

[171] C. F. Macrae, I. J. Bruno, J. A. Chisholm, P. R. Edgington, P. McCabe, E. Pidcock, L. Rodriguez-Monge, R. Taylor, J. van de Streek and P. A. Wood, 2008, 466.

[172] M. H. Anthofer, M. E. Wilhelm, M. Cokoja, I. I. E. Markovits, A. Pöthig, J. Mink, W. A. Herrmann and F. E. Kühn, *Catal. Sci. Technol.*, 2014, **4**, 1749–1758.

List of Publications and Curriculum Vitae

18 Journal or Book Chapter Contributions

1. *“Immobilisation of a molecular epoxidation catalyst on UiO-66 and -67: effect of pore size on catalyst activity and recycling”*

   Marlene Kaposi, Christine H. Hutterer, Simone A. Hauser, Tobias Kaposi, Florian Klappenberger, Mirza Cokoja, Alexander Pöthig, Johannes V. Barth, Wolfgang A. Herrmann, Fritz E. Kühn, *Dalton Trans.*, 2015, doi:10.1039/C5DT01340B

2. *“Structural Studies of Imidazolium Perrhenates: Influence of substituents on the strength of cation-anion contacts”*

   Robert M. Reich, Mirza Cokoja, Iulius E. Markovits, **Marlene Kaposi**, Alexander Pöthig, Wolfgang A. Herrmann, *Dalton Trans.*, 2015, *44*, 8669-8677.

3. “From simple ligands to complex structures: structural diversity of silver(I) complexes bearing tetradentate (alkylenebimpy) NHC ligands”

   Thomas Wagner, Alexander Pöthig, Hannah M. S. Augenstein, Tobias D. Schmidt, **Marlene Kaposi**, Eberhard Herdtweck, Wolfgang Brutting, Wolfgang A. Herrmann, Fritz E. Kühn *Organometallics*, 2015, *34*, 1522–1529.

4. “Reactions of formaldehyde with organometallic reagents”

   Marlene Kaposi, Julia Witt, Mirza Cokoja, Fritz E. Kühn, in *Science of Synthesis: Stereoselective Synthesis*, (Ed.: J. G. de Vries), Thieme: Stuttgart, 2014, Vol. 2, 289.

19 Talks and Poster Presentations

08/2014 248th ACS National Meeting & Exposition

San Francisco, CA, United States of America

Talk *“UiO-type MOFs for Catalyst Immobilization: Effect of Pore Size on Catalyst Activity and Recycling”*

03/2014 47. Jahrestreffen deutscher Katalytiker

Weimar, Deutschland

Poster *“UiO-type MOFs for catalyst immobilization”*

09/2013 ChemKrist-Workshop 2013 - Absolute structure and Twinning

Mühlheim a. d. Ruhr, Deutschland

Poster *“UiO-type MOFs for catalyst immobilization”*

06/2013 Heidelberg Forum of Molecular Catalysis

Heidelberg, Deutschland

Poster *“UiO-type MOFs for catalyst immobilization”*

Marlene **Kaposi**

Born	July 29, 1987 - *Ried i. I., Austria*
Marital status	married
Nationality	Austrian

Education

2012-2015	**PhD Student, Inorganic Chemistry**, *Technische Universität München*, Germany. Supervisor: Prof. Dr. Dr. h.c. mult. W. A. Herrmann Dissertation: "Multiphase epoxidation catalysis of olefins with metal-organic frameworks and ionic liquids"
2010–2012	**Dipl.-Ing. (equiv. MSc), Technical Chemistry - Synthesis**, *Vienna University of Technology*, Austria. Supervisor: Prof. Dr. Karl Kirchner Master's thesis: "Iron Pincer Complexes for Hydration of Ketones"
2005–2010	**BSc, Technical Chemistry**, *Vienna University of Technology*, Austria.
1998–2005	**Matura**, *Bundesgymnasium Blumenstraße, Bregenz*, Austria.

Experience

2012–2015	**Teaching Assistant**, *TU München*, Munich.
2009–2012	**Tutor**, *TU Wien*, Vienna.
2010	**Internship at a pharmacy**, *Seeapotheke Hard*, Hard, Austria.
2008	**Private tutor**, *team-plus! Lernhilfe-Institut*, Vienna.
2007	**Internship in Analytical Chemistry**, *Dr. Nikoopour ZT GmbH*, Günseldorf, Austria.
2006	**Internship at Johnson & Johnson**, *Johnson & Johnson Med. Prod.*, Vienna, Austria.

Languages

German	native speaker
English	fluent
French	basic communication skills
Spanish	basic communication skills

Skills

Analytics	Single-crystal X-ray diffraction, PXRD, NMR, IR, Raman, GC.
Computer	MS Office, LaTeX, Photoshop, SciFinder, ChemDraw, MestreNova, EndNote, Diamond, Mercury, ApexII, ShelXle, Platon.

Hirtenstraße 25 – 85386 Eching – Germany
☎ *+49 (175) 523 68 32* • ✉ *marlene.kaposi@gmail.com*